

QUANTIFYING THE VISCOELASTIC PROPERTIES OF TREATED AND
UNTREATED *PSEUDOMONAS AERUGINOSA* AND *STAPHYLOCOCCUS*
EPIDERMIDIS BIOFILMS USING A RHEOLOGICAL CREEP ANALYSIS

by

Michael Philip Sutton

A thesis submitted in partial fulfillment
of the requirements for the degree

of

Master of Science

in

Environmental Engineering

MONTANA STATE UNIVERSITY
Bozeman, Montana

April, 2008

© COPYRIGHT

by

Michael Philip Sutton

2008

All Rights Reserved

APPROVAL

of a thesis submitted by

Michael Philip Sutton

This thesis has been read by each member of the thesis committee and has been found to be satisfactory regarding content, English usage, format, citation, bibliographic style, and consistency, and is ready for submission to the Division of Graduate Education.

Warren Jones, Ph.D.

Approved for the Department of Civil Engineering

Brett Gunnink, Ph.D.

Approved for the Division of Graduate Education

Dr. Carl A. Fox

STATEMENT OF PERMISSION TO USE

In presenting this thesis in partial fulfillment of the requirements for a master's degree at Montana State University, I agree that the Library shall make it available to borrowers under rules of the Library.

If I have indicated my intention to copyright this thesis by including a copyright notice page, copying is allowable only for scholarly purposes, consistent with "fair use" as prescribed in the U.S. Copyright Law. Requests for permission for extended quotation from or reproduction of this thesis in whole or in parts may be granted only by the copyright holder.

Michael Philip Sutton

April, 2008

TABLE OF CONTENTS

1. INTRODUCTION.....	1
Purpose for Research.....	1
Biofilm.....	2
EPS.....	3
Previous Work Pertaining to Biofilm Mechanical Properties.....	4
Biofilm Defense Mechanisms.....	6
<i>Pseudomonas aeruginosa- FRD1</i>	7
<i>Staphylococcus epidermidis</i>	8
2. TREATMENTS.....	10
Ions- Cations.....	11
Ferric Chloride.....	12
Ferrous Chloride.....	12
Aluminum Chloride.....	12
Urea.....	13
Chelation.....	14
EDTA.....	14
Antimicrobial Agents.....	15
Glutaraldehyde.....	15
Barquat®.....	16
Chlorine.....	17
Rifampin.....	18
Ciprofloxacin.....	19
3. MODELING.....	21
Constitutive Equations.....	21
Elasticity- Hooke's law.....	22
Viscous Fluids-Newtonian.....	24
Viscoelasticity.....	25
Linearity.....	25
Kelvin Model.....	26
Maxwell Model.....	29
Burger's Model.....	30
4. METHODS.....	32
Biofilm Growth.....	32
Sample Preparation.....	33
Rheology.....	34
Test Apparatus.....	34

TABLE OF CONTENTS-CONTINUED

Creep Testing	37
Gap Setting	38
<i>FRDI</i>	39
<i>S. epidermidis</i>	40
Determining Linearity	41
<i>FRDI</i>	41
<i>S. epidermidis</i>	44
Parameter Estimation	45
Statistical Analysis	48
5. RESULTS.....	52
Controls	52
Cations.....	53
Chelation	60
Antimicrobials.....	61
Urea	65
6. DISCUSSION	66
Cations.....	70
<i>FRDI</i>	70
<i>S. epidermidis</i>	73
Chelation	75
EDTA	75
Urea	78
Antimicrobials.....	80
Barquat®	80
Glutaraldehyde	82
Rifampin.....	86
Ciprofloxacin.....	88
Chlorine.....	90
7. SUMMARY	92
REFERENCES CITED.....	95
APPENDICES	100
APPENDIX A: Data Table of Results for all Treatments.....	101
APPENDIX B: Microsoft Visual Basic Code for Curve Fitting Burger Coefficients.....	121

LIST OF TABLES

Table	Page
1. Constituents of EPS for <i>P. aeruginosa</i>	8
2. Constituents of EPS for <i>Staphylococcus epidermidis</i>	9
3. Cations used for treatments.....	11
4. All treatments and concentrations for each species of biofilm	33
5. <i>FRDI</i> linearity testing results	43
6. Results for untreated <i>FRDI</i>	53
7. Results for untreated <i>S. epidermidis</i>	53
8. Ratio between <i>S. epidermidis</i> and <i>FRDI</i> for the four Burger coefficients	53
9. Results for <i>FRDI</i> tested with 0.2 molar concentration of aluminum chloride	54
10. Results for <i>FRDI</i> tested with 0.02 molar concentration of aluminum chloride ...	55
11. Results for <i>FRDI</i> tested with 0.2 molar concentration of ferric chloride.....	55
12. Results for <i>FRDI</i> tested with 0.02 molar concentration of ferric chloride.....	56
13. Results for <i>FRDI</i> tested with 0.2 molar concentration of magnesium chloride...	56
14. Results for <i>FRDI</i> tested with 0.2 molar concentration of calcium chloride.....	57
15. Results for <i>FRDI</i> tested with 0.2 molar concentration of ferrous chloride	57
16. Results for <i>FRDI</i> tested with 0.02 molar concentration of ferrous chloride.....	58
17. Results for <i>FRDI</i> tested with 0.2 molar concentration of sodium chloride.....	58
18. Results for <i>S. epidermidis</i> tested with 0.2 molar concentration of ferric chloride	59
19. Results for <i>S. epidermidis</i> tested with 0.2 molar concentration of calcium chloride	59
20. Results for <i>S. epidermidis</i> tested with 0.2 molar concentration of sodium chloride	60

LIST OF TABLES-CONTINUED

Table	Page
21. Results for <i>FRDI</i> tested with 0.2 molar concentration of EDTA.....	60
22. Results for <i>S. epidermidis</i> tested with 0.2 molar concentration of EDTA.....	61
23. Results for <i>FRDI</i> tested with 50 mg/l molar concentration of Barquat®	61
24. Results for <i>S. epidermidis</i> tested with 0.2 molar concentration of Barquat®	62
25. Results for <i>FRDI</i> tested with a 50 mg/l concentration of glutaraldehyde.....	62
26. Results for <i>S. epidermidis</i> tested with a 50 mg/l concentration of glutaraldehyde.....	63
27. Results for <i>S. epidermidis</i> tested with a 0.1 mg/l concentration of rifampin.....	63
28. Results for <i>FRDI</i> tested with a 1 mg/l concentration of ciprofloxacin	64
29. Results for <i>FRDI</i> tested with a 50 mg/l concentration of chlorine.....	64
30. Results for <i>S. epidermidis</i> tested with a 0.2 molar concentration of urea.....	65
31. Results for <i>FRDI</i> tested with a 0.2 molar concentration of urea.....	65
32. Comparision of biofilm elastisity and viscosity to common substances	67

LIST OF FIGURES

Figure	Page
1. Schematic of biofilm formation (Permission from Peg Dirckx, Center for Biofilm Engineering).....	3
2. Schematic of chemical interactions of a polysaccharide inside the EPS (Mayer et al., 1999 with permission from Hans Curt Flemming).....	10
3. Molecular structure of urea.....	13
4. Molecular structure of EDTA.....	14
5. Molecular structure of glutaraldehyde.....	16
6. Molecular structure of Barquat® MB-80.....	17
7. Molecular structure of rifampin.....	18
8. Molecular structure of ciprofloxacin.....	20
9. Elemental representation of the Burger model.....	21
10. Spring and dashpot representation of Kelvin's model.....	27
11. Spring and dashpot representation of Maxwell's model.....	29
12. Spring and dashpot representation of Burger's model.....	31
13. Biofilm covered membranes on a TSA agar plate.....	32
14. TA Instruments AR1000 rheometer used to perform creep tests.....	34
15. Picture of humidification chamber.....	36
16. Jig created to position membranes in the center of the rheometer base plate.....	36
17. Schematic of loading rate and resulting strain in a creep test.....	37
18. Chart showing the resulting normal force on the rheometer base plate caused by lowering the rheometer head 5 microns on an <i>FRDI</i> biofilm. The linear region representing full membrane coverage can be seen after a normal force just lower than 1 N.....	39

LIST OF FIGURES-CONTINUED

Figure	Page
19. Chart showing the resulting normal force on the rheometer base plate caused by lowering the rheometer head 5 microns on an <i>S. epidermidis</i> biofilm. The linear region representing full membrane coverage can be seen after a normal force just lower than 1 N.	41
20. Chart showing average maximum compliance values for <i>FRDI</i> colony biofilm from a series of creep tests run at varying shear stresses. A notable jump in compliance can be seen between 20 and 25 Pa.	43
21. Chart showing the curve fitting of test data (dash) using Burger's model (solid).	47
22. Distribution of values for the G_K coefficient from the sodium chloride treatment group.	49
23. Histogram of data for the G_K coefficients from the sodium chloride treatment group.	50
24. Distribution of values for the $\log G_K$ coefficient from the sodium chloride treatment group.	51
25. Histogram of logarithmic G_K data set from the sodium chloride treatment group.	51
26. <i>FRDI</i> biofilm before treatment (left) and the same biofilm after one hour with a 0.2 M $FeCl_2$ treatment (right).	54
27. Median values of maximum strains for all <i>FRDI</i> treatments, normalized to maximum strain values for the equivalent control experiments.	68
28. Median values of maximum strains for all <i>S. epidermidis</i> treatments, normalized to maximum strain values for the equivalent control experiments.	69
29. Chart showing ratio between all cation treatments and their controls for the four Burger coefficients for the <i>FRDI</i> biofilm.	71
30. Median representation of typical creep curves for all cation treatments for <i>FRDI</i> biofilm.	72
31. Chart showing ratio between all cation treatments and their controls for the four Burger coefficients for the <i>S. epidermidis</i> biofilm.	73

LIST OF FIGURES-CONTINUED

Figure	Page
32. Median representation of typical creep curves for all cation treatments for <i>S. epidermidis</i> biofilm.	74
33. Atypical creep curve from EDTA treatment of <i>FRDI</i> biofilm.	75
34. Chart showing ratio between 0.2 M EDTA treatments and their controls for the four Burger coefficients for the <i>S. epidermidis</i> and <i>FRDI</i> biofilms.	76
35. Median representation of typical creep curves for 0.2 M EDTA treatment for <i>FRDI</i> biofilm.	77
36. Median representation of typical creep curves for 0.2 M EDTA treatment for <i>S. epidermidis</i> biofilm.	77
37. Chart showing ratio between 0.2 M urea treatments and their controls for the four Burger coefficients for the <i>S. epidermidis</i> and <i>FRDI</i> biofilms.	78
38. Median representation of typical creep curves for 0.2 M urea treatment for <i>FRDI</i> biofilm.	79
39. Median representation of typical creep curves for 0.2 M urea treatment for <i>S. epidermidis</i> biofilm.	79
40. Chart showing ratio between 50 mg/l Barquat® treatments and their controls for the four Burger coefficients for the <i>S. epidermidis</i> and <i>FRDI</i> biofilms.	80
41. Median representation of typical creep curves for 50 mg/l Barquat® treatment for <i>FRDI</i> biofilm.	81
42. Median representation of typical creep curves for 50 mg/l Barquat® treatment for <i>S. epidermidis</i> biofilm.	82
43. Chart showing ratio between 50 mg/l glutaraldehyde treatments and their controls for the four Burger coefficients for the <i>S. epidermidis</i> and <i>FRDI</i> biofilms.	83
44. Median representation of typical creep curves for 50 mg/l glutaraldehyde treatment for <i>FRDI</i> biofilm.	84
45. Median representation of typical creep curves for 50 mg/l glutaraldehyde treatment for <i>S. epidermidis</i> biofilm.	84

LIST OF FIGURES-CONTINUED

Figure	Page
46. Chart showing ratio between 0.1 $\mu\text{g}/\text{ml}$ Rifampin treatment and its control for the four Burger coefficients for the <i>S. epidermidis</i> biofilm.	86
47. Median representation of typical creep curves for 0.1 $\mu\text{g}/\text{ml}$ rifampin treatment for <i>S. epidermidis</i> biofilm.	87
48. Chart showing ratio between 1 $\mu\text{g}/\text{ml}$ ciprofloxacin treatment and its control for the four Burger coefficients for the <i>FRDI</i> biofilm.	88
49. Median representation of typical creep curves for 1 $\mu\text{g}/\text{ml}$ ciprofloxacin treatment for <i>FRDI</i> biofilm.	89
50. Chart showing ratio between 50 mg/l chlorine treatment and its control for the four Burger coefficients for the <i>FRDI</i> biofilm.	90
51. Median representation of typical creep curves for 50 mg/l chlorine treatment for <i>FRDI</i> biofilm.	91

Page of Notations

σ	Stress
C	Stiffness tensor
ε	Strain
λ	Lame constant
G	Shear modulus
δ	Kroneker delta
E	Elastic modulus
ν	Poissons's ratio
γ	Shear strain
τ	Shear stress
G_K	Kelvin elastic element
η_K	Kelvin viscous element
G_M	Maxwell elastic element
η_M	Maxwell viscous element
t	Time
t_1	Time load is relaxed
τ_K	Shear stress on Kelvin element
τ_M	Shear stress on Maxwell element
τ_1	Shear stress on spring element
τ_2	Shear stress on dashpot element
γ_1	Shear strain on spring element
γ_2	Shear strain on dashpot element
γ_K	Shear strain on Kelvin element
γ_M	Shear strain on Maxwell element
τ_0	Constant shear stress applied at beginning of creep test

ABSTRACT

Microbial biofilms are quite difficult to kill and control, and present many problems to industry and medicine. The ability to alter the mechanical properties of biofilms could aid in the control of biofilm. The goal of this research project was to develop techniques for measuring the mechanical properties of biofilms so that the effects of chemical treatments could be assessed. Constitutive material models were developed and applied to assist in this effort to quantify the effects. Biofilms are viscoelastic in nature, therefore, rheological testing techniques were utilized for this research. Creep testing was performed on a parallel plate rheometer to determine biofilm mechanical properties. The rheometer is a mechanical device that can accurately measure and apply shear stress and strain on viscoelastic samples. The Burger material model closely approximated material behavior of most chemical treatments. This model was used for determining constitutive properties.

Pseudomonas aeruginosa (*FRD1*) and *Staphylococcus epidermidis* colony biofilms were used for testing. Several treatment methods were used to investigate their effect on biofilm mechanical properties. As a source of different cations, solutions of NaCl, FeCl₃, AlCl₃, MgCl₂, CaCl₂, FeCl₂ were used for testing. Multivalent cation treatments stiffened the *FRD1* biofilm, but weakened the *S. epidermidis*. Urea treatments weakened both biofilm species. Glutaraldehyde treatments weakened the *FRD1* biofilm, but had little effect on the *S. epidermidis*. Several treatments -- EDTA, Barquat, chlorine, antibiotics (rifampin, and ciprofloxacin) -- weakened biofilms of both species. The effect of the same chemical treatment between the two species of biofilm sometimes had nearly opposite effects on the biofilms mechanical properties.

This research illustrated that it is possible to alter the mechanical properties of biofilm through chemical addition. Further, there are significant differences between the ways that the material properties of biofilms of different species of bacteria will be affected by a chemical treatment. Finally, it was observed that the 4-parameter Burger model for constitutive mechanical properties of biofilms fit the vast majority of the collected data, so that this model proves useful in comparing properties of biofilms grown or treated under various conditions.

INTRODUCTION

Biofouling is a costly and sometimes deadly problem facing industry and the medical community. Millions of dollars in extra costs occurring from pressure losses in pipe systems, increased drag on pipes and ship hulls, down time for cleaning and part replacements are blamed on biofouling every year. Pathogens may be introduced into drinking water systems through biofilm detachment, causing sickness (Van der Wende et al., 1989); also, persistent infections formed on implanted medical devices are one of the greatest obstacles currently facing the medical industry (Habash and Reid, 1999). The main culprits for biofouling are biofilms. Antimicrobials work by stopping or slowing microbial growth, but do not necessarily clear the biofilms from the infected area. Much more is known about killing biofilm than is known about removing biofilm (Chen and Stewart, 1999). A smaller spectrum of biofilm research is focused on altering the mechanical properties of biofilms. The ability to alter the material properties could be helpful in controlling biofilm growth in industrial and medical applications.

Purpose for Research

Understanding how antimicrobial agents or chemical treatments will affect a biofilm may influence the choice of treatment. If the goal is to remove biofilm from a surface then choosing a treatment that weakens the biofilm would most likely be the best choice. If the goal is to prevent the dispersal of many cells from a biofilm into a system, then using a treatment that tightens the biofilm may be a better choice. The ability to

manipulate the material properties of biofilm may prove a valuable tool in controlling biofilm formation and removal.

Knowledge of how different biofilm species or strains respond to similar treatments may provide some insight into the chemical makeup of a particular biofilm's EPS (extracellular polymeric substances). Understanding how biofilm mechanical properties change with chemical treatments could help to determine characteristic differences between biofilm species. Information relating how a certain biofilm species will respond to a chemical treatment may aid in the selection of a biofilm control treatment. The two bacterial biofilms investigated for this thesis were *Pseudomonas aeruginosa* (FRD1) and *Staphylococcus epidermidis*.

Biofilm

Biofilms are the accumulation of microorganisms, extracellular polymeric substances (EPS), cations, organic and inorganic particles, and also colloidal and dissolved compounds (Wingender et al., 1999). Biofilms form when planktonic, single microbial cells, are transported in a bulk fluid and attach to a wetted surface. Once the cells attach to a surface they begin to grow and multiply. The now immobilized group of cells begins to produce an EPS that enhances the survival of the microbial cells in the community (Towler, 2004). A schematic of the sequence of biofilm formation can be seen in Figure 1. Biofilms typically need a solid surface, known as a substratum, in order to form. They also typically need a water interface. However, the solid-water interface is not the only location that biofilm can be found; water-oil, water-air, and solid-air interfaces are also places where biofilms can survive (Wingender et al., 1999).

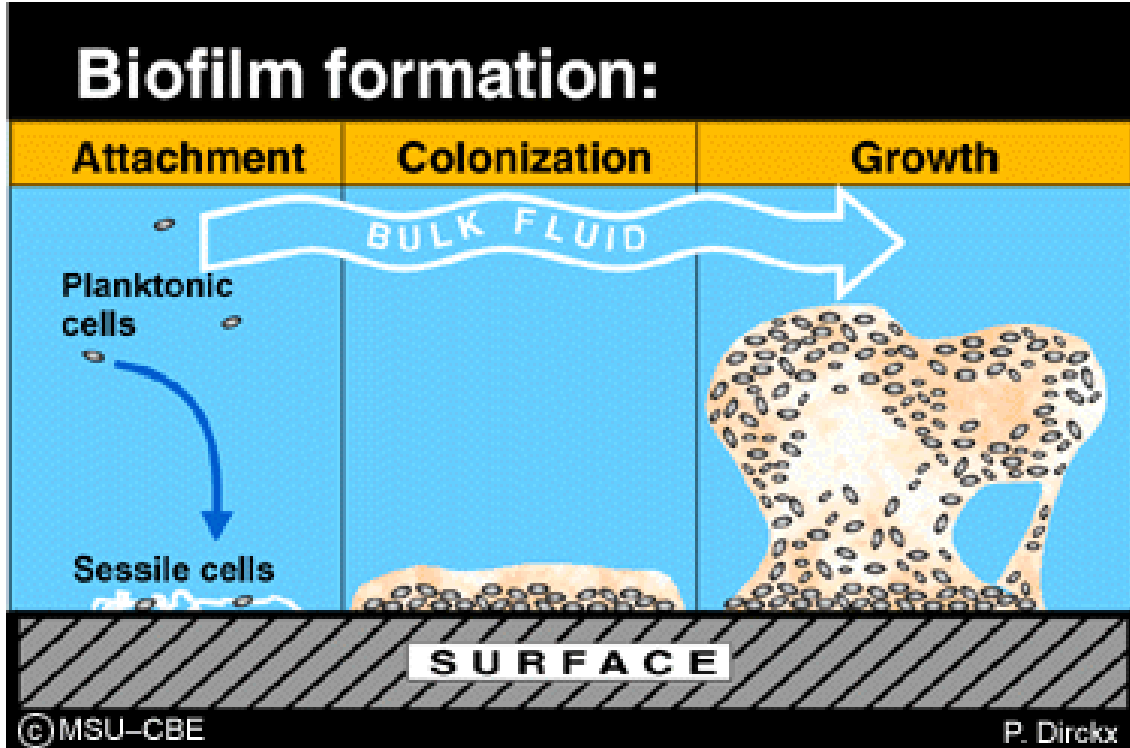


Figure 1: Schematic of biofilm formation (Permission from Peg Dirckx, Center for Biofilm Engineering).

EPS

The chemical makeup of a biofilm is known to differ by species and by genetic mutations within a species; the composition of EPS in a biofilm can vary from between 50 to 90 percent of the total organic matter depending on species (Wingender, 1999). In nature, EPS has been shown to be produced by both prokaryotic (bacteria) and eukaryotic microorganisms (algae, fungi). The structure of EPS can vary widely depending on growth conditions and a range of other variables. The EPS is important for the structural makeup and functionality of a biofilm. The EPS typically carries a charge; electrostatic interactions are thought to be quite important in the structural stability of a biofilms EPS.

The composition of the EPS determines physiochemical and biological properties of the biofilm (Wingender et al., 1999).

Previous Work Pertaining to Biofilm Mechanical Properties

While there has been less work conducted in the field of biofilm mechanics compared to antimicrobial work, a fair amount of prior work has been conducted on biofilm mechanical properties. Earlier work on creating biofilm mechanical models had been performed using microscopy in fluid flow cells where the deformation of a biofilm cluster was measured under a known flow rate. From the flow rate, a shear stress could be calculated and from the microscopy a strain and strain rate could be measured. These tests indicated that the biofilm could be modeled as a viscoelastic fluid (Klapper et al., 2002; Stoodley et al., 2002).

Alteration of the mechanical properties of biofilm has been explored by relatively few researchers (Towler et al., 2003; Klapper et al., 2002; Wloka et al., 2005; Chen and Stewart, 2000). The most researched method for altering biofilm's mechanical properties has been the addition of calcium ions to the EPS (Chen and Stewart, 2001). Calcium in its ionic form is a divalent cation (it has two positive charges). Multivalent cations are capable of binding several negatively charged particles on the surface of the EPS.

Work on determining the cohesive strength of biofilm flocs has been performed using a micro-cantilever technique. The force required to separate a biofilm floc was determined by microscopically measuring the deflection of a small glass pipette tip at mechanical failure of the biofilm sample, and the ultimate stress was determined by

dividing the force by the estimated area of the failure plane (Poppele and Hozalski, 2003).

The effects of chemical treatments on the cohesion of biofilm to surfaces were investigated (Chen and Stewart, 2000). This investigation measured the protein released from biofilm on a stainless steel slide by chemical treatments, and correlated protein removal to biofilm removal. The effect of a chemical on the detachment rate of a biofilm was determined.

Uniaxial compression techniques have been used to help estimate mechanical properties of biofilms. The apparent modulus of elasticity and yield point can be estimated using this method (Korstgens et al. 2001).

Rotational parallel plate rheometers have been used in several instances to investigate the material properties of biofilm. The mechanical properties of the dental plaque bacterium *Streptococcus mutans* were investigated (Vinogradov et al., 2004). Under certain shear stress loading conditions, the biofilm was found to act as a linear viscoelastic material, and the Burger's model was shown to be suitable as a constitutive model. The mechanical properties of a mixed culture biofilm were investigated and were also found to be linearly viscoelastic and fit the Burger's model (Towler et al., 2003). The addition of calcium to the growth media of the alginate producing strain of *Pseudomonas aeruginosa*, *FRD1*, was found to increase the biofilms strength in response to an applied shear stress (Wloka et al, 2006). The change in the viscosity of *P. aeruginosa* and *K. pneumoniae* caused by the addition of salts and chelating agents was investigated using a cone and plate viscometer (Chen and Stewart, 2002).

Biofilm Defense Mechanisms

Biofilm- associated bacteria are much more difficult to kill than their planktonic counterparts. Biofilm growth is inhibited by antimicrobials, but the biofilm will typically re-grow once the biocide is removed (Lewis, 2001). There are several characteristics of biofilms that help them to succeed in hostile environments.

One mechanism that helps biofilm cells resist antimicrobial treatment is diffusion limitation. Diffusion limitations can create situations where the antimicrobial fails to fully penetrate the biofilm during the time the biofilm was exposed to the treatment. The makeup of the EPS causes the diffusion rate of the antimicrobial to be retarded compared to its diffusion rate in water, resulting in lower biocide concentrations and requiring longer exposure times to obtain full penetration. Oxidative agents such as hypochlorite are consumed quickly at the interface of the biofilm and the bulk fluid, and because the reaction rate is more rapid than diffusion, killing occurs only in the exposed outer layers of the biofilm (Costerton et al., 1999; Lewis, 2001).

Nutrient and substrate gradients in the biofilm are another mechanism that help protect biofilm against antimicrobials. Many antimicrobials are most effective when bacterial growth is rapid. Some antimicrobials are completely ineffective without cell growth; penicillin is an example of an antimicrobial that requires growth (Lewis, 2001). Cells located in areas of the biofilm with low or no nutrients will grow very slowly or not at all; these cells are not likely to be killed by most antimicrobials (Costerton et al., 1999).

Persister cells are cells that have a tolerance to a given antimicrobial. Experiments have shown that when an antimicrobial treatment is administered, there will be a large killing event, but a small amount of cells will not die. Increasing the concentration of the antimicrobial has little effect on killing these persisting cells. The persisters will then be able to reseed the biofilm once the antibiotic pressure has been removed (Lewis, 2001).

Pseudomonas aeruginosa- FRDI

The bacterium *Pseudomonas aeruginosa* is Gram-negative, aerobic, and rod shaped. The bacteria typically measure between 0.5 to 0.8 μm by 1.5 to 3.0 μm . *Pseudomonas* can exist as a biofilm or as a singular planktonic cell. The optimum growing temperature is 37 degrees Celsius, but it can tolerate temperatures up to 42 degrees Celsius (Tortora et al, 2005). *P. aeruginosa* is an opportunistic pathogen of humans; it will not colonize healthy tissues, but it can colonize any compromised tissue or people who are immunocompromised.

FRDI is a mutant of *P. aeruginosa*. It expresses a mucoid phenotype due to the excessive production of the exopolysaccharide alginate; this strain was first isolated from a patient with cystic fibrosis. *P. aeruginosa* biofilms are commonly found in lung infections in cystic fibrosis patients (Silo-Suh et al, 2002; Walters et al., 2003). Some of the known constituents of EPS and their corresponding electrostatic charge in a *P. aeruginosa FRDI* biofilm can be seen in Table 1.

Table 1: Constituents of EPS for *P. aeruginosa*.

Constituent	Charge	Locus
Alginate	Negative	<i>alg</i>
Polysaccharide	??	<i>psl</i>
Polysaccharide	??	<i>pel</i>
DNA	Negative	
Lectin		<i>lecA</i>

The Locus in the table refers to a group of genes important for certain functions in a biofilm. The *psl* locus produces a mannose rich polymer; this gene cluster is thought to be important for biofilm initiation in *P. aeruginosa* (Jackson et al., 2004; Matsukawa and Greenberg, 2004). *LecA* is a tetrameric protein; it is known to bind to D-galactose, a monosaccharide, and it is thought *lecA* helps *P. aeruginosa* in the maturation process of the biofilm (Diggle et. al., 2006). The *pel* locus produces a glucose rich polysaccharide (Friedman and Kolter, 2004).

Staphylococcus epidermidis

Staphylococci are gram positive, spherical, facultative anaerobes, and are about one micrometer in diameter (Tortora et al, 2005). *Staphylococcus epidermidis* is present on the skin in the natural flora of humans. Most strains of *Staphylococcus epidermidis* are not pathogenic; however hospital infections can be problematic. *S. epidermidis* is responsible for 33.5% of nosocomial bloodstream infections (Rupp et al., 1999). The most common occurrence for *Staphylococcal* infections are those associated with Hickman catheters, central venous catheters, prosthetic heart valves, and vascular grafts

(Zheng and Stewart, 2002). Catheter and implant caused infection has made *S. epidermidis* a bacterium of interest. Some of the known constituents and corresponding electrostatic charges that compose the EPS of *S. epidermidis* biofilm are shown in Table 2 (Sadovskaya, 2005).

Table 2: Constituents of EPS for *Staphylococcus epidermidis*.

Constituent	Charge	Locus
Polyglucosamine	Positive	<i>ica</i>
Teichoic acid	Negative	

The *ica* locus is thought to encode for polysaccharide/adhesin which mediates cell adherence to biomaterials (Hennig, et al. 2007). Teichoic acids are highly negatively charged cell wall polymers that are thought to play an important role in the first step of biofilm formation (Gross et al., 2007).

TREATMENTS

There are several different chemical and physical characteristics of the EPS that are thought to play important roles in the mechanical properties of biofilms. These include: hydrogen bonding, electrostatic interactions between like-charged polymers that are bridged together by multivalent counter-ions, physical entanglement, electrostatic interactions between oppositely charged EPS strands, covalent bonding, hydrophobic interactions, and weak force interactions (Chen and Stewart, 2002). Several different chemical treatments were used to exploit the intrinsic chemistry of the biofilms, which in turn affected the constitutive behavior of the biofilms. Figure 2 shows a schematic of chemical interactions in a polysaccharide (Mayer et al., 1999)

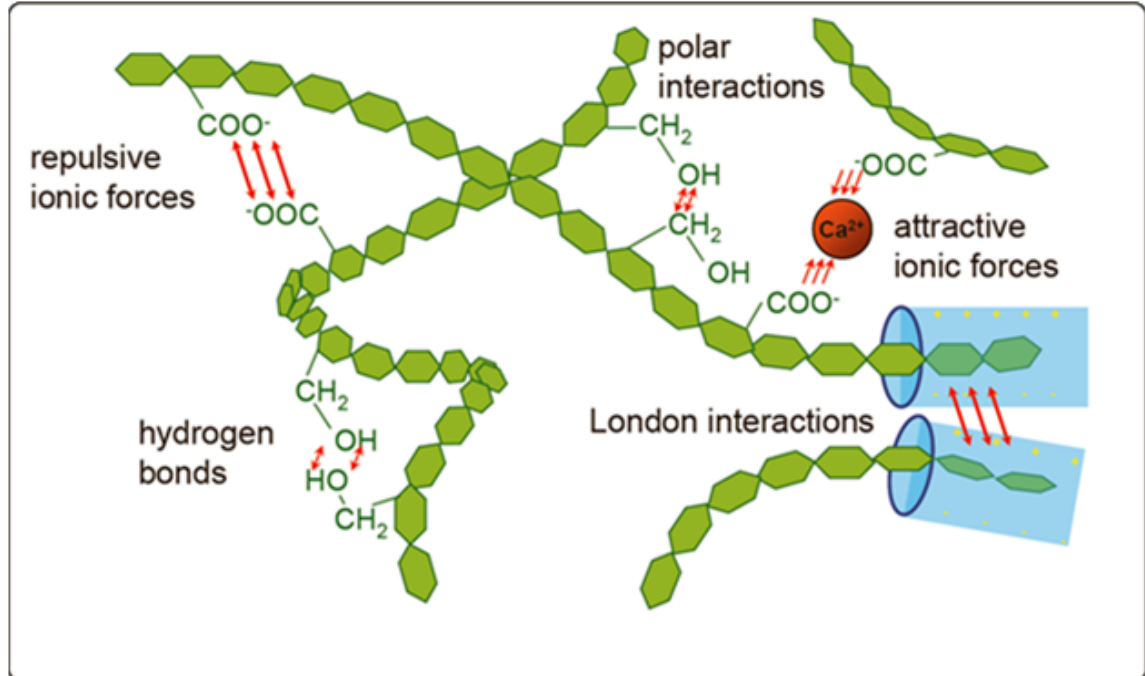


Figure 2: Schematic of chemical interactions of a polysaccharide inside the EPS (Mayer et al., 1999 with permission from Hans Curt Flemming).

Ions- Cations

Cations introduced to a net-negatively charged biofilm can be ionically bound to the anionic sites on a strand of EPS. Divalent cations can bind to two sites simultaneously, which can create a cross-linkage in the EPS, constricting the polymeric matrix and causing an overall tightening of the biofilm, which results in a change of the mechanical properties (Wloka et al., 2005).

Altering the material properties of the biofilm by cationic cross-linkage should not be limited to just calcium-- any multivalent cation should be capable of tightening the EPS by the same mechanism mentioned above. Several divalent, trivalent, and monovalent cations were used in this research. All cations were put into solution with the Cl⁻ anion to limit an uncontrolled variable. All cations were tested at a concentration of 0.2 M, but some were also tested at a 0.02 M concentration to compare the effect of concentration on the change in mechanical properties. Table 3 lists all cation treatments used for this research.

Table 3: Cations used for treatments.

Cation	Binding sites	Comments or issues
Al ³⁺	3	Common water treatment coagulant; forms Al(OH) ₃ (s) at high concentration and alkaline pH
Fe ³⁺	3	Common water treatment coagulant, forms Fe(OH) ₃ at moderate concentration and alkaline pH
Fe ²⁺	2	Can oxidize to Fe ³⁺ with exposure to air
Mg ²⁺	2	
Ca ²⁺	2	Thought to be important for EPS stability
NaCl	1	Should not be able to cross-link, because it only has one binding site. Exchange of 2 Na ⁺ ions for one divalent cation should disrupt existing crosslinking.

Ferric Chloride

Ferric Chloride (FeCl_3) is an ionically bonded salt. When put into solution the cation Fe^{3+} and three Cl^- anions are formed. The cation Fe^{3+} is capable of binding three negatively charged sites on an EPS molecule or interacting with three other negative ions, most notably OH^- ions. $\text{Fe}(\text{OH})_3$ is not very soluble, with a solubility product of 2.79×10^{-39} . The tendency of Fe^{3+} to form iron oxides and hydroxides means it has utility in water treatment as a coagulant chemical. At the Fe^{3+} concentration employed in the current study, some precipitation of iron hydroxides was expected.

Ferrous Chloride

Ferrous Chloride (FeCl_2), when put into solution forms the cation Fe^{2+} and two Cl^- anions. This Fe^{2+} cation is capable of binding two negatively charged sites in the EPS. Rapid reactions can occur with Fe^{2+} and oxidants such as dissolved oxygen to form Fe^{3+} in solution. The reaction rate is accelerated once the pH of the solution becomes 7 or greater (Vance, 1994).

Aluminum Chloride

Aluminum chloride (AlCl_3) is an ionically bonded salt. When put into solution the cation Al^{3+} and three Cl^- anions are formed. The cation is capable of binding three negatively charged sites. Aluminum ions are commonly used in drinking water treatment, and alum ($\text{Al}_2(\text{SO}_4)_3$) is the most widely utilized coagulant in the drinking water treatment industry (Benschoten and Edzwald, 1990). Like iron hydroxides, aluminum hydroxide ($\text{Al}(\text{OH})_3$) is not very soluble, with a solubility product of 3×10^{-34} . At the

concentrations used in this study, some precipitation of aluminum hydroxide was likely to occur.

Urea

Hydrogen-bonding interactions are theorized to be important for EPS mechanical stability. Disrupting the hydrogen bonds should disrupt the EPS matrix resulting in a weaker biofilm. Urea ((NH₂)₂CO) is a chemical known to disrupt hydrogen bonding, so a weakened biofilm would be expected from a urea treatment (Chen and Stewart, 2002). Urea at a concentration of 0.2 molar was used in rheological testing. The molecular structure of urea can be seen in Figure 3.

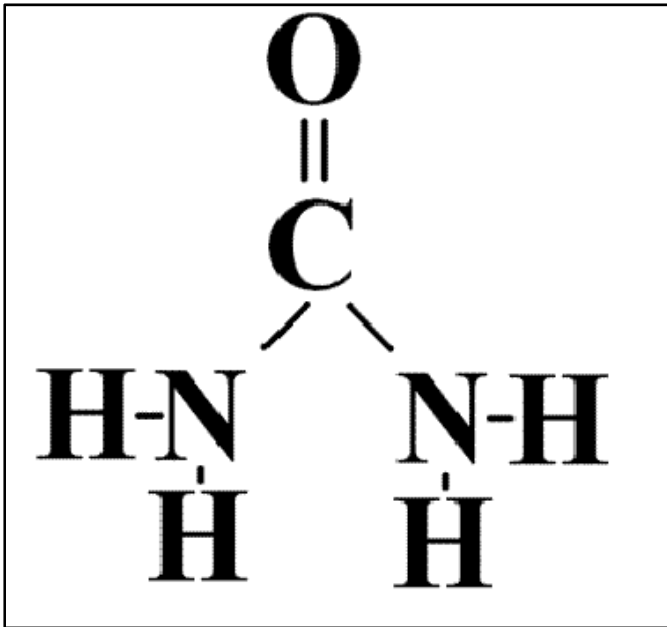


Figure 3: Molecular structure of urea.

Chelation

Chelating agents are chemicals that are capable of sequestering metal ions in solution. Metal ions such as calcium and iron are theorized to be important elements in EPS structure (Wloka et al., 2004). The removal or sequestration of metal ions in the EPS should have some effect on the mechanical properties of biofilms. The chelating agent EDTA was used as a treatment in this study.

EDTA

Ethylenediaminetetraacetic acid (EDTA) is an amino acid commonly used as a chelating agent. EDTA sequesters bi- and trivalent cations by means of its four carboxylate and two amine groups (Holleman and Wiberg, 2001). It has the molecular formula $(\text{HO}_2\text{CCH}_2)_2\text{NCH}_2\text{CH}_2\text{N}(\text{CH}_2\text{CO}_2\text{H})_2$ and a molecular weight of 292. The molecular structure of EDTA can be seen in Figure 4.

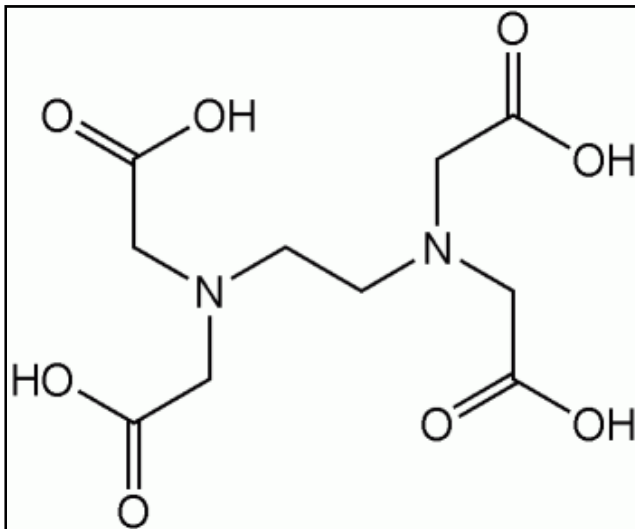


Figure 4: Molecular structure of EDTA.

Antimicrobial Agents

Biofilm have been proven to be quite difficult to kill using antimicrobial treatments. Reduced susceptibility to antibiotics has been thought to be caused by two defense mechanisms in the biofilm. The first explanation is that the antibiotic fails to fully penetrate the biofilm. The second explanation is that nutrient limitations in the biofilm result in slow growth, which in turn limits antimicrobial susceptibility (Walters et al., 2003).

Understanding the effects of antimicrobial agents on the mechanical properties of biofilm could be a helpful tool in choosing a treatment for biofilm control. Not all antimicrobials affect the biofilm the same way. Some create a stronger tighter biofilm while others cause the biofilm to become weaker and looser, and some treatments may not affect the mechanical structure at all (Davidson, 2008). Most antimicrobials should have some killing effect on the bacteria, but the resulting change in the structure of the biofilm after an antimicrobial treatment will differ depending on the strain of bacteria and the treatment used.

Glutaraldehyde

Glutaraldehyde is a colorless liquid with a strong odor. It is most commonly used as an antimicrobial in the hospital and food industry; in high enough concentrations it is considered a sterilizing agent. Glutaraldehyde works as an antimicrobial by denaturing and cross-linking cellular proteins thereby ending microbial metabolic activities involving enzymatic processes, which effectively kills the cell. Because of its cross-linking properties, glutaraldehyde is often used as a fixative agent in microbiological

applications (Marrie et al., 1982). Glutaraldehyde has a molecular weight of 100.1, and its chemical formula is $C_5H_8O_2$ (Davidson, 2008). The molecular structure of glutaraldehyde can be seen in Figure 5. Glutaraldehyde treatments at a concentration of 50 mg/l were used for rheological testing.

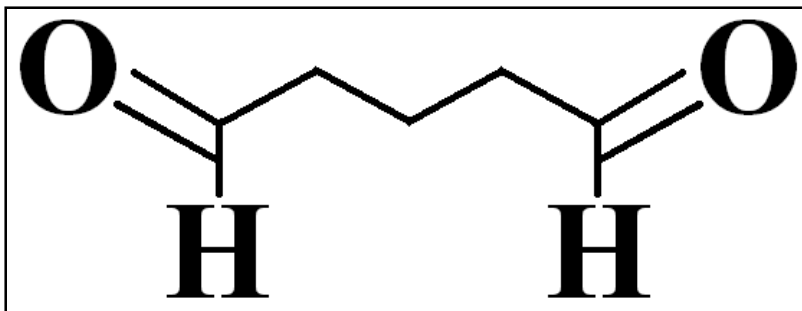


Figure 5: Molecular structure of glutaraldehyde.

Barquat®

Benzalkonium chloride is a generic name for a class of quaternary ammonium compounds often referred to as alkyl dimethyl benzyl ammonium chloride (ADBAC) (Lonza, inc). Quaternary ammonium compounds (QACs) are cationic surfactants; they are commonly used as disinfectants in the food and medical industries (Sundheim et al., 1998). Surfactants are wetting agents that lower the surface tension of liquids. Surfactants are water-soluble surface-active agents, and are comprised of a hydrophobic portion, which is typically a long alkyl chain connected to a hydrophilic functional group (Sigma-Aldrich). Barquat® MB-80 was the QAC used in this research project; it has a molecular weight of 357. Its chemical formula is n-Alkyl (C14-50%, C12-40%, C16-10%) dimethyl benzyl ammonium chloride; the molecular structure of Barquat® can be seen in Figure 6 (Davidson, 2008). Barquat® was tested at a concentration of 50 mg/l for this study.

Because Barquat[®] employs a cationic group for its hydrophobic end, it was theorized that it would intercalate into negatively charged zones of the biofilm matrix.

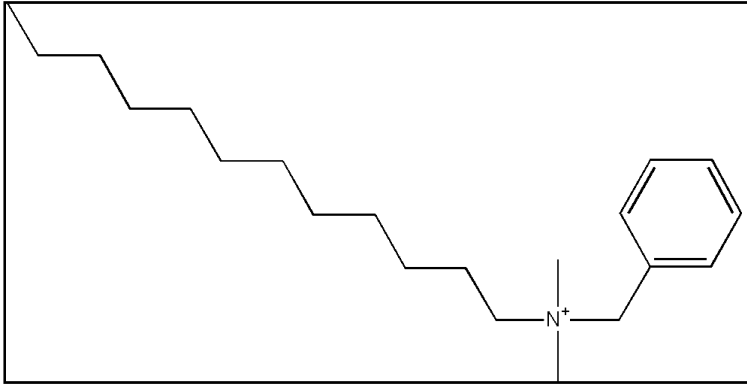


Figure 6: Molecular structure of Barquat[®] MB-80.

Chlorine

Chlorine is commonly used to control biofilm formation in wetted areas such as in drinking water distribution systems, swimming pools, cooling towers, and many more industrial situations. Hypochlorite (OCl^-) or hypochlorous acid (HOCl) is the chemical treatment being referred to by the term “chlorine.” Chlorine is a highly oxidative chemical; its antimicrobial activity is due to its high affinity to oxidize organic material. The high rate of reaction between chlorine and organic material causes chlorine to be quite effective against planktonic bacteria, but creates a diffusion limitation in biofilm (Chen and Stewart, 1996). Only the outer layers of the biofilm exposed to the bulk fluid carrying the chlorine is affected by the treatment (Davison, 2008). Rheological testing for this thesis used chlorine at a concentration of 50 mg/l.

Rifampin

Rifampin is an antibiotic known to be very effective in the killing of planktonic *Staphylococcus epidermidis*. Rifampin works by inhibiting bacterial RNA polymerase (Campbell et al., 2001). Four hour rifampin treatments at a concentration of $0.1 \mu\text{g ml}^{-1}$ on a planktonic culture of *S. epidermidis* resulted in a 4.92 log reduction in viable cells. However, the equivalent rifampin treatment on colony biofilm yielded only a 0.6 log reduction of viable cells. The protection of the biofilm is not due to inadequate penetration of rifampin; the most likely cause for protection is slow growth caused by nutrient limitations (Zheng and Stewart, 2002).

Rifampin was used as treatment in rheological testing for this thesis. TSA plates were poured and rifampin was added before the plates cooled so that the concentration of rifampin in the agar plates was $0.1 \mu\text{g/ml}$. *S. epidermidis* colony biofilms were grown on TSA plates for 48 hours, and then transferred to the plates containing rifampin for 24 hours prior to rheological testing. The molecular structure of rifampin can be seen in Figure 7.

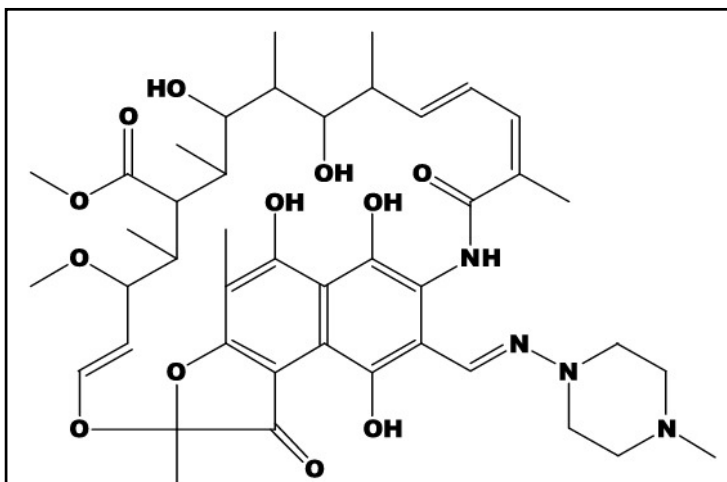


Figure 7: Molecular structure of rifampin.

Ciprofloxacin

Fluoroquinolones are a commonly used class of antimicrobials. They work by inhibiting bacterial replication by their action on DNA gyrase (Riddle et al. 2000). Ciprofloxacin is the most commonly used antibiotic of all the fluoroquinolones. Ciprofloxacin is known to be effective against *Pseudomonas aeruginosa* (Walters et al., 2003). A ciprofloxacin treatment on planktonic cells of the *FRDI* strain of *Pseudomonas aeruginosa* was found to have a Minimum Inhibitory Concentration (MIC) of around $0.01 \mu\text{g ml}^{-1}$. Treatment of planktonic *FRDI* cells with $1 \mu\text{g ml}^{-1}$ resulted in a 5.9 log reduction of viable cells. A four hour treatment of a *FRDI* colony biofilm with a ciprofloxacin treatment of $1 \mu\text{g ml}^{-1}$ resulted in a 1.06 log reduction of viable cells (Walters et al., 2003). The discrepancy in the killing efficacy between the planktonic cell culture and the colony biofilm is immense, and equates to ciprofloxacin being approximately 60,000 times more effective in killing planktonic cells than colony biofilms. Nutrient limitations are thought to be responsible for this phenomenon. In particular, oxygen penetration is most likely the limiting factor, not antimicrobial penetration. Oxygen penetration into the biofilm was found to be only 50 to 90 μm from the air interface; killing was likely to occur in this small portion of the biofilm only (Walters et al., 2003).

While ciprofloxacin is not very effective in the killing of biofilm, the effect of the antimicrobial on the mechanical properties of the biofilm is intriguing. For this thesis, *P. aeruginosa* colony biofilms were grown for 24 hours on TSA plates before being transferred to TSA plates containing $1 \mu\text{g ml}^{-1}$ of ciprofloxacin. Biofilms were treated on

the ciprofloxacin plates for 24 hours prior to testing. The molecular structure of ciprofloxacin can be seen in Figure 8.

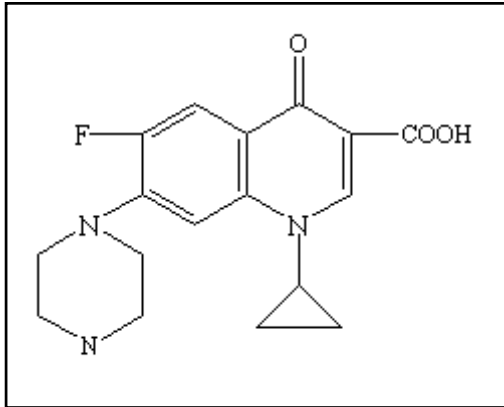


Figure 8: Molecular structure of ciprofloxacin.

MODELING

Constitutive equations for the biofilm treatments were derived by combining elastic and inelastic material models together in a sequence that best fits the experimental data. Elastic and inelastic materials are modeled as discrete elements-- springs and dashpots, respectively. These elements are put together in parallel to create the Kelvin model and are put together in series to create the Maxwell model. Combining the Kelvin and Maxwell models in series creates the Burger model (Figure 9). Solving the differential equations from the Burger's model results in two 4-coefficient equations. The details of these models will be covered later in this chapter.

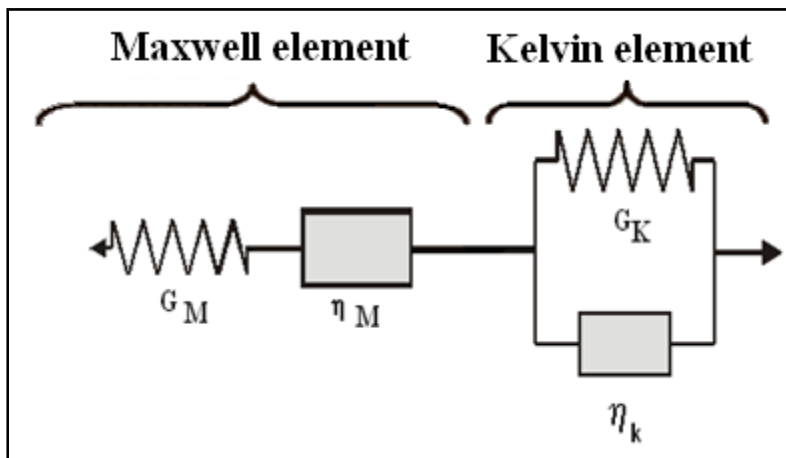


Figure 9: Elemental representation of the Burger model.

Constitutive Equations

Constitutive equations are used to mathematically describe the mechanical (dynamic) response of a material to external stimulation. Constitutive equations are intrinsic to individual materials. There are many factors that may affect how a material will respond to an excitation including temperature, deformation, loading, and pressure.

There are too many variables and materials to create an equation that wholly encompasses a material over the entire range of variables and outside factors. Instead, constitutive equations are created to represent the observed behavior of the material as accurately as possible by restricting the range of variables involved. The most well known examples of constitutive equations are Hooke's law for elastic materials and Newtonian viscosity for viscous fluids. These equations describe how a material will strain in response to a stress. These equations are only valid for a given range of variables. For example, Hooke's law governs how a steel beam will deform, but it is only valid for solid steel. As steel is heated near its melting point, its material properties will change and Hooke's law will no longer hold true.

Elasticity- Hooke's law

When modeling elastic materials, strain is considered to be instantaneous with the application of a load. The strain remains constant while a constant load is applied and the strain recovers instantly returning back to its unloaded configuration with the removal of the load. Purely elastic materials are modeled to be fully reversible, so no energy is considered to be lost to friction during the loading and unloading process.

Most elastic materials behave linear elastically (strain is directly proportional to the stress (Findley, 1989)). For small strains the relationship between stress and strain for linear elastic materials is represented by Hooke's law. In tensor form Hooke's law is given as:

$$\sigma_{ij} = C_{ijkl} * \epsilon_{kl} \quad (1)$$

σ_{ij} is a second order stress tensor and ϵ_{kl} is a second order strain tensor. C_{ijkl} is a 4th order tensor that describes the elastic moduli of a given material. The stiffness tensor, C , is independent of strain and stress in a linear elastic model, and is comprised of 81 coefficients; however, the tensor may be reduced to 36 coefficients using symmetry. For most materials the elastic modulus can be reduced even further by assuming isotropy. Fully isotropic materials behave in the same elastic manner regardless of material orientation. In the case of complete isotropy, only two of the 81 elastic moduli coefficients remain independent. The resulting form of Hooke's law for completely isotropic materials is given by:

$$\sigma_{ij} = \lambda \epsilon_{kk} \delta_{ij} + 2G \epsilon_{ij} \quad (2)$$

λ and G are called the Lamé constants, and δ is the Kronecker delta. G is the shear modulus given by:

$$G = \frac{E}{2(1+\nu)} \quad (3)$$

E is the elastic modulus and ν is Poisson's ratio.

$$\lambda = \frac{\nu * E}{(1+\nu)(1-2\nu)} = \frac{2 * \nu * G}{(1-2 * \nu)} \quad (4)$$

Linear elastic materials are classically modeled using a spring analog.

Viscous Fluids-Newtonian

Fluids are defined as substances that deform continuously when acted on by a shearing stress of any magnitude (Munson, 2002). In contrast to elastic materials whose strain is proportional to the applied stress, fluids will strain indefinitely under an applied load. There are two main classes of fluids, compressible and incompressible.

Incompressible fluids like water undergo small or negligible changes in their density when subjected to varying pressures and temperatures, while compressible fluids like air can experience significant density changes with the variation of temperature and pressure.

All fluids have some viscosity, but some fluids have such a low viscosity that it is considered to be negligible; these fluids are called inviscid fluids. Most common fluids are Newtonian, and for these fluids the strain rate imparted by a shear stress will be linearly proportional to the magnitude of that stress. For Newtonian fluids the stress imparted onto a viscous fluid is a function of the fluids viscosity (η) and the strain rate, where:

$$\sigma = \eta * \frac{d\epsilon}{dt} \quad (5)$$

Viscous fluids are typically modeled as a dashpot element. These elements are essentially shock absorbers filled with a viscous fluid. A dashpot will deform continuously at a constant rate if subjected to a constant stress.

Viscoelasticity

Previous experiments have shown that biofilms are viscoelastic in nature (Towler et al., 2003, Klapper et al., 2002). Most materials fall into a category of either solid or fluid, however, there are many materials that exhibit mechanical behavior of both solids and fluids. These materials are known as viscoelastic. Viscoelastic materials respond elastically upon rapid loading, and then experience a continuously increasing strain with a decreasing strain rate. Upon removal of the stress there is an instantaneous elastic recovery followed by a continuously decreasing strain (Munson, 2002). The most famous example of a viscoelastic material is silly putty. Silly putty bounces when loaded quickly and flows when pulled slowly.

Viscoelastic materials are also known as time dependent materials. In order to develop a constitutive equation for a viscoelastic material, time must be a variable along with stress and strain. This makes the examination of viscoelastic materials more difficult since the time variable cannot be held constant. The three most common types of testing for viscoelastic materials are creep, stress relaxation, and constant rate stressing (Findley, 1989).

Linearity

If a material is to be classified as linearly viscoelastic, the strain response exhibited by the material needs to be proportional to the stress at a given time. Also, the linear superposition principle needs to hold true for a material to be linearly viscoelastic.

The requirements for linear viscoelasticity represented mathematically can be represented in two equations:

$$\varepsilon[c\sigma(t)] = c\varepsilon[\sigma(t)] \quad (6)$$

$$\varepsilon[\sigma_1(t) + \sigma_2(t-t_1)] = \varepsilon[\sigma_1(t)] + \varepsilon[\sigma_2(t-t_1)] \quad (7)$$

Where σ is stress and ε is strain and c is a scalar constant. Equation (6) states that the strain responding to an applied stress $c\sigma(t)$ equals c times the strain if the applied stress is $\sigma(t)$. Equation (7) states the second requirement that if two arbitrary non-equivalent stresses are applied at differing times then the resulting strain $\varepsilon[\sigma_1(t) + \sigma_2(t-t_1)]$ equals the sum of the strains that would result from $\sigma_1(t)$ and $\sigma_2(t-t_1)$ acting independently (Findley, 1989).

Linearity is important in the modeling of viscoelastic materials since the classical Kelvin, Maxwell and Burger models only hold true if the material responds linearly. If a material is deemed to be non-linear then modeling becomes more of an exercise in equation fitting rather than based on equations derived from mechanical models. Most materials are linear over a certain range of stress, strain, time, and temperature; however, over larger ranges of these variables most materials are non-linear.

Kelvin Model

The Kelvin model is made up of a spring and dashpot connected in parallel; this can be seen in Figure 10. The strain experienced in both the spring and dashpot are equivalent in the Kelvin element.

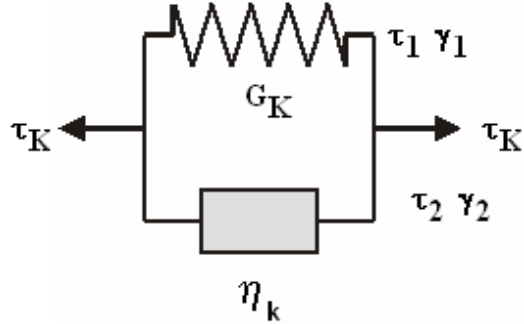


Figure 10: Spring and dashpot representation of Kelvin's model.

The following is a derivation of the differential equation and solution for shear strain in a Kelvin model with respect to time in a creep test.

The stress in spring member (general)

$$\tau = G * \gamma \quad (8)$$

The stress in the dashpot member (general)

$$\tau = \eta * \frac{d\gamma}{dt} \quad (9)$$

From the stress strain relationships developed in (8) & (9) for general springs and dashpots, a stress strain relationship for each element in the Kelvin model can be developed.

$$\tau_1 = G_K * \gamma_K \quad (10)$$

$$\tau_2 = \eta_K * \frac{d}{dt} \gamma_K \quad (11)$$

Both elements are connected in parallel so the total stress is

$$\tau_K = \tau_1 + \tau_2 \quad (12)$$

The strain in the model is the same for both elements

$$\gamma_1 = \gamma_2 = \gamma_K \quad (13)$$

Using equations (10), (11), and (12) and eliminating τ_1 and τ_2

$$\frac{d}{dt}\gamma + \frac{G_K}{\eta_K} * \gamma = \frac{\tau_K}{\eta_K} \quad (14)$$

Solving the differential equation in (14) using a constant stress of τ_o and $\gamma=0$ at $t = 0$

yields the strain equation for loading of the Kelvin model (γ_{Kcreep}).

$$\gamma_{Kcreep} = \frac{\tau_o}{G_K} \left(1 - \exp \left(-G_K * \frac{t}{\eta_K} \right) \right) \quad (15)$$

If the stress is removed at time t_1 , the strain resulting in the stress removal can be determined by the superposition principle. Removing the stress at time t_1 is accomplished by applying the stress ($-\tau_o$). The strain equation for the unloading of the Kelvin model ($\gamma_{Krecovery}$) is given by:

$$\gamma_{Krecovery} = \frac{-\tau_o}{G_K} \left(1 - \exp \left(-G_K * \frac{t-t_1}{\eta_K} \right) \right) \quad (16)$$

If the stress (τ_o) is added at $t = 0$ and removed at $t = t_1$, then the superposition principle yields the combined equation for creep and recovery for the Kelvin model given by

$$\gamma_K = \frac{\tau_K}{G_K} * \exp \left(\frac{-G_K}{\eta_K} * t \right) * \left(\exp \left(-G_K * \frac{-t_1}{\eta_K} \right) - 1 \right) \quad (17)$$

Maxwell Model

The Maxwell model is made up of a spring and dashpot connected in series. In a Maxwell model the dashpot and the spring elements are under the same stress, but the strain in each member is not necessarily the same. The following is a derivation of the solution for shear strain in a Maxwell model with respect to time in a creep test. Figure 11 shows the Maxwell model represented by a spring and dashpot.

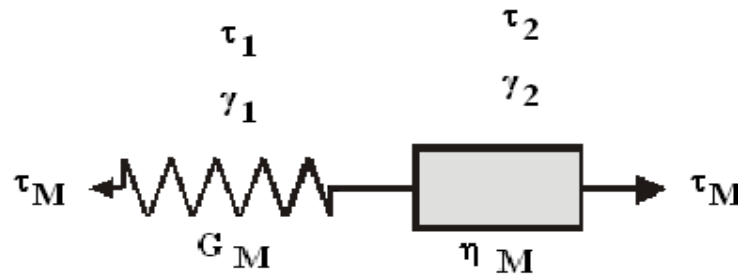


Figure 11: Spring and dashpot representation of Maxwell's model.

Since both elements are connected in series the stress is equal in both elements:

$$\tau_M = \tau_1 = \tau_2 \quad (18)$$

Taking a derivative of (18) to obtain an expression for strain rate,

$$\frac{d}{dt}\gamma_M = \frac{d}{dt}\gamma_1 + \frac{d}{dt}\gamma_2 \quad (19)$$

From equations (8) and (9)

$$\tau_1 = G_M \gamma_1 \quad (20)$$

$$\tau_2 = \eta_M * \frac{d}{dt}\gamma_2 \quad (21)$$

Taking the time derivative of (20) and rearranging

$$\frac{d}{dt} \gamma_1 = \frac{d}{dt} \tau_M / G_M \quad (22)$$

Inserting (22) and (21) into (19) yields

$$\frac{d}{dt} \gamma_M = \frac{d}{dt} \tau_M / G_M + \frac{d}{dt} \gamma_2 \quad (23)$$

Solving the differential equation in equation (23) with a constant stress of τ_0 and $t = 0$ yields the equation for shear strain for the creep portion of a creep test ($0 < t < t_1$)

$$\gamma_M = \frac{\tau_0}{G_M} + \frac{\tau_M}{\eta_M} * t \quad (24)$$

If the stress is removed at time t_1 ($-\tau_0$ is added), the elastic strain of the spring will return to zero. The elastic strain recovery portion is

$$\frac{\tau_0}{G_M} \quad (25)$$

The strain equation for the recovery portion of the creep test ($t > t_1$)

$$\gamma_M = \frac{\tau_0}{\eta_M} * t_1 \quad (26)$$

Burger's Model

Burger's model is made up of a Kelvin and a Maxwell model connected in series.

The two models can be simply added together to obtain the time strain response to a constant stress. Since the elements are in series the stresses are the same in both elements.

The derivation of Burger's model is given below. The spring and dashpot representation of Burgers model can be seen in Figure 12.

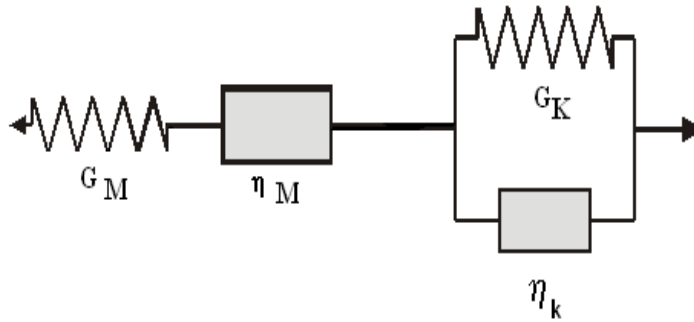


Figure 12: Spring and dashpot representation of Burger's model.

The stress in the Kelvin model and the Maxwell model are the same

$$\tau = \tau_M = \tau_K \quad (27)$$

The results for the Maxwell and Kelvin model in equations 17, 24, and 26 can be added together to obtain the Burger's equation for strain.

The Burger's model for time $0 < t < t_1$

$$\gamma(t) = \frac{\tau}{G_M} + \frac{\tau}{\eta_M} * t + \frac{\tau}{G_M} * \left(1 - \exp \left(-G_K * \frac{t}{\eta_K} \right) \right) \quad (28)$$

The Burger's model for time $t > t_1$

$$\gamma(t) = \frac{\tau}{\eta_M} * t_1 - \frac{\tau}{G_K} \left(1 - \exp \left(-G_K * \frac{t-t_1}{\eta_K} \right) \right) \quad (29)$$

METHODS

Biofilm Growth

The two species of biofilms, the *FRD1* strain of *Pseudomonas aeruginosa* and the *Staphylococcus epidermidis*, ATCC strain #35984, were grown using the colony biofilm method. An overnight culture, using tryptic -soy broth (TSB) as the growth media, was diluted to an absorbance of 0.05 using a spectrophotometer emitting light at 600 angstroms. Polycarbonate filter membranes were used as the substratum on which to grow the biofilm. The membranes are 25 mm in diameter and have 0.22 micron pore size. They were disinfected by exposing each side of the membrane to ultraviolet light for ten minutes. Sterilized membranes were placed onto a tryptic -soy agar plate. A volume of 0.3 ml of the diluted overnight culture was then pipetted onto each of the filter membranes. Care was taken to evenly spread the fluid over the entire area of the

membrane without spilling the inoculum over the edge of the membrane. The inoculated membranes were then allowed to grow in an incubator at 37 degrees Celsius for 24 hours before testing. Figure 13 shows an agar plate with four membranes covered with an approximately 160 μ m thick layer of *FRD1* biofilm.

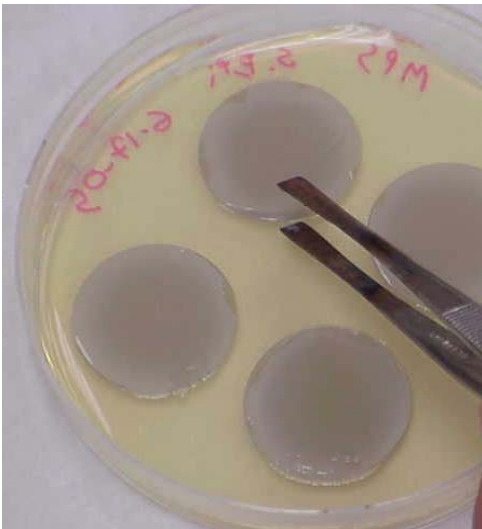


Figure 13: Biofilm covered membranes on a TSA agar plate.

Sample Preparation

Several control membranes were tested for every set of test samples. Control membranes were given no treatment before being tested. The treated test samples were prepared by pipetting 0.47 ml of the desired treatment onto a 25 mm filter pad. The treated biofilm membranes were taken from the agar plate, placed on top of the filter pad and allowed to soak for one hour prior to testing. Table 4 displays all the treatments and concentrations tested for each species of biofilm.

Table 4: All treatments and concentrations for each species of biofilm.		
Bacteria	Test	Concentration
<i>P. aeruginosa</i>	Untreated	No Treatment
<i>P. aeruginosa</i>	AlCl ₃	.2 M
<i>P. aeruginosa</i>	AlCl ₃	.02 M
<i>P. aeruginosa</i>	CaCl ₂	.2 M
<i>P. aeruginosa</i>	EDTA	.2 M
<i>P. aeruginosa</i>	FeCl ₂	.2 M
<i>P. aeruginosa</i>	FeCl ₂	.02 M
<i>P. aeruginosa</i>	Ciprofloxacin	1 µg/ ml
<i>P. aeruginosa</i>	FeCl ₃	.2 M
<i>P. aeruginosa</i>	FeCl ₃	.02 M
<i>P. aeruginosa</i>	Chlorine	50 mg/l
<i>P. aeruginosa</i>	Glutaraldehyde	50 mg/l
<i>P. aeruginosa</i>	MgCl ₂	.2 M
<i>P. aeruginosa</i>	NaCl	.2 M
<i>P. aeruginosa</i>	Barquat	50 g/ml
<i>P. aeruginosa</i>	Urea	.2 M
<i>S. epidermidis</i>	CaCl ₂	.2 M
<i>S. epidermidis</i>	EDTA	0.2 M
<i>S. epidermidis</i>	Glutaraldehyde	50 mg/l
<i>S. epidermidis</i>	Barquat	50 mg/l
<i>S. epidermidis</i>	NaCl	.2 M
<i>S. epidermidis</i>	Rifampin	.1 µg/ ml
<i>S. epidermidis</i>	FeCl ₃	.2M
<i>S. epidermidis</i>	Urea	.2 M
<i>S. epidermidis</i>	Untreated	No Treatment

Rheology

Rheology is defined as a science dealing with the deformation and flow of matter (Webster's). The true interest in rheology is how matter deforms and flows under applied stresses. Rheology deals mostly with substances like tar, toothpaste, putty, slurries, substances that behave as solids if a small shearing stress is applied, but flow like a fluid once some critical stress is reached. Normal Newtonian fluids such as water and oil are covered by classical fluid mechanics (Munson, 2002).

Test Apparatus

A TA Instruments AR1000 rheometer was used for all rheological testing (Figure 14).



Figure 14: TA Instruments AR1000 rheometer used to perform creep tests.

The AR1000 is a disk type rheometer in which a sample is placed between a base plate and a cylindrical head that can be lowered into position for testing.

A 25 mm aluminum plate geometry was used in all tests. Aluminum was chosen over steel for the plate geometry because aluminum is less dense and experiences less inertial effects. The use of a rheometer allows for the applied shear stress and shear strains to be more accurately measured.

The disadvantage of the circular disks used for rotating disk rheometer tests is that the shear rate is not constant across the area of the geometry. This makes calculation of shear rates difficult. However, the advent of computers has made it possible to overcome this problem. Computers linked to the rheometer can numerically calculate shear strain rates, shear stress, and shear strain from applied torque. This makes it possible to run creep tests and form a one-dimensional mechanical model from shear strain (γ) and shear stress (τ) (Towler et al., 2003).

The biofilm membranes needed to be positioned directly in the center of the base plate in order for the plate geometry to completely cover the biofilm sample. Complete coverage was important because the computer being used to conduct the calculations based the calculations on the full surface area of the top plate geometry. If parts of the membrane were not covered then error was introduced into the testing results. A jig was created to assist in membrane placement; it can be seen in Figure 15. A humidification chamber was created to help keep the sample moist while testing was carried out. A picture of the humidification chamber can be seen in Figure 16.



Figure 16: Jig created to position membranes in the center of the rheometer base plate.

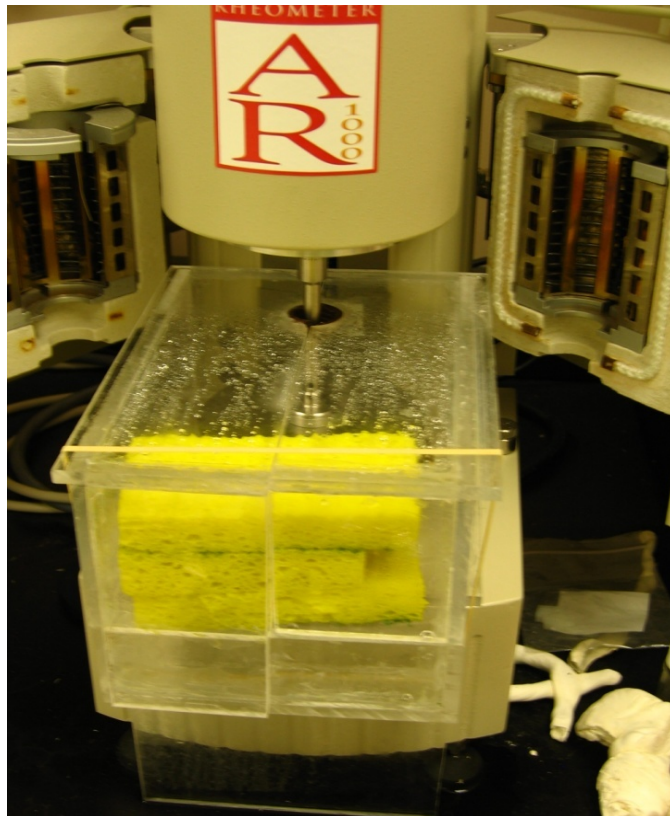


Figure 15: Picture of humidification chamber.

Creep Testing

Creep tests were conducted on the rheometer to determine mechanical properties of the biofilm. Creep tests are composed of two discrete parts, creep and recovery. In the creep portion of the test a constant shear stress is applied and the resulting strain is recorded over a given time span. After a predetermined time, the load from the creep portion was removed and the test specimen was allowed to recover (unload). Immediately after the load was removed a reverse elastic strain occurred, followed by decreasing strain over time. Figure 17 show the shear stress loading schematic (top) and the resulting shear strain with respect to time (bottom).

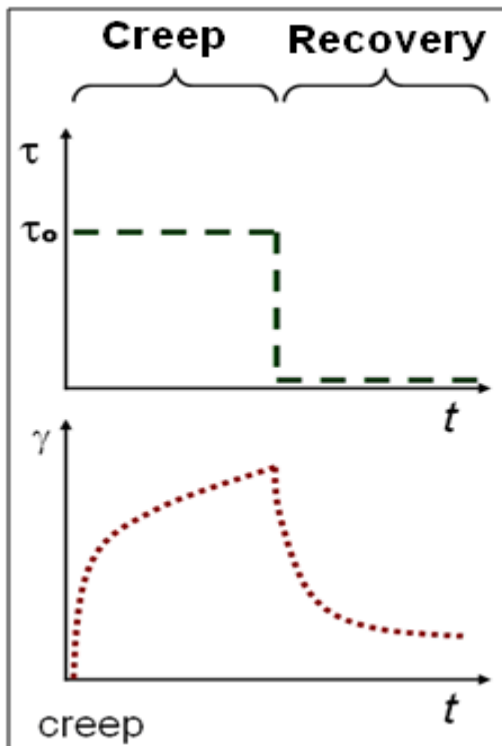


Figure 17: Schematic of loading rate and resulting strain in a creep test.

The linear elastic region for the test specimen was used in determining the loading criteria for the creep tests. For these tests, a 5 minute creep period (loading) and a five minute recovery (unloading) phase was run. Approximately 970 data points were taken during a 10 minute test.

Gap Setting

The gap is the distance between the aluminum top plate geometry and the base plate. Setting the gap was a very important consideration in the testing methods. If the gap was set too close, the sample would be overly compressed. Over-compression of the biofilm was not desirable because the mechanical properties of the biofilm would likely be changed due to the increased density caused by the compression. Also, additional stresses would be imparted on the biofilm, which would have an effect on the results of the test. The converse was also true, as setting the gap without properly contacting the full surface of the biofilm would lead to misleading test results, and it would overstate the actual shear strain. Biofilms do not generally form a smooth, even surface; they typically grow non-uniformly with peaks, valleys, flow channels and much heterogeneity. Consistency in loading the samples was important to help reduce variability in test results. A method was needed to set the gap consistently between tests. The two sections below describe the technique used to determine the gap setting method for the *FRDI* and *S. epidermidis* biofilms.

FRD1

A series of data points were created by lowering the rheometer head by 5 microns and recording the normal force registered by the rheometer's load cell; the normal force was allowed to dissipate back to zero, then the head was lowered another 5 microns and the process was repeated until it was clear that complete coverage of the rheometer head plate against the top surface of the biofilm was achieved. The chart shown in Figure 18 shows the loading result from one test on the *FRD1* biofilm.

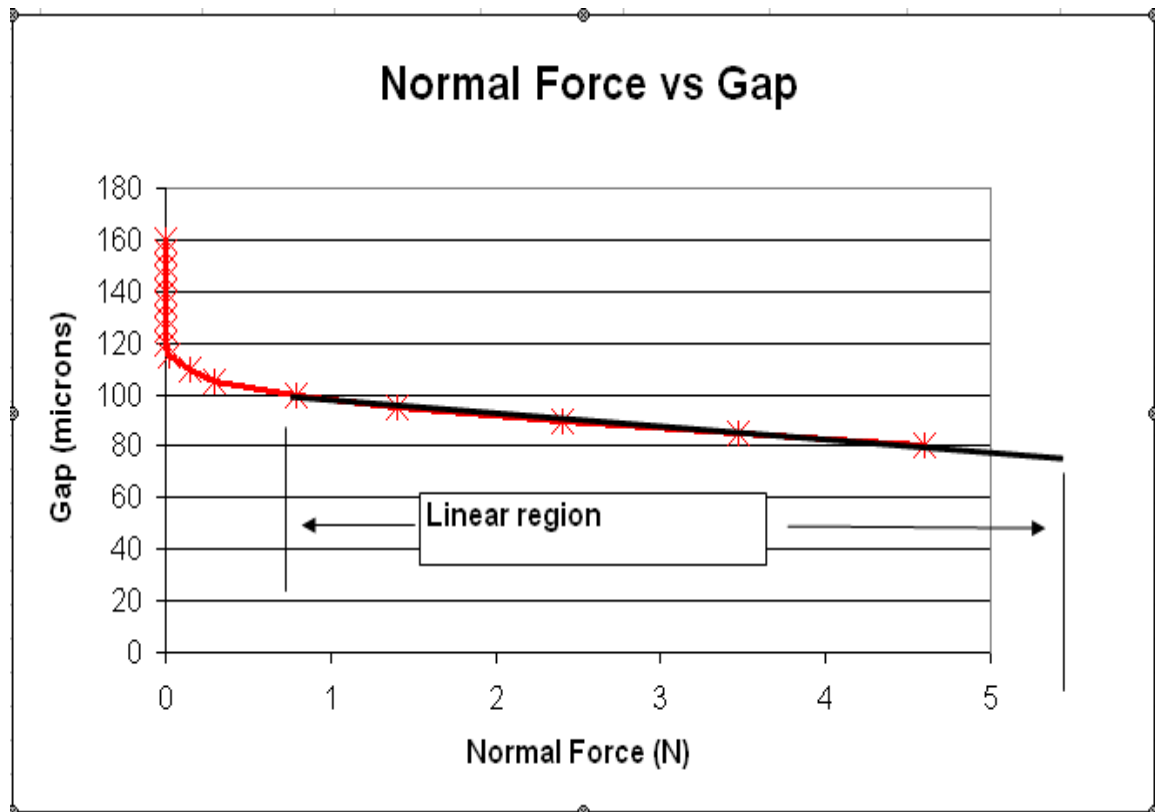


Figure 18: Chart showing the resulting normal force on the rheometer base plate caused by lowering the rheometer head 5 microns on an *FRD1* biofilm. The linear region representing full membrane coverage can be seen after a normal force just lower than 1 N.

It is obvious that at approximately a 1 N normal force the loading rate becomes linear. This is likely due to complete biofilm contact with the upper geometry plate. Up to

the 1 N force there was incomplete plate coverage. From these tests, the method for setting the gap was established. It was determined that the best method was to set the gap by lowering the head 5 microns at a time, waiting for the normal force to return to zero before lowering again. The correct gap was set once a 5 micron lowering resulted in a normal force between 1-1.5 N.

S. epidermidis

The same testing method for determining the gap for the *FRD1* biofilm was used to determine the appropriate gap for the *S. epidermidis* biofilm. Figure 19 shows a chart of the normal force verse gap curve for *S. epidermidis*. The linear region was reached at approximately 0.4 N. A normal force between 0.4- 0.9 N resulting from a lowering of the rheometer head 5 μm was the method established for setting the gap for *S. epidermidis* biofilm.

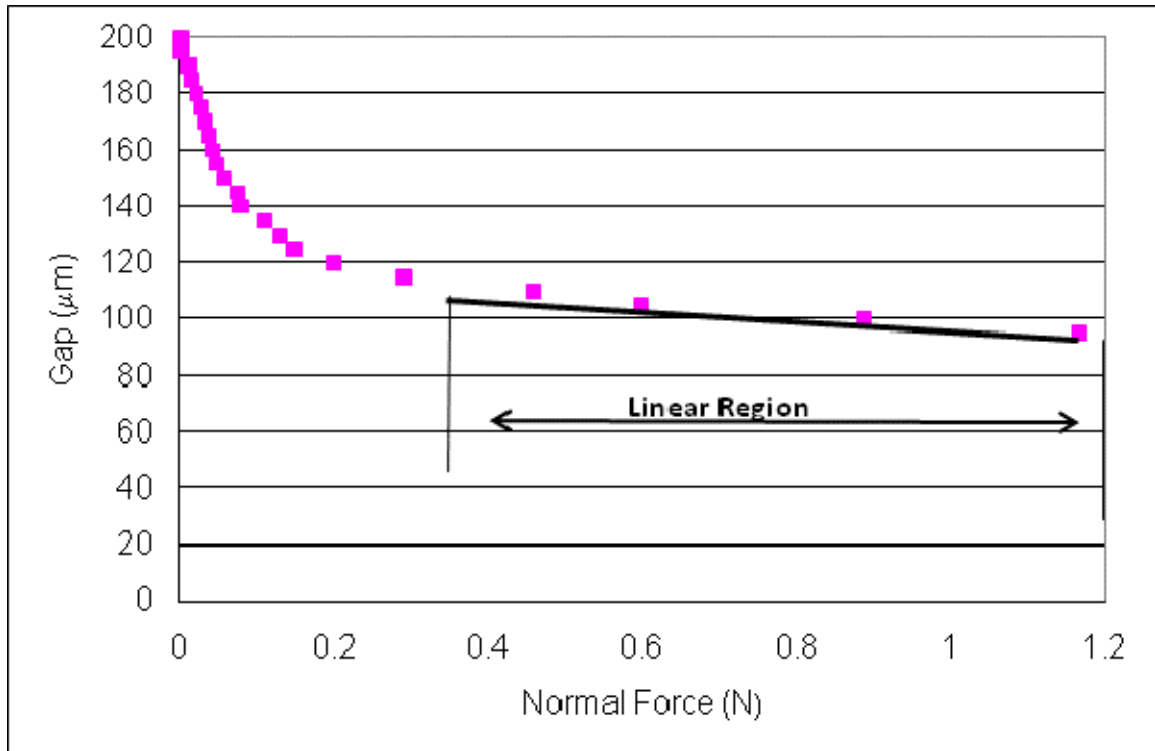


Figure 19: Chart showing the resulting normal force on the rheometer base plate caused by lowering the rheometer head 5 microns on an *S. epidermidis* biofilm. The linear region representing full membrane coverage can be seen after a normal force just lower than 1 N.

Determining Linearity

In order to apply linear modeling techniques developed for the application of the Burger model, testing had to be performed in the linear-elastic stress-strain regime. The sections below describe how the appropriate shear stress for testing in the linear region was determined for the *FRDI* and the *S. epidermidis* biofilms.

FRDI

A series of creep tests were run to determine the linear region of the untreated *FRDI* biofilm. A series of tests were run at different shear stresses between 10 Pa and 30 Pa. Compliance is the strain divided by the stress; it is a measure of stiffness. When the

stress is changed from one test to another, the change in strain should be proportional if the material is linear or in a linear region. Therefore the compliance of the tests should be the same for all tests if the material is linear. Figure 20 shows a chart of the average maximum compliance values recorded from these linearity tests. Several creep tests were run for each shear stress tested in the linearity evaluation. Table 5 shows the specific values of stress and strain during linearity evaluation. It is clear that at a shear stress from 20 to 25 Pa there is a notable jump in the average maximum compliance. This jump indicates that at about 25 Pa the untreated biofilm leaves the linear region, so linear modeling methods should not be used at any stress above 20 Pa. Considering these series of tests, a constant shear stress of 15 Pa was determined to be the optimal shear stress to run the creep tests on the treated samples, since enough strain was created to create a notable difference when the biofilm was stiffened and hopefully not too much strain so when the film was weakened the change in properties was measurable. This stress was also well within the determined linear stress region.

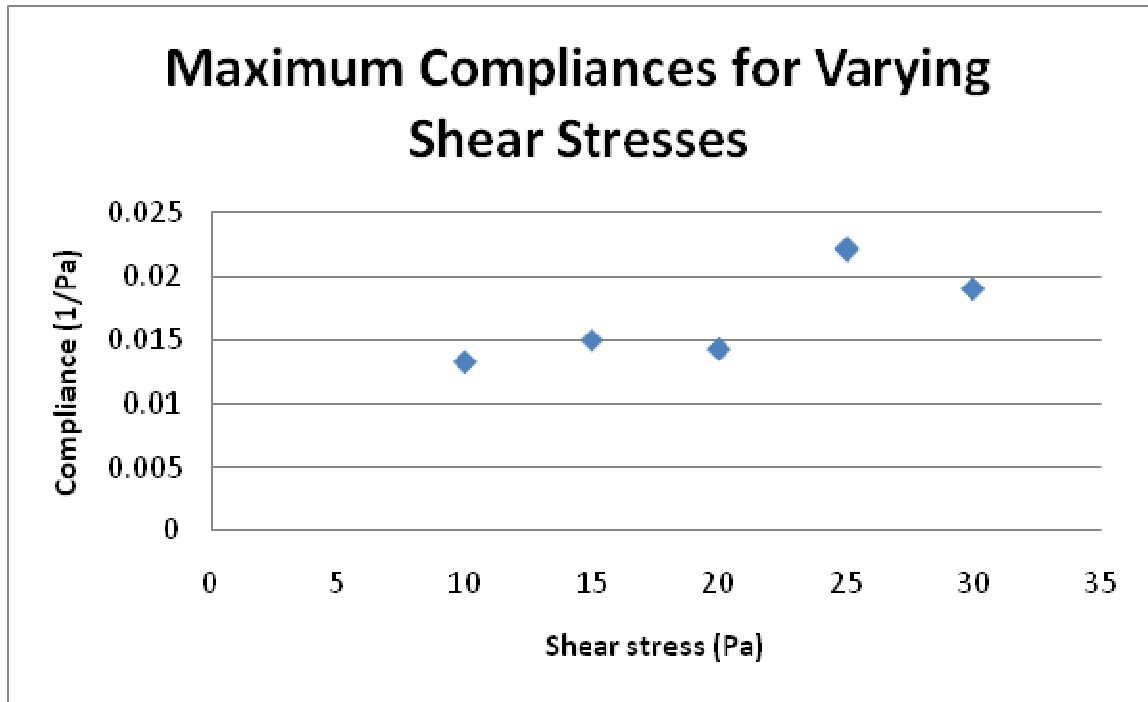


Figure 20: Chart showing average maximum compliance values for FRD1 colony biofilm from a series of creep tests run at varying shear stresses. A notable jump in compliance can be seen between 20 and 25 Pa.

Table 5: *FRD1* linearity testing results.

Applied Stress (Pa)	5	10	15	20	25	30
Avg. Max Strain	0.078	0.152	0.225	0.319	0.554	0.529
Avg. Compliance	0.016	0.015	0.015	0.016	0.022	0.018
# of tests	4	9	41	10	18	22

S. epidermidis

Determining the linear elastic region for *S. epidermidis* was performed in a different manner than for *FRDI*. *S. epidermidis* biofilm is a much stronger material than *FRDI* biofilm. Creep tests performed at 15 Pa with the *S. epidermidis* samples (as was run on *FRDI* biofilms) resulted in almost no noticeable strain. A series of creep tests were run with increasing shear stress values. A 100 Pa shear stress resulted in an average maximum shear strain of about 0.023, this strain value was large enough that a change in strain from different treatments would be noticeable. There was some concern that increasing the shear stress value much higher might result in slippage at the membrane-base plate interface. Therefore the testing at a shear stress of 100 Pa was chosen. This value was surely in the linear elastic region since this stress level is just large enough to create a notable shear strain.

Parameter Estimation

Assuming the biofilm tested in the creep experiments responded in a nearly linear-viscoelastic manner, the four material coefficients from the Burger's model equations (28, 29) can be numerically optimized to fit the data. Non-linear regression techniques would be the preferred method for optimizing the four material coefficients; however, the nature of creep tests makes gradient methods impossible. The applied shear stress during creep testing experiences a step change that occurs between the loading and unloading phases of the test. The step change in applied shear stress causes a discontinuity in the derivatives of the equations describing material behavior. The discontinuity of the derivatives prohibits many analytical methods that employ calculus based optimization techniques (Towler, 2004).

A regression method using the Microsoft Excel solver was created to optimize the material coefficients of the Burger's model. Time and shear strain data from the creep test experiments were placed into the Excel template. The template works by minimizing the error between the strain from the creep tests and the calculated strain values created from two equations for the loading and unloading portion of the Burger's model (equations: 28 & 29). The sampling rates from the creep tests were not consistent and varied from every 0.0016 seconds to 6.5 seconds. The variation in the sampling rates was generated by the rheological software in response to the rate of change in the strain values. When a test begins the sampling rate is at the highest frequency, at the end of a test the sampling rate is at its lowest. A weighting function in the curve fitting template was created to ensure that every point carried equal weight in the optimization of the

material coefficients. The weighting function (WT) was given by the change in time (Δt) between data points, divided by total test time ($\Sigma \Delta t$).

$$WT = \Delta t / \Sigma \Delta t$$

The error function (ERR), used to optimize the material coefficients, was calculated by computing the absolute value of the difference between the strain from the experimental data and the strain calculated from the Burger's equations. The resulting value was then multiplied by the weighting function. Because the Δt values can be quite small and the difference between the experimental data points and the Burger's equations data points can be very small, the error function was multiplied by one million to overcome numerical limitations in the software. Most numerical software has tolerance limits typically around 10^{-7} ; multiplying by one million increases the magnitude of the error function overcoming this limitation, resulting in more accurate regression values.

$$ERR = \text{ABS}(\text{Test Strain} - \text{Burger Strain}) * WT * 10^6$$

The function used to optimize material coefficients (OPT), sums and squares the error function.

$$OPT = \Sigma (ERR^2)$$

A solver routine was then used to minimize the value of the OPT function by changing the values of the four material coefficients. The excel solver uses a quasi-Newtonian method (Excel Help). The problem with a Newtonian method in solving a non-linear problem was that when the solver reaches a local minimum it stops. However, "bumping" the solver past a local minimum allows the solver to iterate to a better fit until another minimum was reached. Arriving at the best fit values for the 4 Burger

coefficients required multiple runs of the solver varying the material coefficient or coefficients being solved. A Visual Basic macro was created to automate the process, the macro routine rotated through the four Burger parameters optimizing with respect to one parameter at a time, then the solver solved globally for all four parameter. This process was then repeated multiple times until the global minimum was reached. The macro routine is displayed in the Appendix.

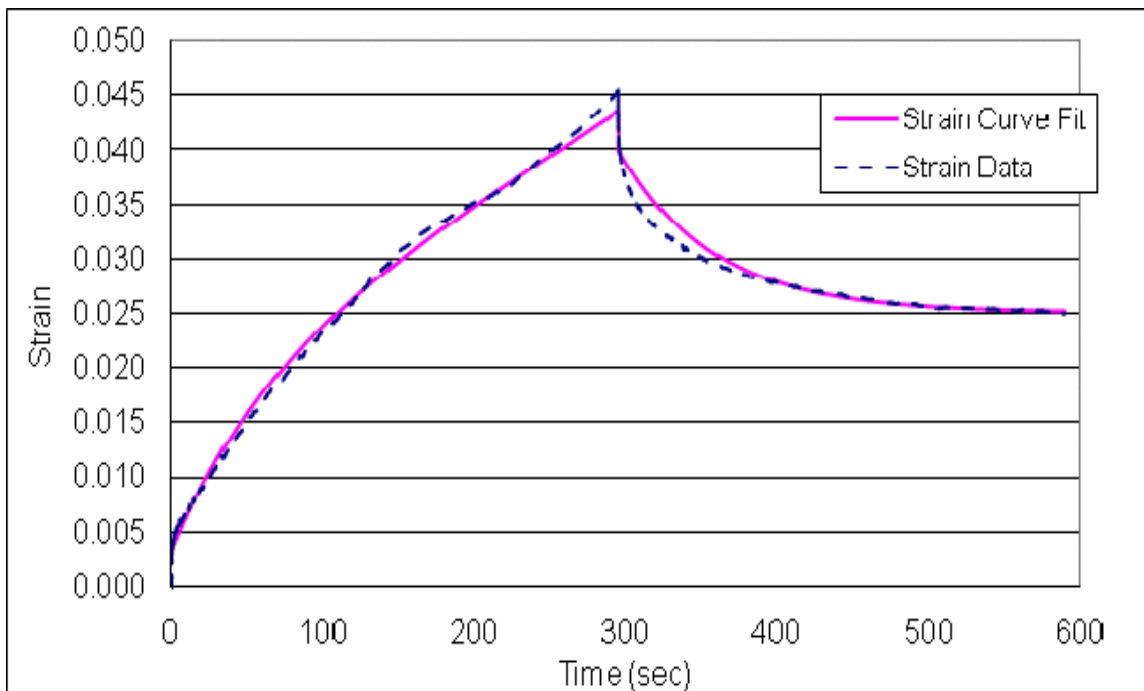


Figure 21: Chart showing the curve fitting of test data (dash) using Burger's model (solid).

Higher strain values from creep tests result in higher error values in the curve fitting routine. In order to relate the error in curve fitting between high strain tests to low strain tests the total error from the tests needed to be normalized (WGTErr). The 10^6 multiplier in the ERR function used to increase accuracy in curve fitting was removed; to

normalize the error function, the ERR function was then divided by the maximum strain experienced ($\text{Max}(\gamma)$) in the creep test.

$$\text{WGERR} = \text{ERR} / (10^6 * \text{Max}(\gamma))$$

The sum of the WGERR function gives a value that indicated the quality of the curve fit. Higher values indicate a lower quality curve fit.

Statistical Analysis

Once the curve fitting was completed, statistical analysis was needed to determine if the treatments resulted in statistical changes to the fitted material properties. Two variable t-tests were used to assess whether the means of the treatment and the control test groups were *statistically* different from each other. The formula for the t-test is shown below. Variance (var) is the square of the standard deviation and \bar{X} is the mean for a test, the subscript T refers to the treatment and C refers to the control, n is the number of tests in either the treatment or control test groups (Devore and Farnum, 1999).

$$t = \frac{\bar{X}_T - \bar{X}_C}{\sqrt{\frac{\text{var}_T}{n_T} + \frac{\text{var}_C}{n_C}}}$$

Once a t-value is computed the significance value (alpha or p-value) can be determined using a table of significance. A p-value of 0.05 or less is typically used by statisticians in determining whether or not the difference between means is statistically significant; smaller p-values indicate a stronger probability that there is a statistical difference between the means.

In order for a t-test to be used, the data needs to be approximately normally distributed. A normally distributed group closely resembles a bell shaped distribution curve (Devore and Farnum, 1999). In general, the curve fit coefficients for the data were not normally distributed. The mean of the treatment groups is skewed towards the outlying values; as a consequence the median value is much more representative for an expected value. A chart showing the range of values for the G_1 coefficient of the sodium chloride treatment group can be seen in Figure 22. This type of distribution is common for Burger's coefficient distributions in all of the treatment groups. The corresponding histogram of the data is shown in Figure 23, where this data is clearly seen to not be normally distributed.

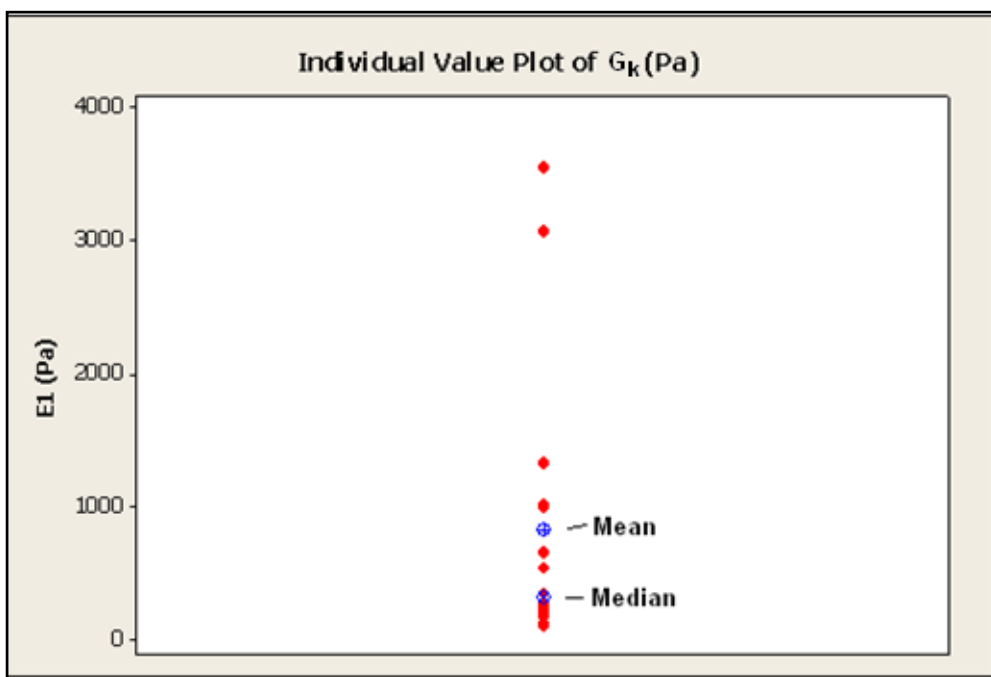


Figure 22: Distribution of values for the G_k coefficient from the sodium chloride treatment group.

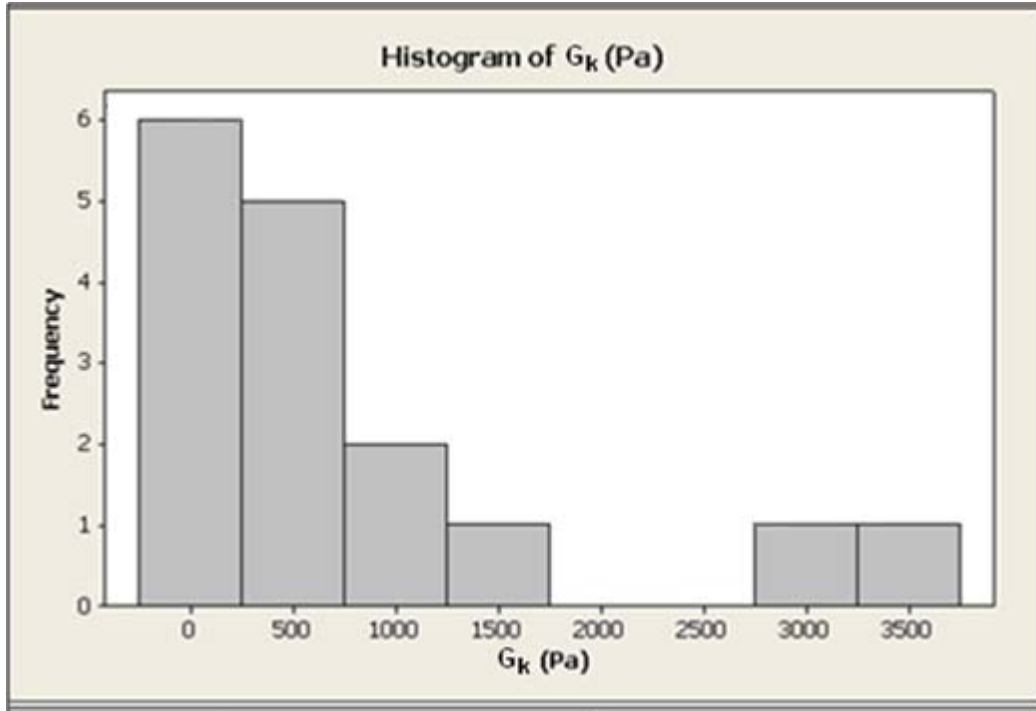


Figure 23: Histogram of data for the G_k coefficients from the sodium chloride treatment group.

Taking the logarithm of the data with this kind of skewness often yields a normally distributed data set. Figure 24 shows the same data set as Figure 22, but on a logarithmic scale. A histogram of the logarithmic data in Figure 25 shows a closer to normal bell curve distribution.

Statistical analysis of the four Burger coefficients and maximum strain values was performed on the logarithmically transformed data sets in order to overcome the problem of normal distributions. Minitab® statistical software was used to perform all two-variable t-tests.

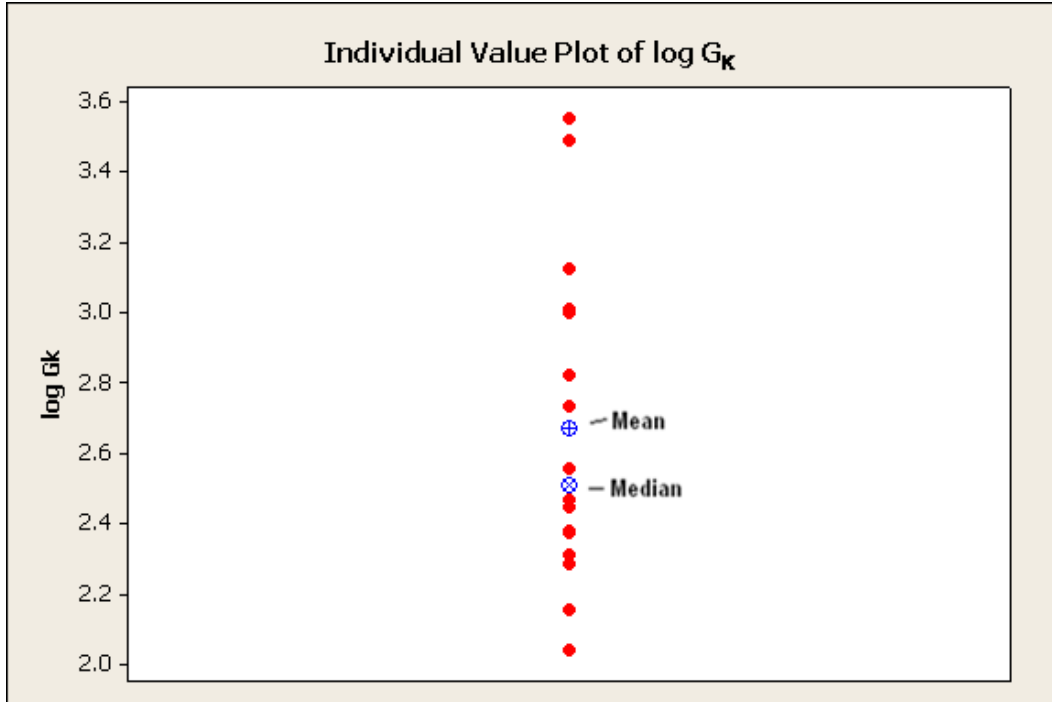


Figure 24: Distribution of values for the $\log G_K$ coefficient from the sodium chloride treatment group.

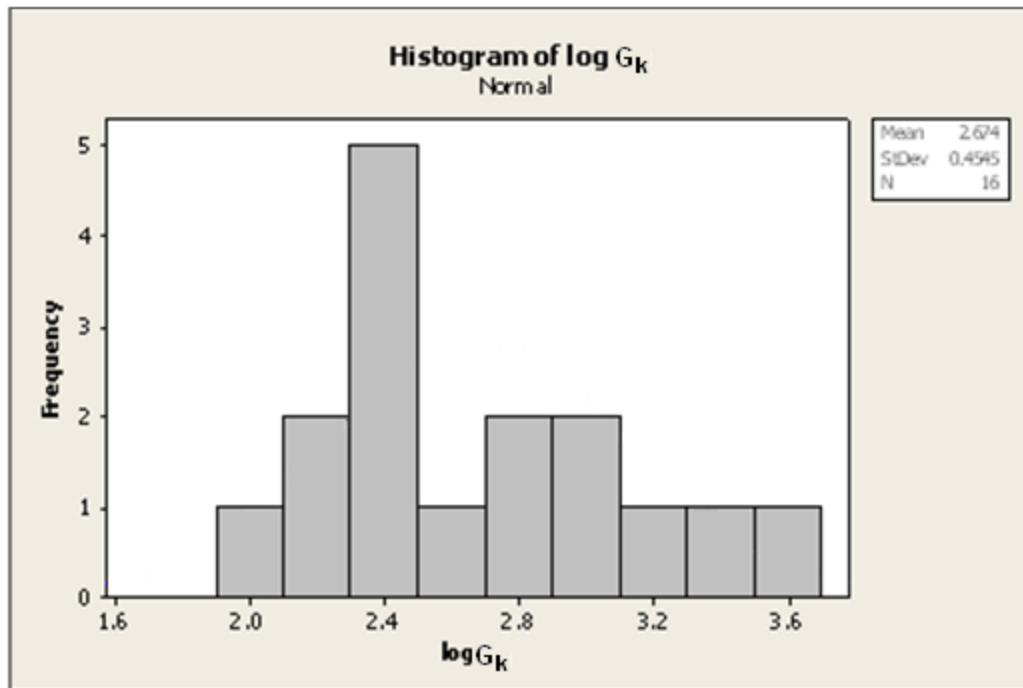


Figure 25: Histogram of logarithmic G_K data set from the sodium chloride treatment group.

RESULTS

The results of all rheological tests are displayed in the tables below. The arithmetic mean, median, and standard deviation, and logarithmic transformed mean of each of the four Burger parameters are given. Statistical analysis between the logarithmically transformed treatments and their controls were performed for all four Burger coefficients and the maximum strain. The ratios between the treatments are given and the confidence value (p value) for the ratio is also displayed. Statistical analysis of the gap setting was performed using the arithmetic mean values. If the ratio between tests was statically significant ($p < 0.05$) then the ratio between control and treatment value is displayed in a **bolded** font. The numbers of tests for each treatment and the number of controls are displayed in the upper left corner. Tables of individual test results are displayed in the appendix.

Controls

The difference in material properties between the *FRDI* and *S. epidermidis* biofilm are quite remarkable. Table 31 shows the ratio of the four Burger coefficients between the two biofilm species. *S. epidermidis* coefficients are 8- 97 times higher than the *FRDI* coefficients. *S. epidermidis* is a much stiffer biofilm than *FRDI*.

Table 6: Results for untreated *FRDI*.

# of TRTMENTS	G_K (Pa)	η_K (Pa.s)	η_M (Pa.s)	G_M (Pa)	Max γ	WGT ERR	Gap (μm)
153							
Arithmetic Mean	1024	38915	97445	3024	0.2869	0.0204	129
Standard Deviation	1805	79846	141281	5083	0.3121	0.0081	33
Median	312	8637	33965	804	0.1895	0.0191	135
Logarithmic Mean	432	11158	39749	1137	0.1570	-	-

Table 7: Results for untreated *S. epidermidis*.

# of TRTMENTS	G_K (Pa)	η_K (Pa.s)	η_M (Pa.s)	G_M (Pa)	Max γ	WGT ERR	Gap (μm)
34							
Arithmetic Mean	33120	946798	4616745	11463	0.0234	0.0231	82
Standard Deviation	27592	659017	2719188	6683	0.0151	0.0118	15
Median	25873	854288	3774165	9638	0.0209	0.0208	83
Logarithmic Mean	27683	773385	3885109	9988	0.0204	-	-

Table 8: Ratio between *S. epidermidis* and *FRDI* for the four Burger coefficients.

	G_K (Pa)	η_K (Pa.s)	η_M (Pa.s)	G_M (Pa)
Ratio between <i>S. epi.</i> and <i>FRDI</i>	64	69	98	8.8

Cations

All multivalent cation treatments tested on the *FRDI* biofilm resulted in a stiffer biofilm. Visible physical changes occurred to the biofilm during treatment. Figure 26 shows a *FRDI* biofilm before and after a 0.2 M treatment with FeCl_2 . The biofilm becomes dimpled and physically becomes stiffer. The dimpling effect was most pronounced for the iron treatments and the aluminum. Dimpling still occurred to a lesser extent in the other divalent cations *FRDI* treatments (magnesium and calcium), no

dimpling was experienced for sodium, which was the only monovalent cation treatment.

No visible changes occurred to the *S. epidermidis* biofilm from cation treatments.

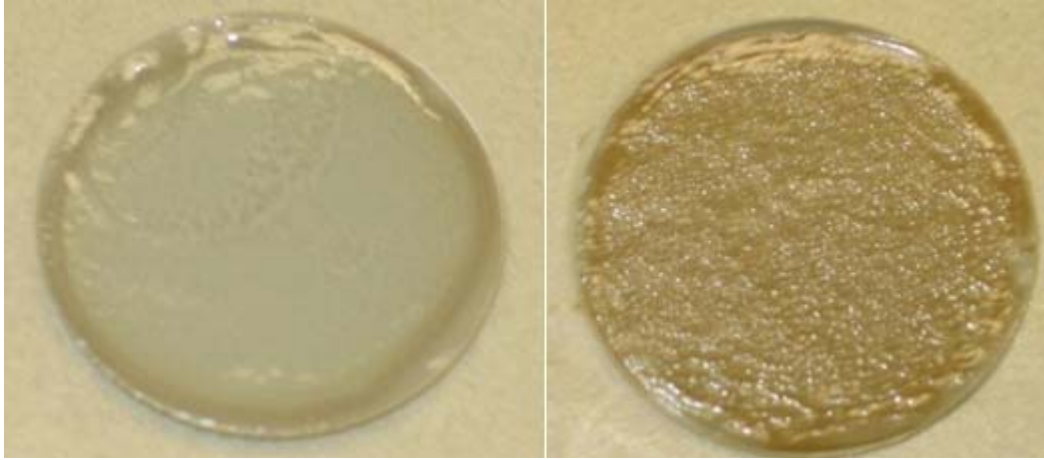


Figure 26: FRDI biofilm before treatment (left) and the same biofilm after one hour with a 0.2 M FeCl_2 treatment (right).

Table 9: Results for *FRDI* tested with 0.2 molar concentration of aluminum chloride.

# of TRTMENTS	# of CNTRLS				G_M (Pa)	$\text{Max } \gamma$	WGT ERR	Gap (μm)
23	16	G_K (Pa)	η_K (Pa.s)	η_M (Pa.s)				
Arithmetic Mean		2531	96523	1557896	3779	0.039	0.0274	110.67
Standard Deviation		2928	147014	3899879	2738	0.031	0.0117	19.55
Median		1426	48159	381378	3159	0.028	0.0238	112.50
Logarithmic Mean		1529	47980	419223	2911	0.027	-	-
Ratio between control and treatment		4.436	6.209	11.614	3.802	0.156	-	0.880
p value		$<10^{-3}$	$<10^{-3}$	$<10^{-3}$	$<10^{-3}$	$<10^{-3}$	-	0.025

The 0.2 M aluminum treatment significantly stiffened the *FRDI* biofilm. The thickness of the biofilm was also significantly reduced according to the gap setting.

Table 10: Results for *FRDI* tested with 0.02 molar concentration of aluminum chloride.

# of TRTMENTS	# of CNTRLS							
14	8	G_K (Pa)	η_K (Pa.s)	η_M (Pa.s)	G_M (Pa)	Max γ	WGT ERR	Gap (μm)
Arithmetic Mean		2156	46797	265334	2447	0.116	0.0232	91.79
Standard Deviation		2708	54852	323580	2315	0.133	0.0091	19.47
Median		1036	29363	133453	1455	0.055	0.0211	95.00
Logarithmic Mean		1058	21690	134076	1249	0.0606	-	-
Ratio between control and treatment		4.009	3.342	4.539	1.683	0.284	-	1.020
p value		0.006	0.038	0.012	0.285	0.019	-	0.91

The 0.02 M concentration of aluminum chloride resulted in less stiffening of the *FRDI* biofilm than the 0.2 M treatment.

Table 11: Results for *FRDI* tested with 0.2 molar concentration of ferric chloride.

# of TRTMENTS	# of CNTRLS							
15	12	G_K (Pa)	η_K (Pa.s)	η_M (Pa.s)	G_M (Pa)	Max γ	WGT ERR	Gap (μm)
Arithmetic Mean		11371	352209	2323075	14773	0.006	0.0376	112.47
Standard Deviation		4290	203958	1419585	21375	0.003	0.0181	17.17
Median		11523	331342	2064251	8991	0.005	0.0335	110.00
Logarithmic Mean		10513	175637	1971295	9931	0.0058	-	-
Ratio between control and treatment		13.49	24.210	28.774	4.932	0.065	-	0.928
p value		$<10^{-3}$	0.002	$<10^{-3}$	0.002	$<10^{-3}$	-	0.332

The 0.2 M ferric iron treatment stiffened the *FRDI* biofilm more than any other treatment.

Table 12: Results for *FRDI* tested with 0.02 molar concentration of ferric chloride.

# of TRTMENTS	# of CNTRLS							
22	12	G_K (Pa)	η_K (Pa.s)	η_M (Pa.s)	G_M (Pa)	Max γ	WGT ERR	Gap (μm)
Arithmetic Mean		2481	62832	361454	3118	0.057	0.0334	95.27
Standard Deviation		2467	110323	405550	3014	0.063	0.0116	29.62
Median		1525	23363	179871	1737	0.039	0.0311	90.00
Logarithmic Mean		1553	20490	216483	1937	0.0357	-	-
Ratio between control and treatment		4.943	3.141	7.015	2.265	0.182	-	0.959
p value		$<10^{-3}$	0.031	$<10^{-3}$	0.01	$<10^{-3}$	-	0.689

The 0.02 M concentration of Ferric chloride resulted in less stiffening of the *FRDI* biofilm than the 0.2 M treatment.

Table 13: Results for *FRDI* tested with 0.2 molar concentration of magnesium chloride.

# of TRTMENTS	# of CNTRLS							
18	8	G_K (Pa)	η_K (Pa.s)	η_M (Pa.s)	G_M (Pa)	Max γ	WGT ERR	Gap (μm)
Arithmetic Mean		1034	26814	144270	3536	0.079	0.0215	86.67
Standard Deviation		766	19092	98263	2184	0.063	0.0073	11.38
Median		946	18822	125299	3305	0.057	0.0207	87.50
Logarithmic Mean		802	21040	112521	2797	0.0603	-	-
Ratio between control and treatment		2.143	1.820	2.234	1.849	0.456	-	0.738
p value		0.026	0.107	0.037	0.078	0.03	-	0.001

The magnesium chloride treatment significantly stiffened the *FRDI* biofilm. It stiffened the biofilm less than calcium chloride, the other divalent cation treatment. This treatment also significantly reduced the thickness of the biofilm.

Table 14: Results for *FRDI* tested with 0.2 molar concentration of calcium chloride.

# of TRTMENTS	# of CNTRLS	G_K (Pa)	η_K (Pa.s)	η_M (Pa.s)	G_M (Pa)	Max γ	WGT ERR	Gap (μm)
18	11							
Arithmetic Mean		1735	47978	335931	2539	0.0528	0.0262	110.50
Standard Deviation		1327	38213	311169	3054	0.044	0.0080	11.42
Median		1588	36647	225307	1282	0.0437	0.0259	111.00
Logarithmic Mean		1419	33954	231117	1412	0.0410	-	-
Ratio between control and treatment		8.128	7.727	15.812	2.188	0.100	-	0.704
p value		$<10^{-3}$	0.003	$<10^{-3}$	0.122	$<10^{-3}$	-	0

The calcium chloride treatment significantly stiffened the *FRDI* biofilm. It stiffened the biofilm the most of the two divalent cation treatments. It also significantly reduced the thickness of the biofilm.

Table 15: Results for *FRDI* tested with 0.2 molar concentration of ferrous chloride.

# of TRTMENTS	# of CNTRLS	G_K (Pa)	η_K (Pa.s)	η_M (Pa.s)	G_M (Pa)	Max γ	WGT ERR	Gap (μm)
20	9							
Arithmetic Mean		4072	214545	793802	4817	0.026	0.0257	98.00
Standard Deviation		3075	216595	1027497	4539	0.024	0.0151	9.65
Median		2732	150897	459618	3896	0.022	0.0209	95.00
Logarithmic Mean		3054	141406	503883	3230	0.0183	-	-
Ratio between control and treatment		6.368	7.551	12.882	7.709	0.111	-	0.828
p value		0	0	0	0	0	-	0

The 0.2 M ferrous chloride treatment significantly stiffened the *FRDI* biofilm. It stiffened the biofilm the second most of all cation treatments, and it also reduced the thickness of the biofilm.

Table 16: Results for *FRDI* tested with 0.02 molar concentration of ferrous chloride.

# of TRTMENTS	# of CNTRLS							
11	6	G_K (Pa)	η_K (Pa.s)	η_M (Pa.s)	G_M (Pa)	Max γ	WGT ERR	Gap (μm)
Arithmetic Mean		1203	37434	169268	2173	0.074	0.0292	72.58
Standard Deviation		1030	35315	145013	2192	0.099	0.0145	30.64
Median		911	23081	129125	1352	0.049	0.0312	95.00
Logarithmic Mean		967	30289	136329	1326	0.0525	-	-
Ratio between control and treatment		2.113	3.631	2.897	1.671	0.387	-	1.055
p value		0.171	0.013	0.055	0.304	0.081	-	0.813

The 0.02 M concentration of ferrous chloride resulted in less stiffening of the *FRDI* biofilm than the 0.2 M treatment, but still significantly stiffened the biofilm.

Table 17: Results for *FRDI* tested with 0.2 molar concentration of sodium chloride.

# of TRTMENTS	# of CNTRLS							
16	12	G_K (Pa)	η_K (Pa.s)	η_M (Pa.s)	G_M (Pa)	Max γ	WGT ERR	Gap (μm)
Arithmetic Mean		830	60120	121228	5044	0.227	0.0200	133.50
Standard Deviation		1038	94800	172270	6503	0.229	0.0105	20.85
Median		328	9878	30417	1542	0.195	0.0155	140.00
Logarithmic Mean		472	20477	50243	2276	0.1316	-	-
Ratio between control and treatment		1.164	1.327	0.867	1.213	1.052	-	0.959
p value		0.663	0.574	0.768	0.699	0.905	-	0.417

The sodium chloride treatment had no statistical effect on the *FRDI* biofilm.

Table 18: Results for *S. epidermidis* tested with 0.2 molar concentration of ferric chloride.

# of TRTMENTS	# of CNTRLS							
9	4	G_K (Pa)	η_K (Pa.s)	η_M (Pa.s)	G_M (Pa)	Max γ	WGT ERR	Gap (μm)
Arithmetic Mean		17,985	1,256,459	3,069,187	10,686	0.031	0.016	62
Standard Deviation		10,153	1,155,423	2,050,340	6,467	0.017	0.004	9
Median		14,196	695,903	2,318,985	9,016	0.029	0.017	60
Logarithmic Mean		16061	920701	2595647	9251	0.027	-	-
Ratio between control and treatment		0.461	1.469	0.471	0.564	1.807	-	0.990
p value		0.024	0.108	0.064	0.504	0.058	-	0.907

The ferric chloride treatment on *S. epidermidis* seems to weaken the biofilm slightly.

There is a fairly weak statistical significance. This treatment affected the *S. epidermidis* biofilm the least of all cation treatments.

Table 19: Results for *S. epidermidis* tested with 0.2 molar concentration of calcium chloride.

# of TRTMENTS	# of CNTRLS							
7	4	G_K (Pa)	η_K (Pa.s)	η_M (Pa.s)	G_M (Pa)	Max γ	WGT ERR	Gap (μm)
Arithmetic Mean		11684	213606	1381641	4656	0.125	0.0262	79.5714
Standard Deviation		10843	173169	1284555	3922	0.157	0.0088	8.7342
Median		10240	187307	1277033	4383	0.049	0.0202	77.00
Logarithmic Mean		8978	231978	950575	5967	0.0626	-	-
Ratio between control and treatment		0.357	0.124	0.248	0.401	2.924	-	0.827
p value		0.045	0.002	0.051	0.071	0.063	-	0.007

The calcium chloride treatment on *S. epidermidis* weakened the biofilm significantly.

This treatment weakened the *S. epidermidis* biofilm the second most of the three cation treatments.

Table 20: Results for *S. epidermidis* tested with 0.2 molar concentration of sodium chloride.

# of TRTMENTS	# of CNTRLS							
7	4	G_K (Pa)	η_K (Pa.s)	η_M (Pa.s)	G_M (Pa)	Max γ	WGT ERR	Gap (μm)
Arithmetic Mean		2038	151974	209898	631	0.125	0.0259	79.57
Standard Deviation		2785	258131	192571	506	0.157	0.0081	8.73
Median		1531	32124	210052	553	0.049	0.0207	77.00
Logarithmic Mean		7828	146305	827461	3401	0.0714	-	-
Ratio between control and treatment		0.372	0.566	0.250	0.256	2.924	-	0.827
p value		0.117	0.643	0.054	0.048	0.063	-	0.007

The sodium chloride treatment on the *S. epidermidis* weakened the biofilm the most of the three cation treatments tested.

Chelation

Table 21: Results for *FRDI* tested with 0.2 molar concentration of EDTA.

# of TRTMENTS	# of CNTRLS							
13	12	G_K (Pa)	η_K (Pa.s)	η_M (Pa.s)	G_M (Pa)	Max γ	WGT ERR	Gap (μm)
Arithmetic Mean		1202	78063	118574	3473	55.33	0.0262	128.66
Standard Deviation		1473	138823	162810	5529	124.70	0.0209	32.678
Median		369	8272	25761	701	1.091	0.0188	141.0
Logarithmic Mean		465	12290	7210	323	1.0759	-	-
Ratio between control and treatment		0.986	0.535	0.249	0.564	5.188	-	0.893
p value		0.238	0.713	0.903	0.653	0.457	-	0.288

There was no statistical change in material properties of the *FRDI* biofilm from the EDTA treatment.

Table 22: Results for *S. epidermidis* tested with 0.2 molar concentration of EDTA.

# of TRTMENTS	# of CNTRLS							
8	4	G_K (Pa)	η_K (Pa.s)	η_M (Pa.s)	G_M (Pa)	Max γ	WGT ERR	Gap (μm)
Arithmetic Mean		21871	1012602	3607564	11159	0.030	0.0187	73.1250
Standard Deviation		14370	634786	2357626	8477	0.017	0.0048	4.5806
Median		19561	1146605	3077172	9130	0.022	0.0179	75.0000
Logarithmic Mean		18607	745692	2980195	8997	0.0253	-	-
Ratio between control and treatment		0.780	1.035	0.583	0.904	1.297	-	0.929
p value		0.081	0.083	0.075	0.931	0.239	-	0.06

There was a statistically weak indication that the EDTA treatment slightly weakened the *S. epidermidis* biofilm

Antimicrobials

Table 23: Results for *FRDI* tested with 50 mg/l molar concentration of Barquat[®].

# of TRTMENTS	# of CNTRLS							
22	11	G_K (Pa)	η_K (Pa.s)	η_M (Pa.s)	G_M (Pa)	Max γ	WGT ERR	Gap (μm)
Arithmetic Mean		790	2661	3454	1152	6.110	0.0218	170.45
Standard Deviation		2389	996917	98535	6316	14.072	0.0181	16.68
Median		33	1296	3831	299	1.345	0.0187	165.00
Logarithmic Mean		33	6328	4090	678	1.2515	-	-
Ratio between control and treatment		0.053	0.340	0.075	0.288	11.169	-	1.205
p value		$<10^{-3}$	0.207	$<10^{-3}$	0.065	0.001	-	$<10^{-3}$

The Barquat[®] treatment significantly weakened the *FRDI* biofilm. The Barquat[®] treatment caused the biofilm to have a “watery” appearance. The treatment caused the biofilm to become significantly thicker.

Table 24: Results for *S. epidermidis* tested with 0.2 molar concentration of Barquat®.

# of TRTMENTS	# of CNTRLS	G_K (Pa)	η_K (Pa.s)	η_M (Pa.s)	G_M (Pa)	Max γ	WGT ERR	Gap (μm)
7	4							
Arithmetic Mean		3024	39400	181999	1573	11,302.9	0.0138	72.85
Standard Deviation		1952	29140	159503	580	26,373.0	0.0161	3.93
Median		2375	33617	121819	1418	0.5	0.0112	70
Logarithmic Mean		2632	31330	139955	1501	23.6207	-	-
Ratio between control and treatment		0.096	0.037	0.037	0.187	1030.386	-	1.040
p value		0.009	0.279	0.001	0.034	0.018	-	0.193

The Barquat® treatment significantly weakened the *S. epidermidis* biofilm. This treatment statistically weakened the *S. epidermidis* biofilm the most of all treatments. The Barquat® treatment caused the biofilm to have a “watery” appearance.

Table 25: Results for *FRDI* tested with a 50 mg/l concentration of glutaraldehyde.

# of TRTMENTS	# of CNTRLS	G_K (Pa)	η_K (Pa.s)	η_M (Pa.s)	G_M (Pa)	Max γ	WGT ERR	Gap (μm)
10	6							
Arithmetic Mean		17545110	30417	22928	3719	5.682	0.0354	157.00
Standard Deviation		37343793	70034	56383	6388	9.039	0.0286	20.58
Median		51	855	3005	499	1.821	0.0280	162.50
Logarithmic Mean		696	2405	3149	808	1.6341	-	-
Ratio between control and treatment		0.521	0.063	0.031	0.149	30.061	-	1.345
p value		0.763	0.026	0.001	0.032	0.001	-	0.003

The glutaraldehyde treatment significantly weakened the *FRDI* biofilm. There is a large discrepancy between the arithmetic mean and the median value for the G_K coefficient.

The treatment caused the biofilm to become considerably thicker.

Table 26: Results for *S. epidermidis* tested with a 50 mg/l concentration of glutaraldehyde.

# of TRTMENTS	# of CNTRLS							
9	7	G_K (Pa)	η_K (Pa.s)	η_M (Pa.s)	G_M (Pa)	Max γ	WGT ERR	Gap (μm)
Arithmetic Mean		66568	2886065	6593222	7697	0.023	0.0226	96.88
Standard Deviation		101693	5907398	2653682	2542	0.007	0.0101	10.7
Median		33487	422942	5820380	6718	0.027	0.0191	100.
Logarithmic Mean		40948	720488	6196093	7351	0.0214	-	-
Ratio between control and treatment		1.042	1.052	1.472	0.736	1.120	-	1.246
p value		0.92	0.001	0.027	$<10^{-3}$	0.496	-	0.001

The glutaraldehyde treatment did not seem to have a major affect on the *S. epidermidis* biofilm. While there were statistically significant changes for individual coefficients, the net effect is negligible. The Maxwell elastic coefficient becomes less stiff, and the Maxwell viscous coefficient becomes stiffer. The thickness of the biofilm increases significantly due to the glutaraldehyde treatment.

Table 27: Results for *S. epidermidis* tested with a 0.1 mg/l concentration of rifampin.

# of TRTMENTS	# of CNTRLS							
9	3	G_K (Pa)	η_K (Pa.s)	η_M (Pa.s)	G_M (Pa)	Max γ	WGT ERR	Gap (μm)
Arithmetic Mean		5616	135207	613724	5231	0.209	0.0418	55
Standard Deviation		4215	238627	460165	5028	0.326	0.0139	5
Median		3886	25897	515962	3520	0.070	0.0393	55
Logarithmic Mean		4167	41909	398225	3385	0.1109	-	-
Ratio between control and treatment		0.203	0.057	0.152	0.385	4.519	-	0.993
p value		0.021	0.279	0.011	0.058	0.016	-	0

The rifampin treatment significantly weakened the *S. epidermidis* biofilm.

Table 28: Results for *FRDI* tested with a 1 mg/l concentration of ciprofloxacin.

# of TRTMENTS	# of CNTRLS	G_K (Pa)	η_K (Pa.s)	η_M (Pa.s)	G_M (Pa)	Max γ	WGT ERR	Gap (μm)
10	4							
Arithmetic Mean		906	536874137427	71724	1443	36.450	0.0148	101.
Standard Deviation		1951	1697733793277	209018	2391	37.381	0.0124	20.1
Median		69	63685	228	836	23.253	0.011	90.0
Logarithmic Mean		69	134509	786	534	6.1854	-	-
Ratio between control and treatment		0.408	25.704	0.053	1.167	14.894	-	0.33
p value		0.348	0.199	0.025	0.777	0.028	-	0

The ciprofloxacin treatment significantly weakened the *FRDI* biofilm. This treatment weakened the biofilm the most out of all the treatments for *FRDI*. The value of the η_K coefficient is extremely large, indicating a nearly solid dashpot element. The testing of the ciprofloxacin treated biofilm did not match the typical Burger curve, so a single dashpot model is more appropriate.

Table 29: Results for *FRDI* tested with a 50 mg/l concentration of chlorine.

# of TRTMENTS	# of CNTRLS	G_K (Pa)	η_K (Pa.s)	η_M (Pa.s)	G_M (Pa)	Max γ	WGT ERR	Gap (μm)
14	8							
Average		613	24495	50247	3210	0.784	0.0278	184.29
Median		426	8397	16295	2743	0.339	0.0268	187.50
Standard Deviation		674	34940	69649	3626	1.431	0.0167	34.63
Logarithmic Mean		274	6508	20007	1635	0.2793	-	-
Ratio between control and treatment		0.540	0.764	0.653	1.067	1.455	-	1.010
p value		0.425	0.778	0.594	0.918	0.652	-	0.896

The Burger parameters indicate that the chlorine treatment had a slight weakening of the *FRDI* biofilm, but statistically there was no significant change.

Urea

Table 30: Results for *S. epidermidis* tested with a 0.2 molar concentration of urea.

# of TRTMENTS	# of CNTRLS								
6	4	G_K (Pa)	η_K (Pa.s)	η_M (Pa.s)	G_M (Pa)	Max γ	WGT ERR	Gap (μm)	
		Arithmetic Mean	5384	428938	1012069	2580	4.218	0.0564	82.5
		Standard Deviation	5710	537425	1422835	2838	6.933	0.0306	14.05
		Median	4381	218144	264732	1942	0.898	0.0577	87.5
		Logarithmic Mean	2099	58394	91636	580	0.5180	-	-
		Ratio between control and treatment	0.064	0.052	0.017	0.048	33.651	-	0.825
		p value	0.014	0.019	0.018	0.072	0.027	-	0.048

The urea treatment significantly weakened the *S. epidermidis* biofilm.

Table 31: Results for *FRDI* tested with a 0.2 molar concentration of urea.

# of TRTMENTS	# of CNTRLS								
19	8	G_K (Pa)	η_K (Pa.s)	η_M (Pa.s)	G_M (Pa)	Max γ	WGT ERR	Gap (μm)	
		Arithmetic Mean	574	41353	30997	2234	3.238	0.0187	163.26
		Standard Deviation	824	69685	51507	3927	6.268	0.0134	21.91
		Median	215	15743	16719	762	0.361	0.0172	160.00
		Logarithmic Mean	186	8914	8818	778	0.6141	-	-
		Ratio between control and treatment	0.635	1.143	0.287	0.682	2.897	-	1.100
		p value	0.455	0.855	0.113	0.554	0.128	-	0.048

The Burger parameters indicate a significantly weakened biofilm for the *FRDI* urea treatment. However, the confidence values do not statistically support the change in material properties.

DISCUSSION

Simply viewing the tables of results makes it quite difficult to decipher what effect the treatments are having on the biofilms. Graphically representing the data helps to clarify the results. In this section, the results are represented in two different ways. The ratios of each of the four Burger's coefficients in the treated biofilms to their values in the controls are displayed. This ratio is developed from the statistical analysis of the logarithmically transformed data, and thus uses the log-mean value of each coefficient. Secondly, representative creep curves are shown for each treatment along with the representative control results. The median values of the four Burger coefficients were used to create these curves. These graphical comparisons help to assess the effects of each of the individual treatments.

It is interesting to compare the rheological results from biofilm testing to common substances in order to better understand the material properties of the biofilms. Table 32 roughly compares the viscosities and elastic moduli of the two biofilms tested to common substances. Both biofilm species are considerably more viscous than most common fluids, but much less stiff than elastic substances like rubber.

Table 32: Comparison of biofilm elasticity and viscosity to common substances.

Substance	Viscosity (Pa-s)	Elastic modulus (Pa)
<i>S. epidermidis</i>	$\sim 10^6$	$\sim 15,000$
<i>FRDI</i>	$\sim 15,000$	~ 500
Water	8.9×10^{-4}	-
Rubber	-	$10^7 - 10^8$
Castrol oil	.1	-
Honey	10	-
Sour cream	100	-

A simple method for comparing the stiffening or weakening effects of all treatments together is to compare the maximum strain value. A larger strain value indicates a softer biofilm, a while lower strain indicates a stiffer biofilm. To put all the treatments on the same basis, the median value of the maximum strain (the strain at the peak value, normally occurring at 5 minutes) for each treatment was divided by the corresponding value for the control (untreated) biofilm. These are shown in Figure 27 and Figure 28 for all *FRDI* and *S. epidermidis* treatments, respectively. The *FRDI* biofilm shows a wide range of maximum strain values, from significant stiffening to significant loosening. The *S. epidermidis* biofilm seemed to only be weakened by the treatments tested.

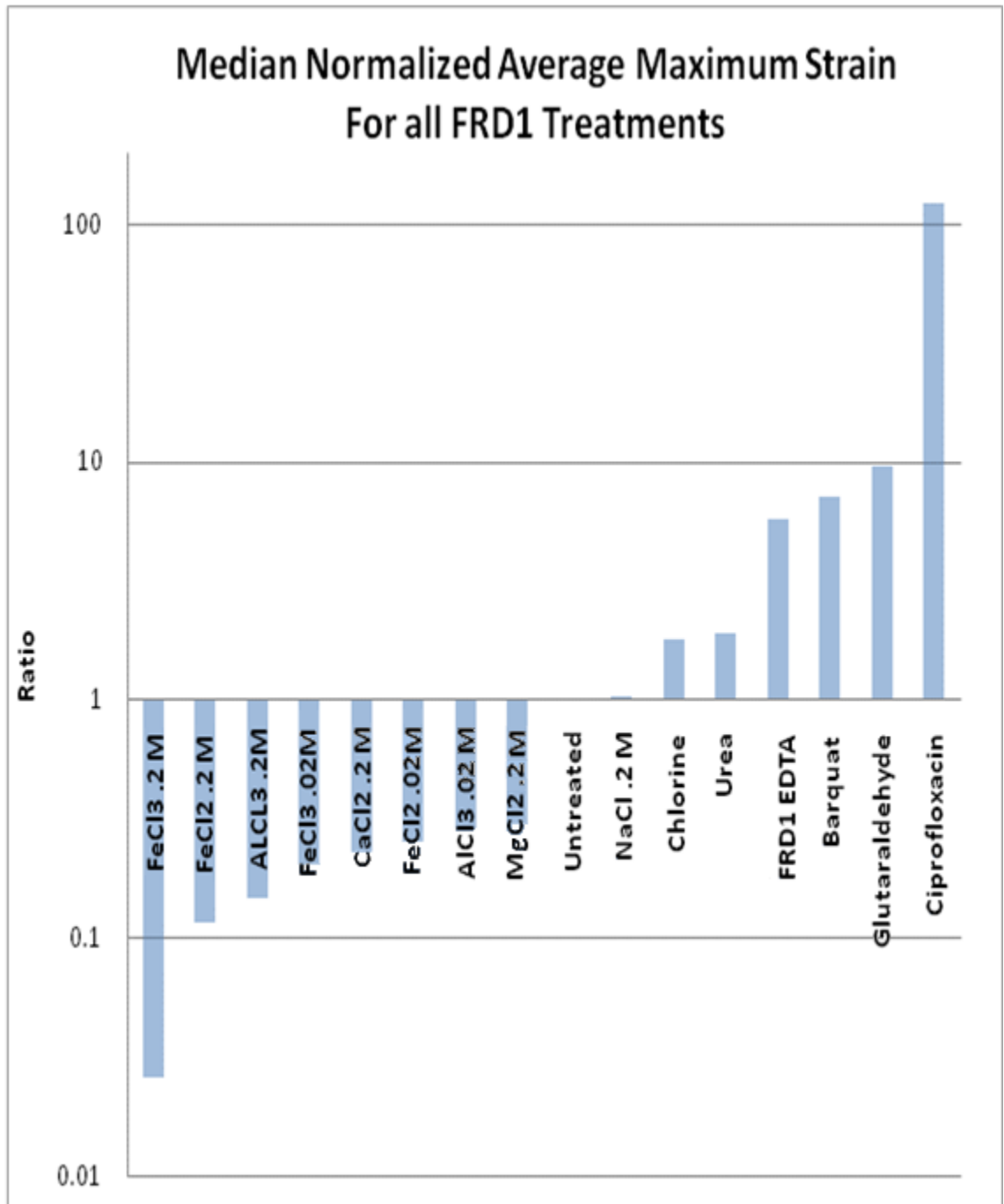


Figure 27: Median values of maximum strains for all *FRD1* treatments, normalized to maximum strain values for the equivalent control experiments.

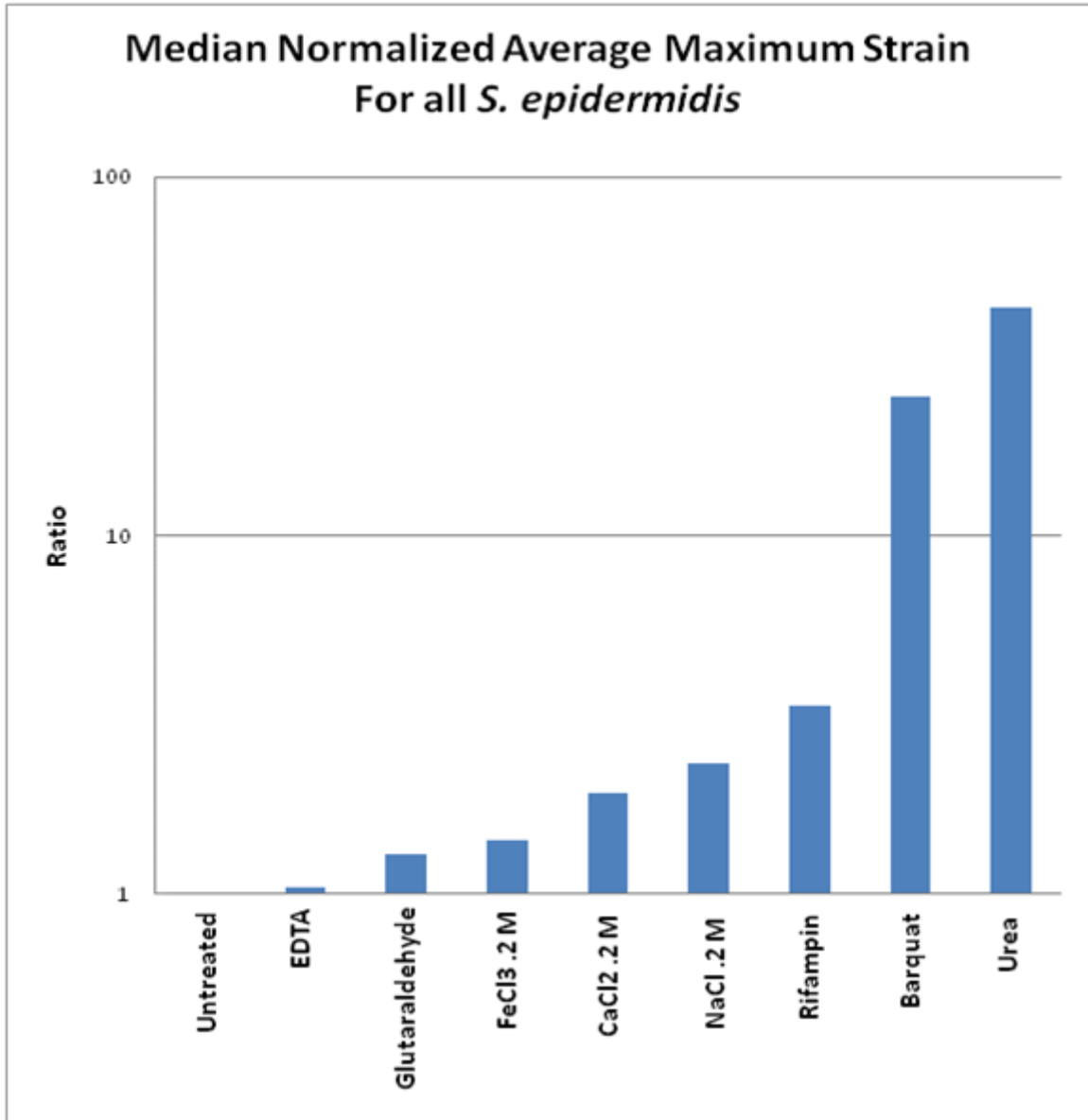


Figure 28: Median values of maximum strains for all *S. epidermidis* treatments, normalized to maximum strain values for the equivalent control experiments.

CationsFRDI

All multivalent cation treatments on the *FRDI* biofilm resulted in a reduction of maximum strain and an increase of the value of all Burger coefficients. Figure 29 displays the ratios of the treatment to the control means for all four Burger coefficients for all cation treatments. The concentration of applied cation did appear to have an effect on the material properties. Lower multivalent cation concentrations resulted in less stiffening than the corresponding treatment at higher concentrations. The valence number seemed to also have an effect on stiffening. Trivalent cations created stiffer biofilms than divalent cations, except ferrous chloride had a greater stiffening effect than aluminum chloride; this is likely due to the oxidization of ferrous iron to ferric iron during treatment. Trivalent cation treatments resulted in a stiffer biofilm likely because of two factors. Trivalent ions are capable of cross-linking three sites, rather than just two for divalent cations and only one for the monovalent cation. The increase in stiffening for the trivalent cations could also be partly caused by precipitation of aluminum hydroxide ($\text{Al}(\text{OH})_3$) and iron(III) hydroxide ($\text{Fe}(\text{OH})_3$). At high cation concentrations (0.02 and 0.2 M) and pHs between 6 and 8, some precipitation is likely to occur (Johnson and Amirtharajah, 1982). Cross-linking and precipitation likely explain the increased stiffening of the iron and aluminum treated *FRDI* biofilm.

Sodium chloride, a monovalent cation, showed a statistically insignificant change in material properties. Sodium could potentially weaken the biofilm if monovalent ions replace sites that are cross-linked with multivalent cations. The results show that

monovalent cation replacement is not a significant factor in the material properties of *FRDI* biofilm.

Molecular weight seemed to affect the stiffness of the biofilm. The molecular weight of iron is 55.75, the molecular weight of aluminum is 26.98; iron treatments resulted in a stiffer biofilm than the aluminum treatments, even though both are trivalent ions. The same result held true for divalent cations; iron (MW 55.75) was stiffer than calcium (MW 40.08) which was stiffer than magnesium (MW 24.305).

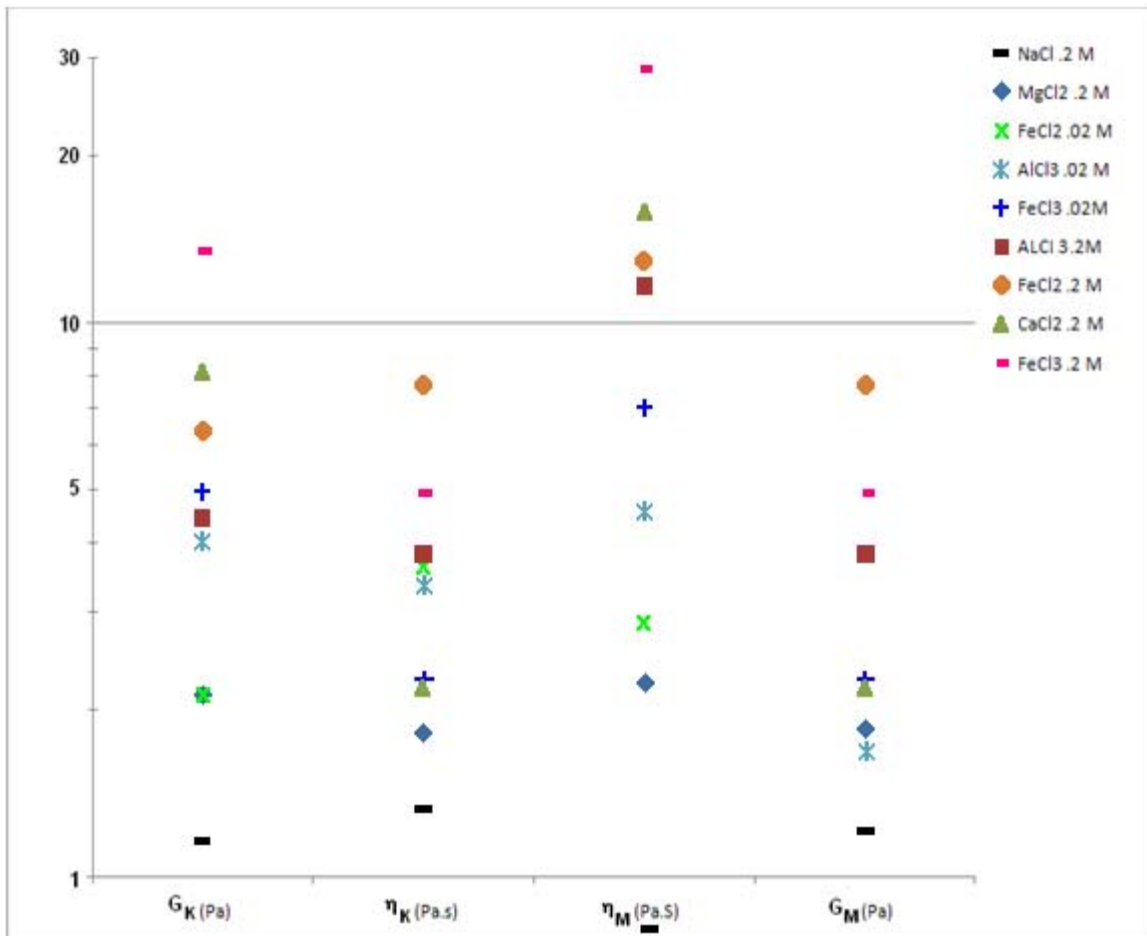


Figure 29: Chart showing ratio between all cation treatments and their controls for the four Burger coefficients for the *FRDI* biofilm.

The median value of the four Burger coefficients was used to graphically represent the typical creep curve for each treatment. The median values were used rather than the mean values because the median is not as influenced by outlier data that can be orders of magnitude different than the mean. The curves for all cation treatments can be seen in Figure 30.

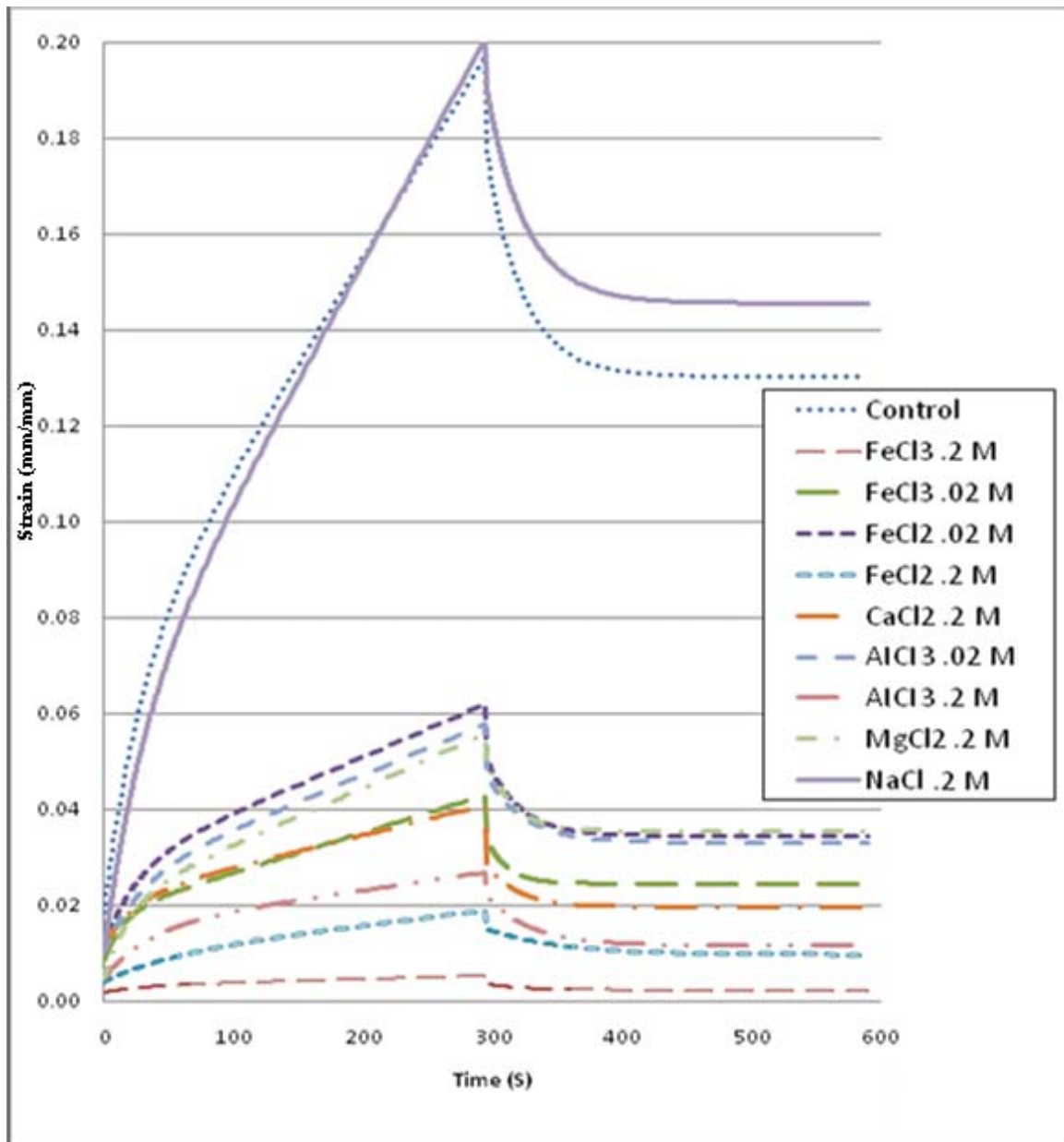


Figure 30: Median representation of typical creep curves for all cation treatments for *FRDI* biofilm.

S. epidermidis

Cation treatments on *S. epidermidis* biofilms yielded drastically different results than with the *FRDI* biofilm. Rather than tightening the biofilm as with the *FRDI*, the cation treatments reduced the stiffness of the *S. epidermidis* biofilm. Figure 31 shows a chart of the ratio between the treatment and the control for the four Burger coefficients. For practically all treatments, the ratio between the treatments and the controls is less than one, and lower values for the coefficients indicate reduced stiffness or increased compliance for the material. The change in the Burger parameters was not statistically significant in all cases, but in most cases the p-values were low (previously shown in Table 18, Table 19, and Table 20).

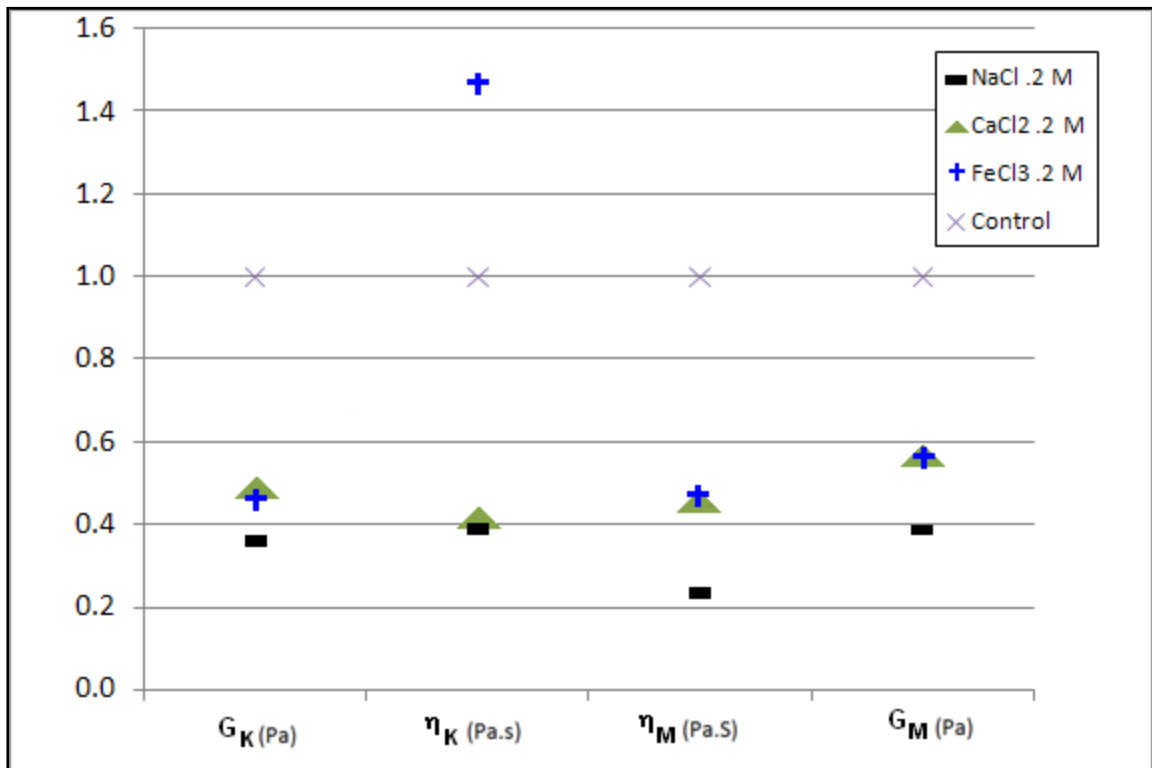


Figure 31: Chart showing ratio between all cation treatments and their controls for the four Burger coefficients for the *S. epidermidis* biofilm.

Figure 32 shows a chart displaying the response curves using the median Burger coefficient values for all *S. epidermidis* cation treatments. This chart shows a correlation between the valence of the cation and its effect on the strength of the biofilm.

Interestingly, the trivalent cation (Fe^{+3}) seems to slightly weaken the biofilm, the divalent cation (Ca^{+2}) weakens the biofilm more than (Fe^{+3}) and the monovalent cation (Na^{+}) weakens the biofilm the most of all the cations. An explanation for this phenomenon could be that the strong *S. epidermidis* biofilm is heavily cross-linked and the addition of cations results in cross-linked sites being replaced with less efficient cross-linkers. The unlinking of these heavily cross-linked site results in a more compliant biofilm.

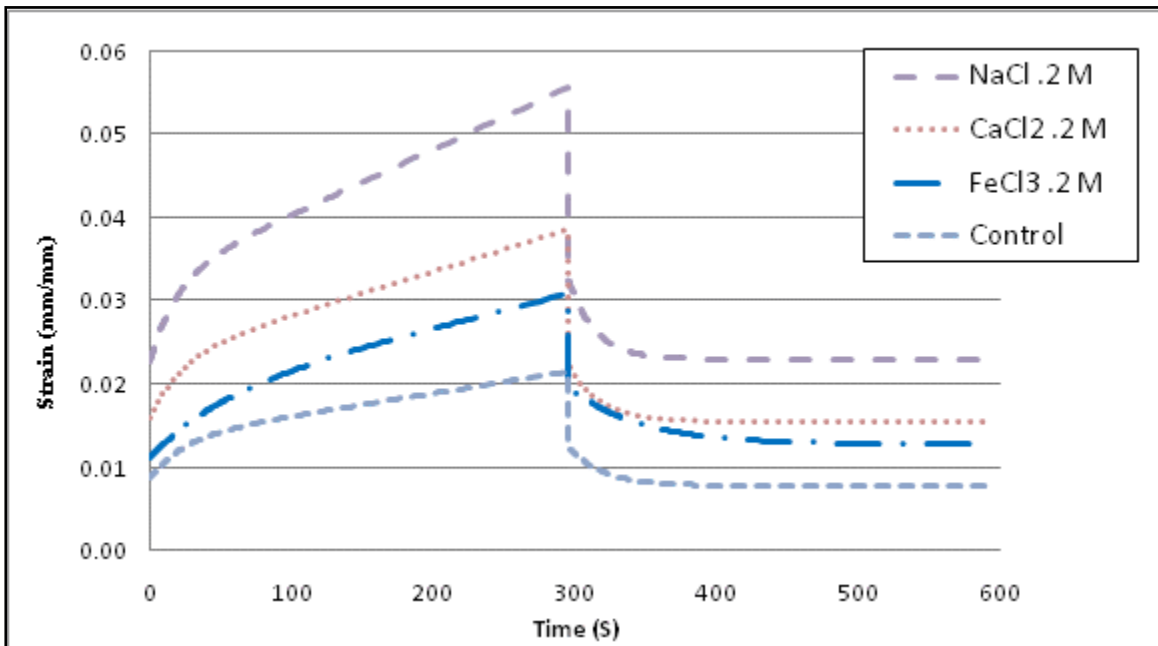


Figure 32: Median representation of typical creep curves for all cation treatments for *S. epidermidis* biofilm.

ChelationEDTA

EDTA treatments yielded interesting results for the *FRDI* biofilm. Approximately half of the *FRDI* treatments resulted in large maximum strain values (>1), but the other half of the test resulted in smaller than average strains (<0.2). Some of the creep tests had creep curves that were not typical of the classic Burger curves seen in the majority of creep tests. Figure 33 shows an example of one of these atypical creep curves. The curves that did not resemble the typical Burger creep curve were not used to fit the Burger coefficients, however, the maximum strain and gap values were used in the results.

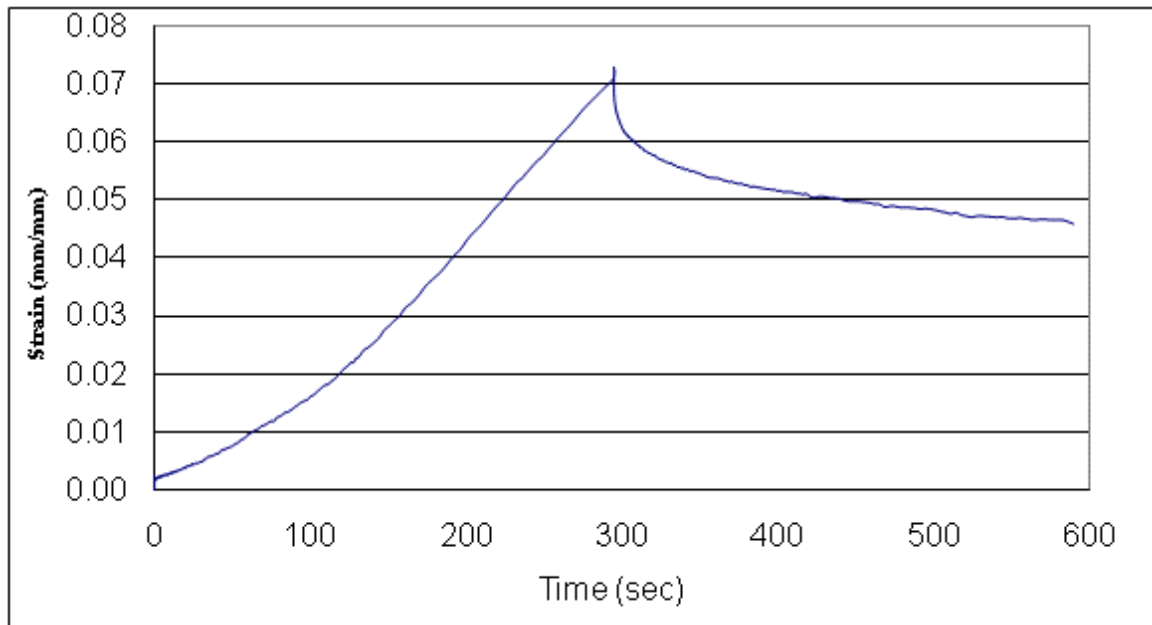


Figure 33: Atypical creep curve from EDTA treatment of *FRDI* biofilm.

Figure 34 shows the ratio of the treatment to their controls for the Burger coefficients for both species of biofilm. Three *FRDI* Burger coefficients are significantly reduced; the G_K coefficient does not experience much change. The *S. epidermidis*

treatment has three coefficients reduced and the η_K coefficient increased slightly. None of these changes had statistically significant p-values. The change in the shape of the creep curves indicates that the EDTA did have some effect on the material properties of the biofilm, even if the change was not statistically significant.

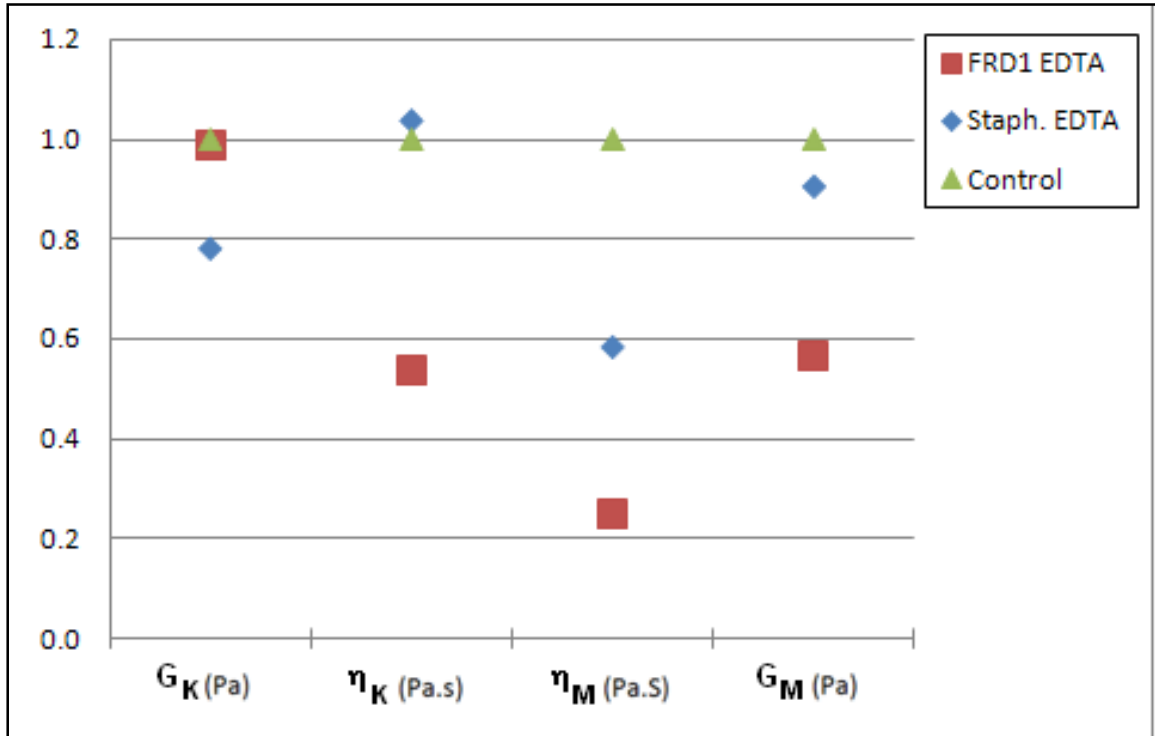


Figure 34: Chart showing ratio between 0.2 M EDTA treatments and their controls for the four Burger coefficients for the *S. epidermidis* and *FRDI* biofilms.

Figure 35 and Figure 36 show the representative creep curves for EDTA treatments of both species of biofilm. The median Burger values indicate a slight increase in the overall strain of both biofilm species, but not a significant change. It was expected both biofilm species would experience a reduction in strength; metal ions involved in cross-linking biofilm would be sequestered causing a loss in biofilm stiffness (Holleman and Wiberg, 2001). However, the EDTA seemed to have little effect changing the

material properties of both biofilm species, indicating that metal cation cross-linkage may not be a major factor in the structure of these biofilms.

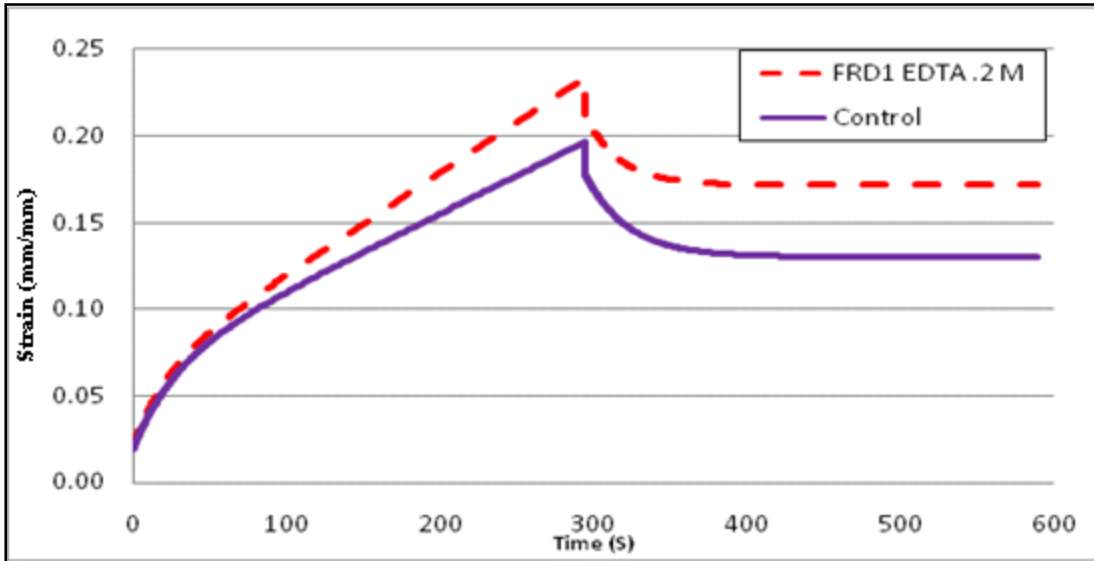


Figure 35: Median representation of typical creep curves for 0.2 M EDTA treatment for *FRD1* biofilm.

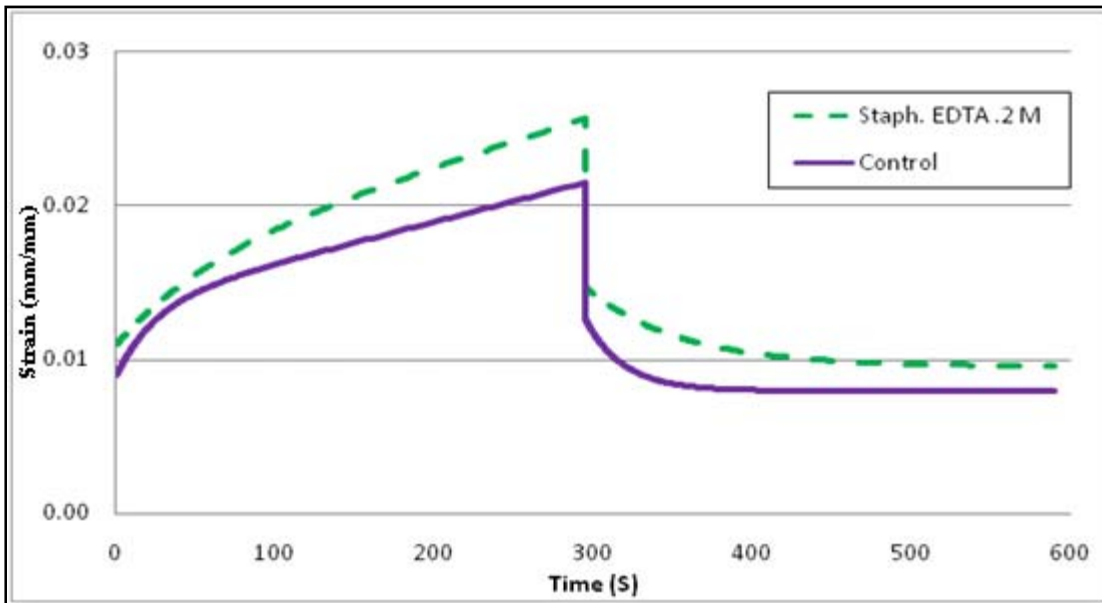


Figure 36: Median representation of typical creep curves for 0.2 M EDTA treatment for *S. epidermidis* biofilm.

Urea

Urea treatment on the *S. epidermidis* biofilm significantly weakened the biofilm; the treatment on the *FRDI* biofilm seems to create a weaker biofilm, however the t-testing on *FRDI* did not show statistical significance. Figure 37 shows the ratio of the four Burger coefficients of the urea treatments vs. their controls for both species of biofilms. The *S. epidermidis* coefficients are drastically reduced, while the *FRDI* Burger coefficients show a modest reduction in magnitude.

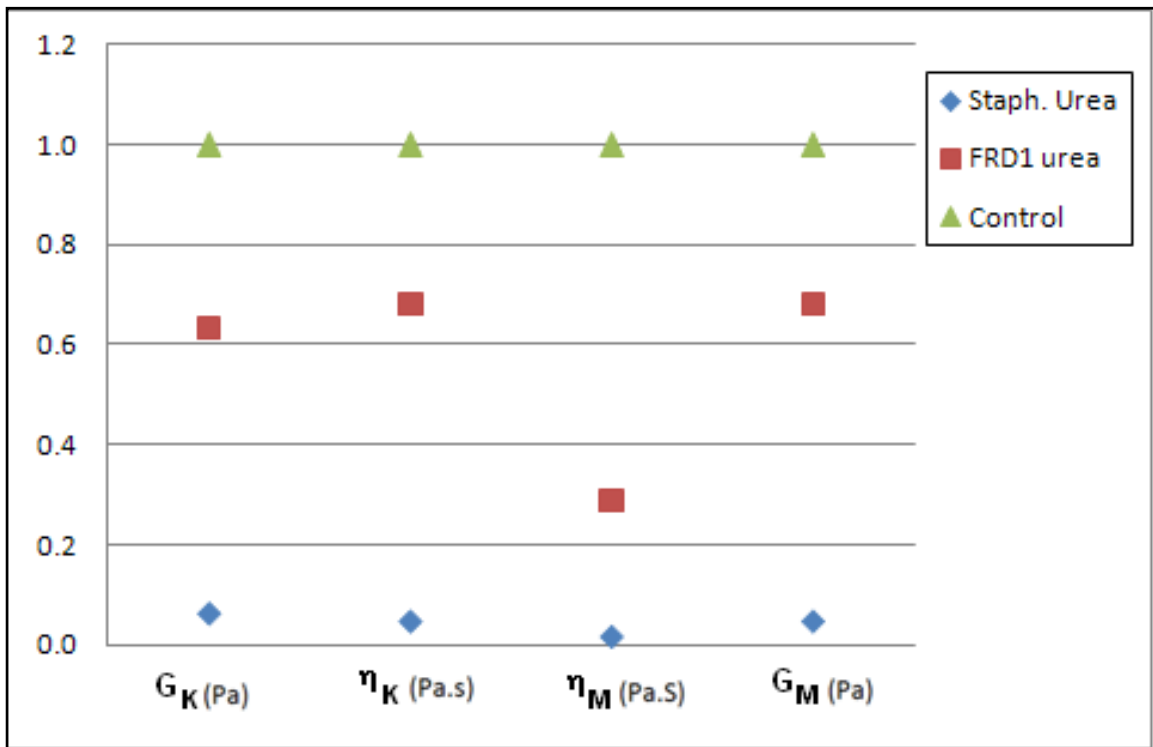


Figure 37: Chart showing ratio between 0.2 M urea treatments and their controls for the four Burger coefficients for the *S. epidermidis* and *FRDI* biofilms.

Urea treatment likely disrupts hydrogen bonding in the biofilms (Chen and Stewart, 2002). It seems that hydrogen bonds are quite important to the mechanical properties of *S. epidermidis* and to a lesser degree for *FRDI*. Figure 38 and Figure 39

show the representative median creep curves for urea treatments and their controls for *FRD1* and *S. epidermidis* biofilm respectively. Increased strain can be seen in both urea treatments.

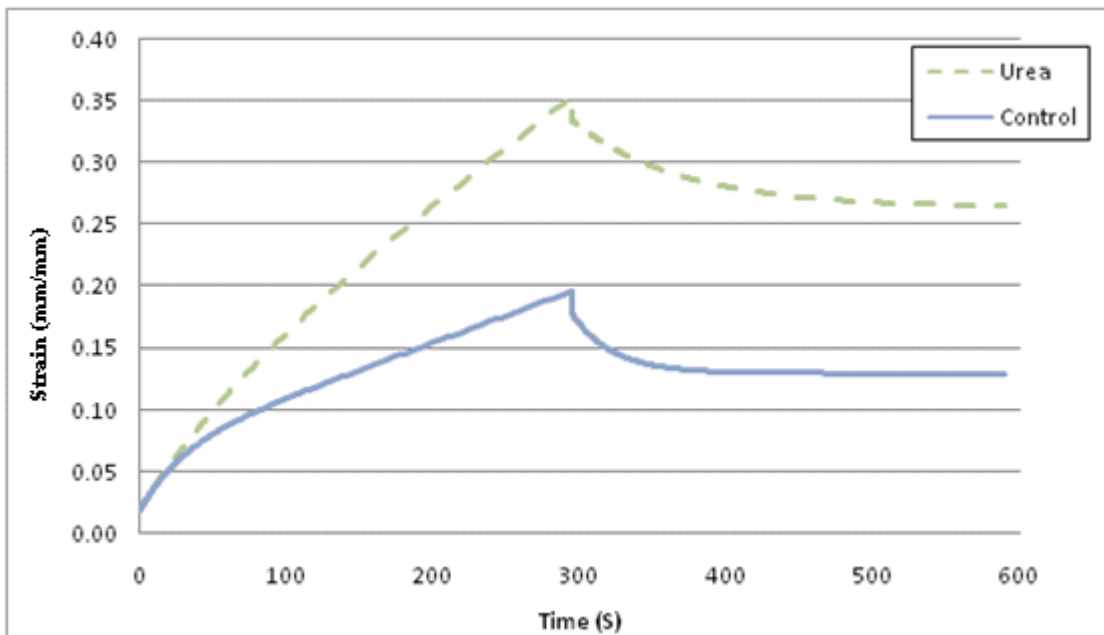


Figure 38: Median representation of typical creep curves for 0.2 M urea treatment for *FRD1* biofilm.

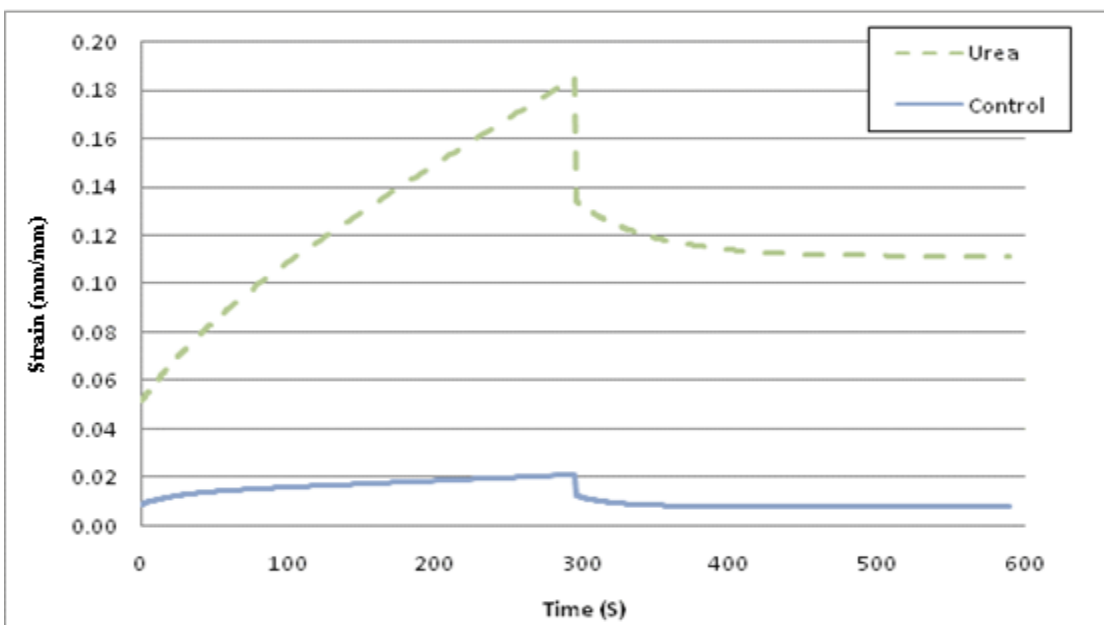


Figure 39: Median representation of typical creep curves for 0.2 M urea treatment for *S. epidermidis* biofilm.

Antimicrobials

Barquat®

The surfactant, Barquat®, had similar effects on both *S. epidermidis* and *FRD1* biofilms. The treatment caused both biofilm species to become much more compliant. Figure 40 shows the ratios between the controls and Barquat® treatments for both biofilm species. All four Burger coefficients are significantly reduced compared to their controls.

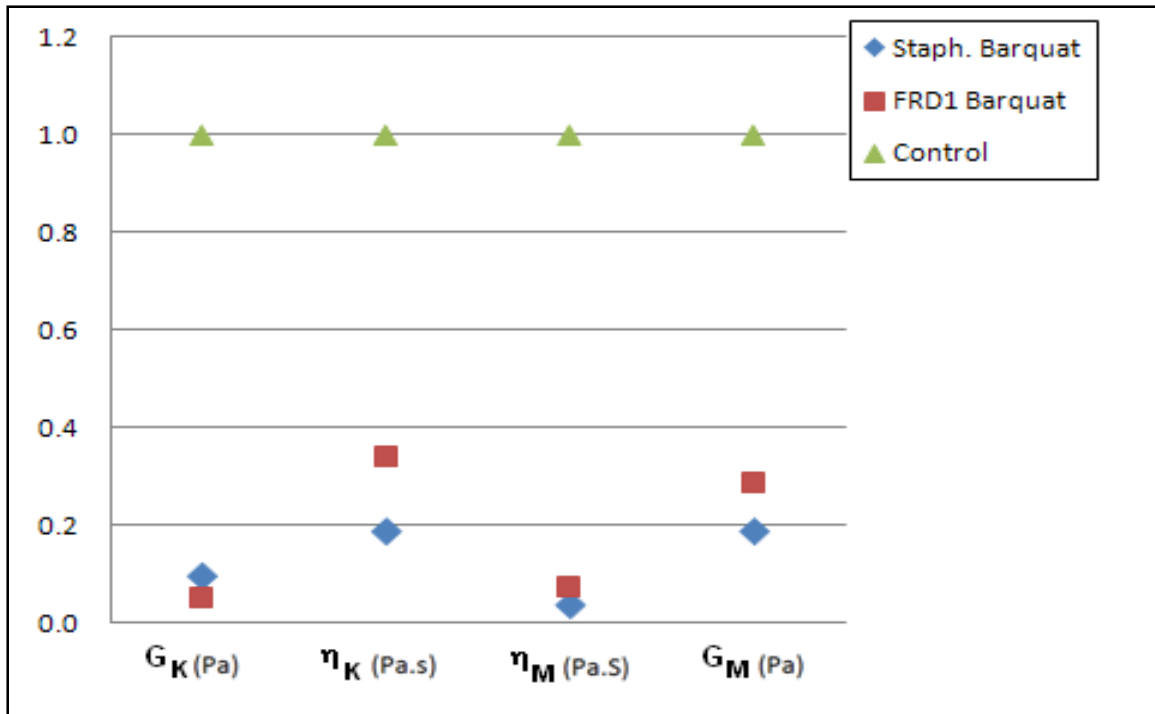


Figure 40: Chart showing ratio between 50 mg/l Barquat® treatments and their controls for the four Burger coefficients for the *S. epidermidis* and *FRD1* biofilms.

Figure 41 and Figure 42 show the typical creep curves for both species of biofilm treated with Barquat®. The increase in the strain compared to the control is quite noticeable. Barquat's® chemical effect on the two biofilm species seems to be quite similar; the ratio between the treatment and the control seems to move in step for both

species of biofilms. The EPS of both *S. epidermidis* and *FRD1* become slightly “liquefied” by this surfactant treatment – that is, the biofilms become more viscous than elastic. The Barquat® treatment on the two biofilms seems to affect the biofilm’s ability to retain water, so this treatment results in reduced stiffness for the biofilms material properties. The loss of ability for the biofilm to retain water in a gel form may be partially explained by the reduced surface tension of water cause by the surfactant (Sundheim et al., 1998).

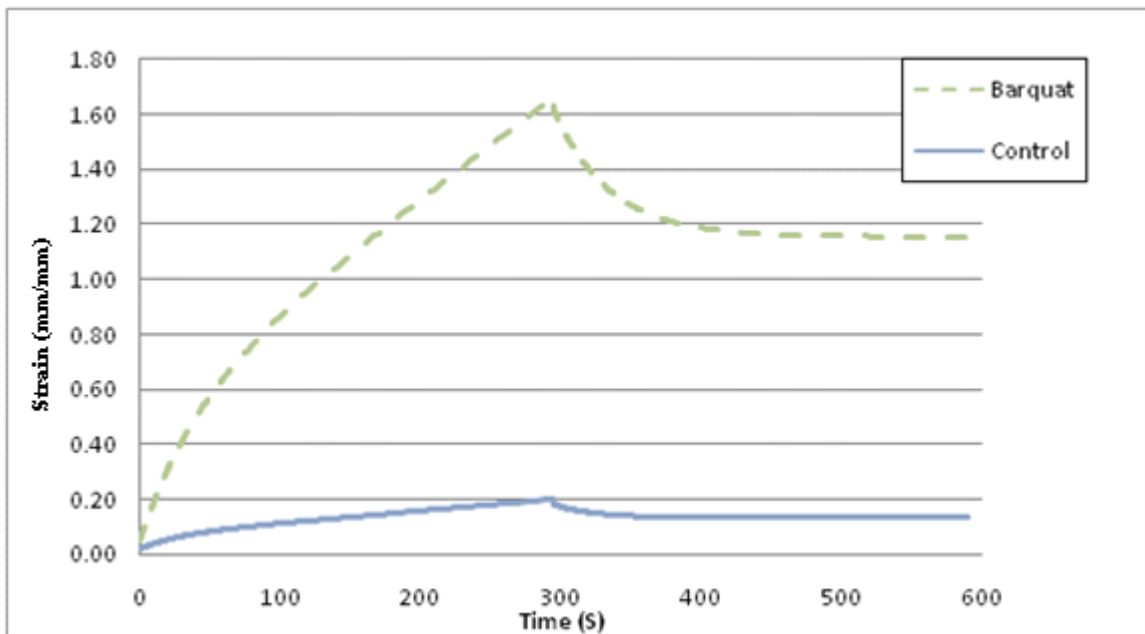


Figure 41: Median representation of typical creep curves for 50 mg/l Barquat® treatment for *FRD1* biofilm.

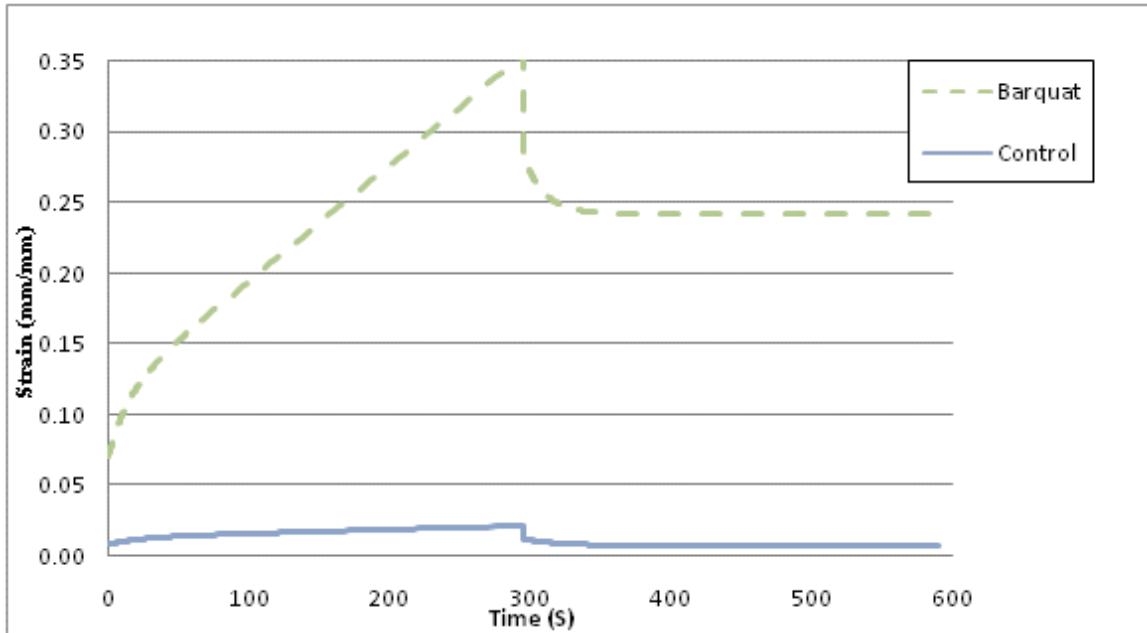


Figure 42: Median representation of typical creep curves for 50 mg/l Barquat® treatment for *S. epidermidis* biofilm.

Glutaraldehyde

Glutaraldehyde treatments yielded very different results between the two species of biofilm. *FRDI* became much weaker and the *S. epidermidis* did not experience much change in material properties. Figure 43 shows the ratio of the Burger coefficients for the glutaraldehyde treatments versus their controls for both species of biofilms. All *FRDI* Burger coefficients see a drastic reduction in coefficient values; this reduction was unexpected since glutaraldehyde is known to be a fixative agent. Three of the four Burger coefficients for the treated *S. epidermidis* biofilm showed a slight increase in coefficient values compared to their treatments, possibly indicating a slight tightening of the biofilm which was the expected result given glutaraldehyde's cross-linking properties (Davidson, 2008). The t-tests indicated the differences were statistically significant for nearly all parameters tested for both biofilm species.

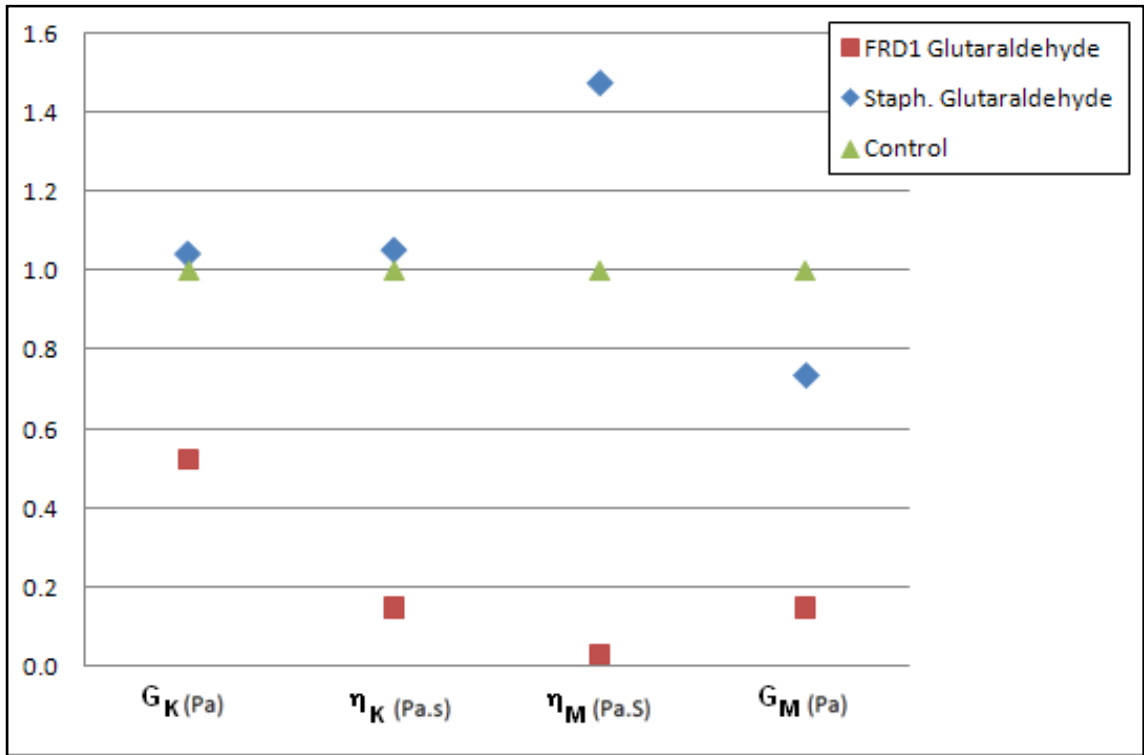


Figure 43: Chart showing ratio between 50 mg/l glutaraldehyde treatments and their controls for the four Burger coefficients for the *S. epidermidis* and *FRD1* biofilms.

Figure 44 and Figure 45 show the typical creep curves for glutaraldehyde treated *FRD1* and *S. epidermidis* biofilms, respectively. The treated *FRD1* clearly becomes more compliant given the large strain experience in the typical creep curve. The treated *S. epidermidis* seems to have a slightly larger maximum strain than its control, but its elastic response is larger than the control indicating a more elastic biofilm. In addition, the return to nearer the original position with the *S. epidermidis* biofilm treated with glutaraldehyde is as expected from the stronger Maxwell dashpot (η_M). There seems to be a nearly opposite effect of the material properties between the glutaraldehyde treatment of the *FRD1* and the *S. epidermidis* biofilms.

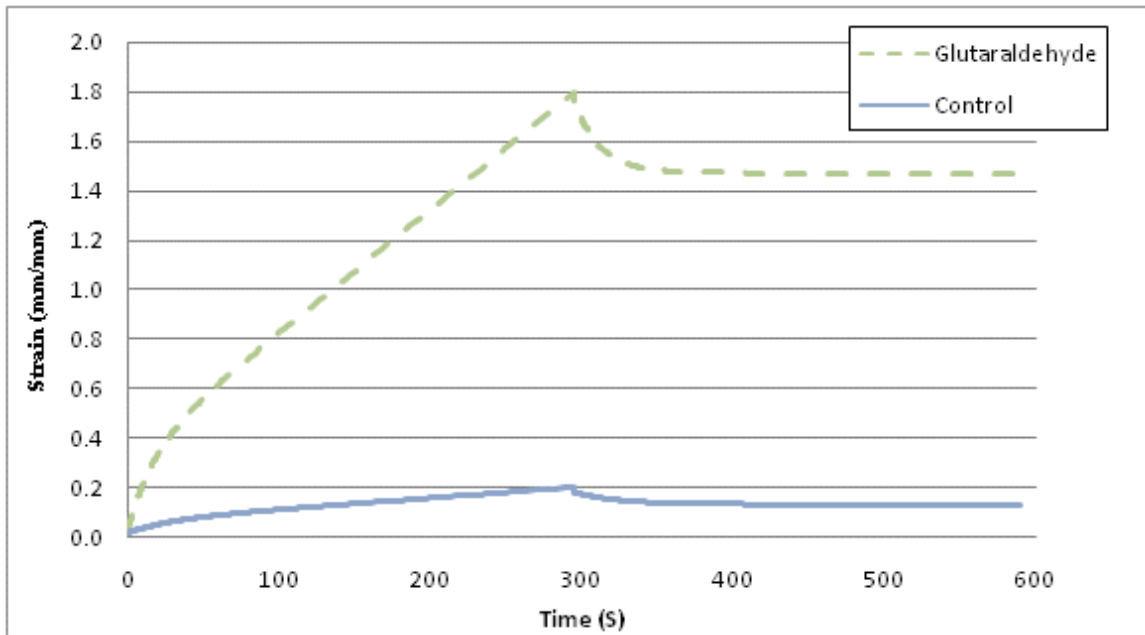


Figure 44: Median representation of typical creep curves for 50 mg/l glutaraldehyde treatment for *FRDI* biofilm.

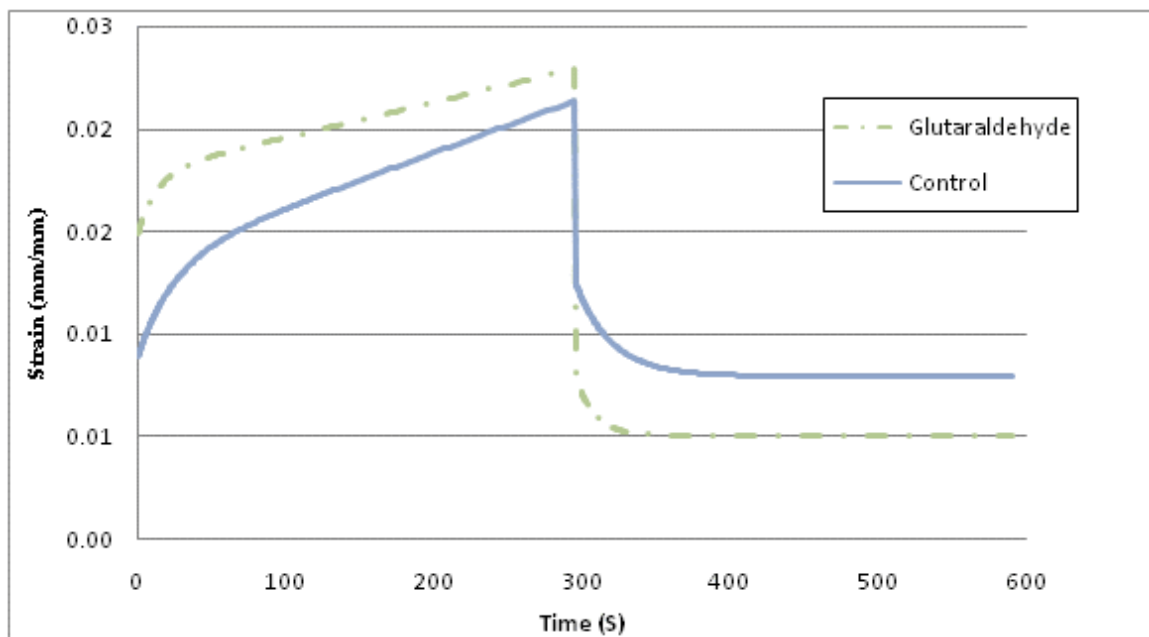


Figure 45: Median representation of typical creep curves for 50 mg/l glutaraldehyde treatment for *S. epidermidis* biofilm.

Glutaraldehyde is known to be effective as a fixative agent on some staphylococcus biofilm species, so the treatment was expected to stiffen the *S. epidermidis* biofilm.

(Marrie et al., 1982). The results from the creep testing were less than what was expected. This reduced variation could be caused by a limitation of the testing technique. *S. epidermidis* creates a much stiffer biofilm than *FRDI*. It may be that it is difficult to detect tightening of the *S. epidermidis* biofilm because of the high shear stress (100 Pa) needed to test the biofilm. A tightened biofilm may be slipping on the base plate rather than straining the biofilm. It would be nearly impossible to detect slippage with such tiny strains, but such slippage could explain the lack of significant tightening from the glutaraldehyde treatment as measured.

Rifampin

The rifampin treatment greatly reduced the stiffness of the *S. epidermidis* biofilm.

Figure 46 shows the ratio of the rifampin treatment to its control. All four Burger coefficients are reduced by at least a factor of 0.4. There was a strong statistical significance to support the displayed change in material properties.

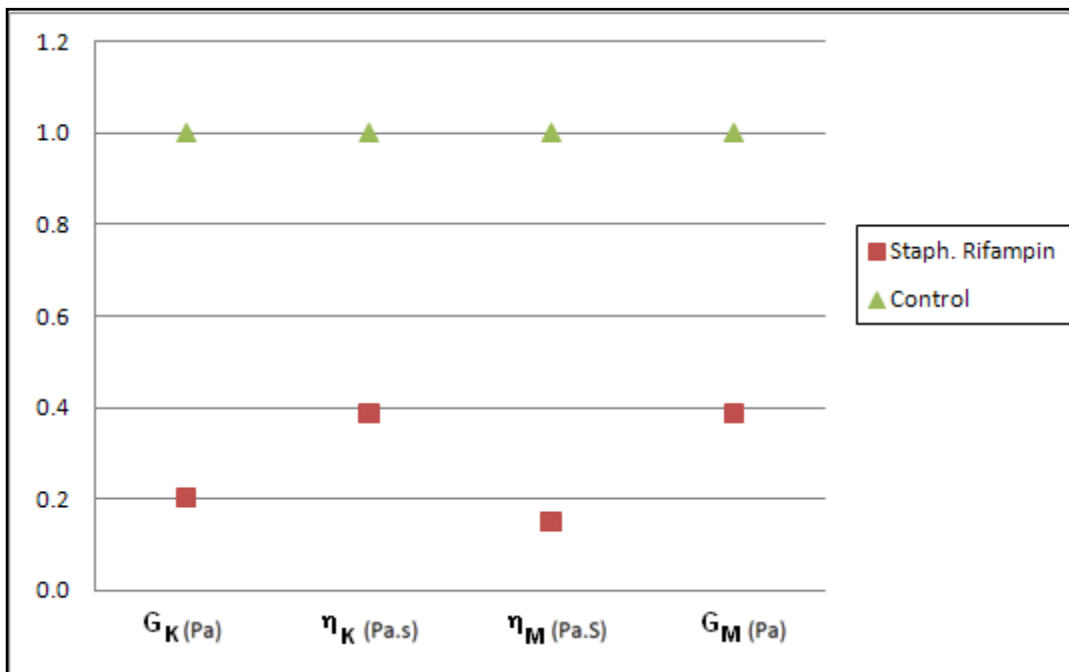


Figure 46: Chart showing ratio between 0.1 $\mu\text{g/ml}$ Rifampin treatment and its control for the four Burger coefficients for the *S. epidermidis* biofilm.

Figure 47 shows the typical creep curve for *S. epidermidis* treated with rifampin. The stiffness of biofilm was clearly reduced by the antimicrobial treatment. The antibiotic's inhibition of bacterial growth caused a significant softening of the *S. epidermidis* biofilm (Campbell et al., 2001). The lack of bacterial growth could result in the degradation of the biofilm.

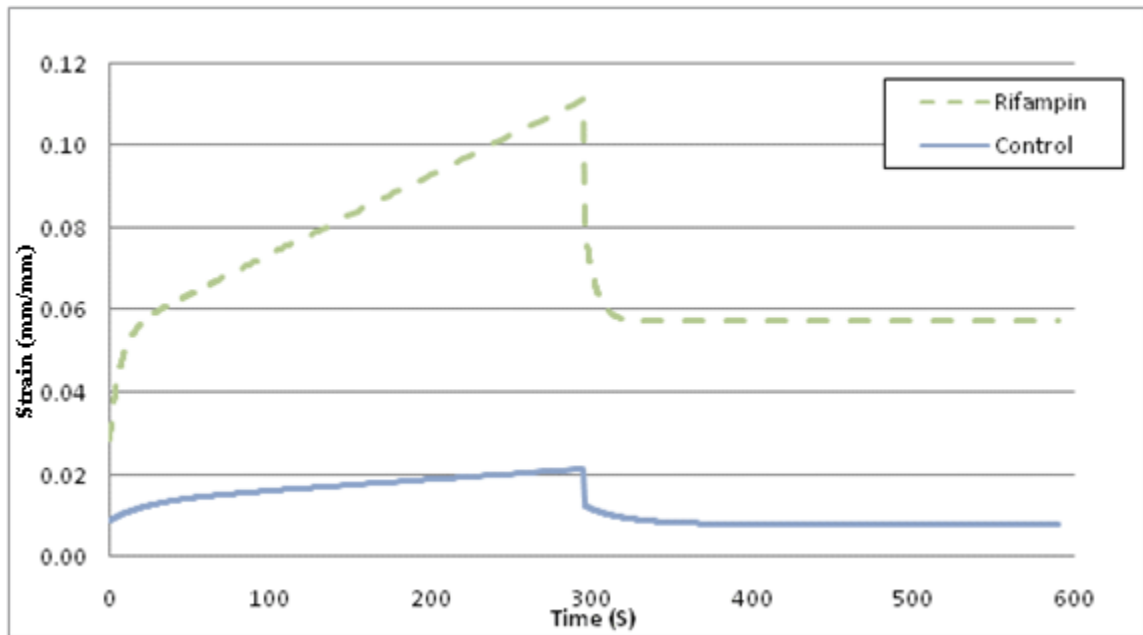


Figure 47: Median representation of typical creep curves for 0.1 µg/ml rifampin treatment for *S. epidermidis* biofilm.

Ciprofloxacin

Ciprofloxacin treatment on *FRDI* biofilm resulted in the most compliant biofilm of all the treatments. Figure 48 shows the ratio of the ciprofloxacin treatment relative to its control. The values of the Burger coefficients are a little misleading; the η_K and G_M coefficients are larger than the values of their controls. This would seem to indicate a tightened or stiffened biofilm, but the η_M parameter is so severely reduced that the other parameters do not significantly influence the shape of the creep curve. Essentially, the biofilm is nearly fluidized by this treatment. Only the η_M coefficient is statistically significant from the t-testing of the Burger coefficients.

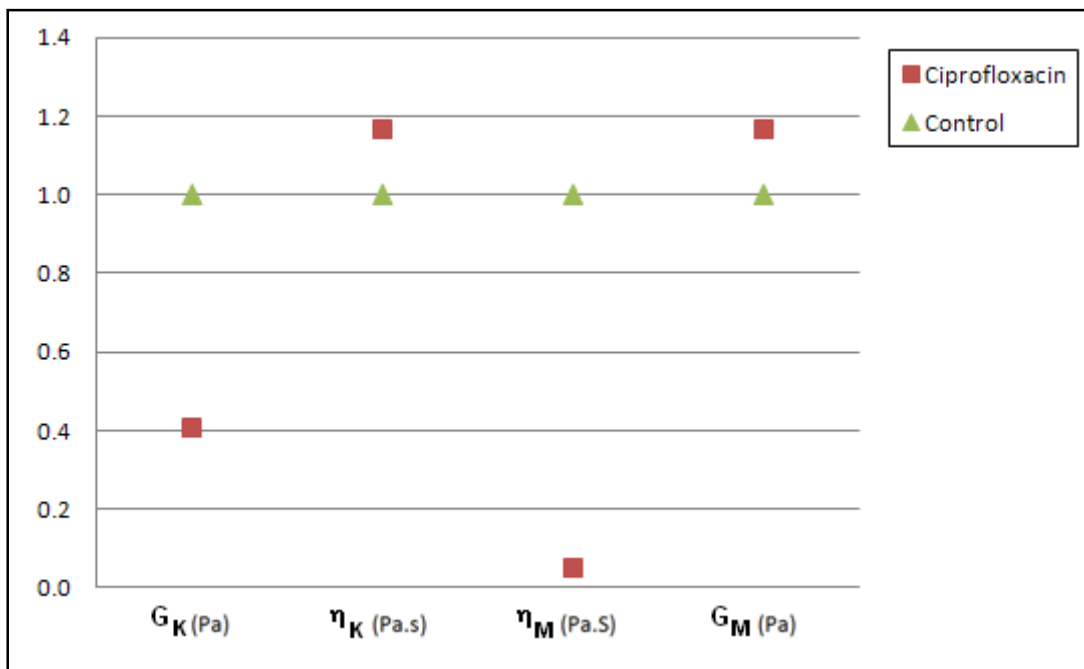


Figure 48: Chart showing ratio between 1 $\mu\text{g/ml}$ ciprofloxacin treatment and its control for the four Burger coefficients for the *FRDI* biofilm.

Figure 49 shows the typical creep curve for *FRDI* treated with Ciprofloxacin and the typical untreated *FRDI* creep curve. The shape of this curve resembles the creep curve of a lone dashpot – a simple viscous fluid. The inhibition of cellular growth has a major effect on the overall strength of the *FRDI* biofilm (Riddle et al. 2000). Like the rifampin treatment on the *S. epidermidis*, the lack of bacterial activity seems to result in biofilm degradation.

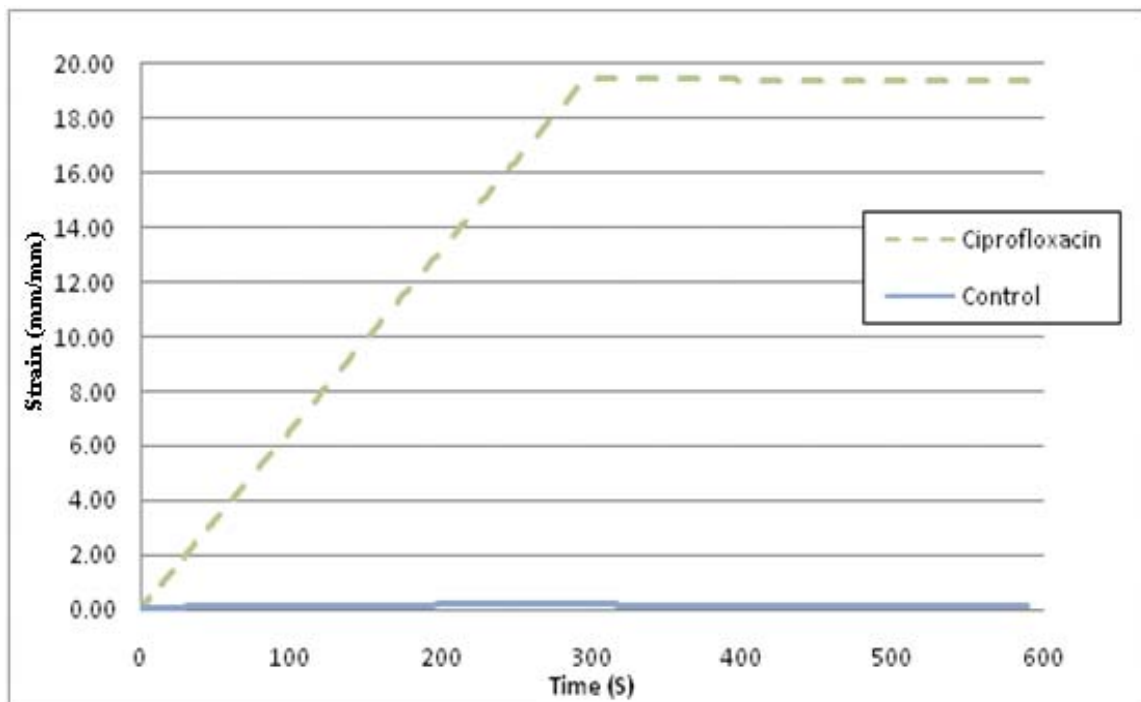


Figure 49: Median representation of typical creep curves for 1 µg/ml ciprofloxacin treatment for *FRDI* biofilm.

Chlorine

Chlorine treatments on the *FRDI* biofilm seemed to lead to a slight reduction in stiffness for the biofilm. Figure 50 shows the ratio between the Burger coefficients for the chlorine treated biofilm and their controls. Two of the four coefficients show decreases in their coefficient values and the other two remain relatively unchanged. However, the t-tests did not show a statistically significant change in material properties.

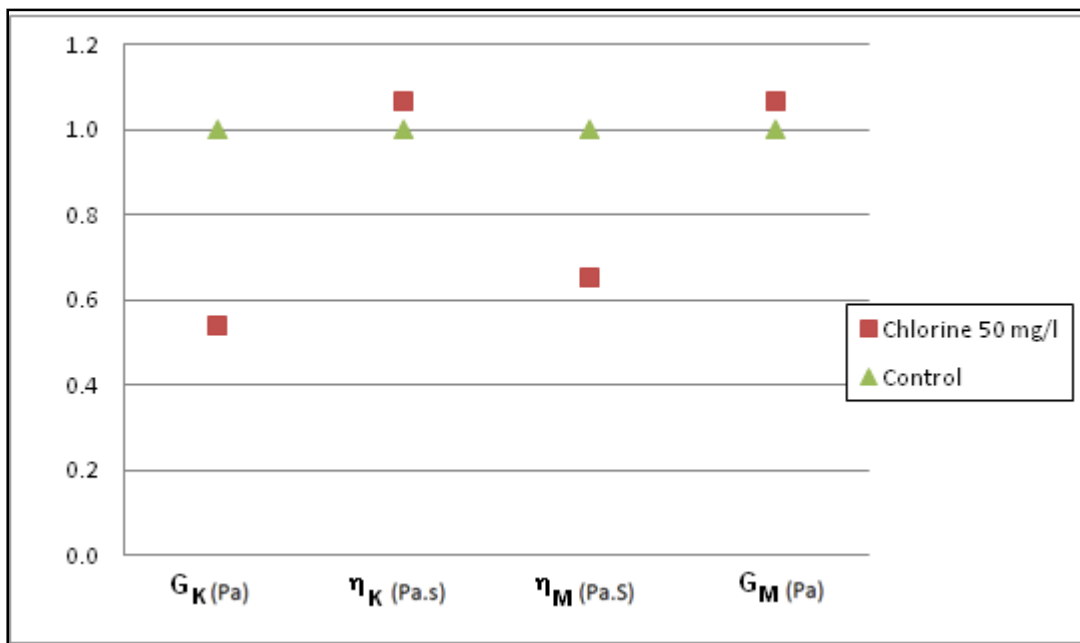


Figure 50: Chart showing ratio between 50 mg/l chlorine treatment and its control for the four Burger coefficients for the *FRDI* biofilm.

Figure 51 shows the typical creep curve for chlorine treated *FRDI* biofilm. There seems to be an increase in overall strain, and a decrease in the elastic recovery. The chlorine treatment is likely oxidizing the EPS causing the biofilm to weaken. Diffusion limitation of the chlorine into the biofilm is likely responsible for the lack of significant changes to material properties (Chen and Stewart, 1996).

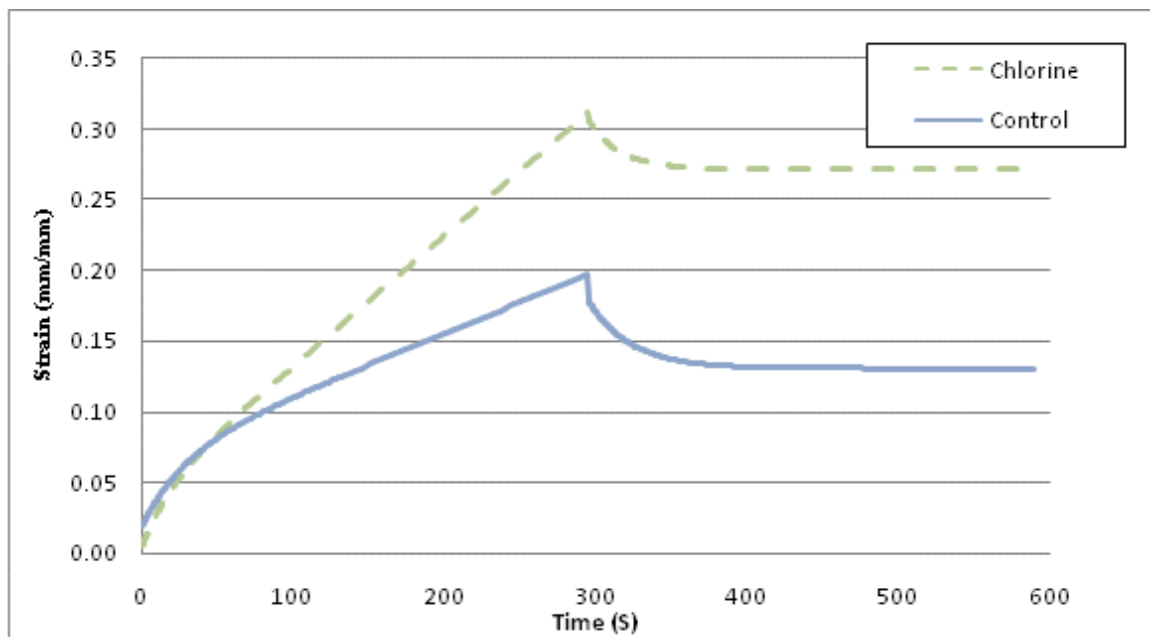


Figure 51: Median representation of typical creep curves for 50 mg/l chlorine treatment for *FRDI* biofilm.

SUMMARY

Biofilms present a costly and sometimes deadly challenge to industry and medicine. The ability to alter the mechanical properties of biofilm could provide an alternate method to biocidal compounds, or aid in the effectiveness of other biofilm control techniques. Little work has been conducted on methods for altering biofilm mechanical properties. This thesis documents the alteration of biofilms' mechanical properties through the addition of chemical treatments. The mechanical properties were measured using a parallel plate rotational disk rheometer. Two species of biofilm were chosen for experimentation, *S. epidermidis* and *FRD1*, a mucoid strain of *Pseudomonas aeruginosa*.

Before experimentation could begin, experimental methods needed to be established. The method for setting the gap distance on the rheometer was determined for each species to ensure complete sample coverage by the rheometer head, but to also minimize the disturbance of the sample's structure. The applied shear stress for creep testing needed to be determined so that linear modeling methods could be employed. This was accomplished for the *FRD1* biofilm by running several tests at various shear stresses to determine where the biofilms became non-linear relative to the linear superposition principle. A similar method was employed for the *S. epidermidis* biofilm, but due to its stiffer material properties the outer bounds of its linear region was not established.

Determination of constitutive laws for each of the treatments began once all of the treatments had been tested on the rheometer. Previous experimentation had determined that most biofilms could be described by the Burger's material model. Burger's model is

composed of four elements; a spring and dashpot in series connected to a spring and dashpot in parallel, the coefficients are G_M , η_M , G_K , η_K . The quasi-Newtonian solver in Microsoft Excel was used to curve-fit the data to Burger's material equation for creep testing. A Microsoft Visual Basic macro routine was created to ensure that the solver arrived at the global minimum of the error function.

Once the four coefficients for the Burger model had been computed for all treatments, statistical analysis of the treatments was performed. The four Burger's coefficients were not normally distributed, but the data became normally distributed under a logarithmic transformation. Statistical two sample t-tests were run using the logarithmically transformed data for the treatments versus their controls in order to determine if changes in the parameters were statistically significant.

The results showed that manipulation of the mechanical properties of biofilm through chemical addition is clearly possible. The stiffness of the *FRDI* biofilm was significantly increased by multivalent cation addition, and decreased by most antimicrobial treatments. The stiffness of the *S. epidermidis* biofilm was reduced by most treatments, in some cases quite significantly. The contrast between the response of the *FRDI* and *S. epidermidis* biofilms was drastic for multiple treatments. The opposite response of the two biofilms to the same treatment (e.g., urea, multivalent cations, glutaraldehyde) highlights the biological and chemical differences between the biofilms and their extracellular matrices. It is apparent that global generalizations cannot be made about affecting a change in biofilm material properties for biofilm control. The results of this thesis show that manipulation of biofilm mechanical properties is possible, hopefully

further work in this area will create new biofilm control techniques. Testing chemical treatments along with mechanical removal techniques would be interesting to better understand and manipulate cohesive biofilm strength.

REFERENCES CITED

1. Campbell E. A., Korzheva N., Mustaev A., Murakami K., Nair S., Goldfarb A., Darst S. A., (2001) Structural Mechanism for Rifampicin Inhibition of Bacterial RNA Polymerase. *Cell* 104, 901–912
2. Chen X., Stewart P. S. (2002) Role of electrostatic interactions in cohesion of bacterial biofilms. *Appl Microbiol Biotechnol* **59**: 718-720
3. Chen, X. and P. S. Stewart. (1996). Chlorine penetration into artificial biofilm is limited by a reaction-diffusion interaction. *Environmental Science & Technology*
4. 30:2078-2083.
5. Costerton J W, Stewart P S, Greenberg E P, (1999) Bacterial Biofilms: A Common Cause of Persistent Infections. *Science* Vol. 284. no. 5418, pp. 1318 - 1322
6. Davidson, W. M. (2008) Visualizing spatial and temporal patterns of antimicrobial action against biofilms of *staphylococcus epidermidis* analyzed by time-lapse confocal microscopy flow cytometry, and mathematical modeling. Doctoral Thesis, Montana State University, Bozeman, MT.
7. Devore J., Farnum N., (1999). *Applied Statistics for Engineers and Scientists*. Brooks/Cole Publishing Company. Pacific Grove, CA.
8. Diggle SP, Stacey RE, Dodd C, Camara M, Williams P, Winzer K. 2006. The galactophilic lectin, LecA, contributes to biofilm development in *Pseudomonas aeruginosa*. *Environ Microbiol.* 8:1095-1104.
9. Dirckx P., Montana State University Center for Biofilm Engineering. Biofilm formation slide.
10. Findley W N, Lai SJ, Onaran K, (1989). *Creep and relaxation of nonlinear viscoelastic materials*. Dover Edition. Dover Publications, Inc. Mineola, NY.
11. Goldberg J B, Gorman W L, Flynn J L, Ohman D E (1993) A mutation in algN permits trans activation of alginate production by algT in *Pseudomonas* species. *J Bacteriol.* 175(5): 1303-1308
12. Gross M., Cramton S. E., **Götz F., Peschel A., (2001)** Key Role of Teichoic Acid Net Charge in *Staphylococcus aureus* Colonization of Artificial Surfaces, *Infection and Immunity.* 69(5):3423-2426

13. Habash M and Reid G (1999) Microbial biofilms: their development and significance for medical device-related infections. *Journal of Clinical Pharmacology*. **39** 887
14. Hennig S., Wai S. N., Ziebuhr W., (2007) Spontaneous switch to PIA-independent biofilm formation in an *ica*-positive *Staphylococcus epidermidis* isolate. *International Journal of Medical Microbiology* 297(2):117-122
15. Holleman, A. F.; Wiberg, E. (2001) *Inorganic Chemistry*. Academic Press. San Diego, CA.
16. Irving S H, Cozzarelli F A, (1997) *Elastic and Inelastic Stress Analysis*. Talyor & Francis. Philadelphia, Pa.
17. Jackson K. D., Starkey M., Kremer S., Parsek M. R., Wozniak D. J, (2004) Identification of *psl*, a Locus Encoding a Potential Exopolysaccharide That Is Essential for *Pseudomonas aeruginosa* PAO1 Biofilm Formation. *Journal of Bacteriology* 186(14): 4466-4475
18. Johnson, P. N., Amirtharajah A., (1982) Ferric chloride and alum as single and dual coagulents. *Journal AWWA*, 74(4):210-216
19. Klapper I, Rupp C J, Cargo R, Purevdorj B, Stoodley P (2002) A viscoelastic fluid description of bacterial biofilm material properties. *Biotech Bioeng* **80**: 289-296
20. Korstgens V, Flemming H C, Wingender J, Dorchard W, (2001) Uniaxial compression measurement device for investigation of the stability of biofilms. *Journal Microbial Method s* 46(1): 9-17
21. Lewis K. (2001) Riddle of Biofilm Resistance. *Antimicrob Agenns Chemother* 45(4): 999-1007
22. Matsukawa M., Greenberg E. P., (2004) Putative exopolysaccharide synthesis genes influence *Pseudomonas aeruginosa* biofilm development. *J Bacteriol*. **186**:4449-4456.
23. Marrie T.J., Nelligan J.,and Costerton J.W. (1982) A scanning and transmission electron microscopic study of an infected endocardial pacemaker lead. *Circulation* 66:1339-1341

24. Mayer C, Moritz R, Kirschner C, Dorchard W, Maibaum R, Wingender J, Flemming HC (1999) The role of intermolecular interactions: studies on model systems for bacterial biofilms. *Int J Biol Macromol* 26:3-16
25. Munson B. R., Young D. F., Okiishi T. H., (2002) *Fundamentals of Fluid Mechanics*. John Wiley & Sons. Hoboken, NJ.
26. Poppele E H, Hozalski R M, (2003) Micro-canilever method for measuring the tensile strength of biofilms and microbial flocs. *Journal of Microbiological Methods* 55(3): 607-615
27. Riddle C., Lemons C. L., Papich M. G., Altier C., (2000) Evaluation of Ciprofloxacin Representative of Veterinary Fluoroquinolones in Susceptibility Testing. *J Clin Microbiol* 38(4): 1636–1637
28. Rupp M. E., Ulphani J. S., Fey P. D., Mack D., (1999) Characterization of *Staphylococcus epidermidis* Polysaccharide Intercellular Adhesin/Hemagglutinin in the Pathogenesis of Intravascular Catheter-Associated Infection in a Rat Model. *Infection and Immunity* 67(5): 2656-2659
29. Sadovskaya, I., Vinogradov E., Flahaut S. F., Kogan G., Jabbouri S., (2005) Extracellular Carbohydrate-Containing Polymers of a Model Biofilm Producing Strain, *Staphylococcus epidermidis* RP62A. *Infection and Immunity* 73(5): 3007-3017
30. Sigma-Aldrich: Surfactants- structures, information, and application http://www2.sigmaaldrich.com/Area_of_Interest/Biochemicals/BioUltra/Detergents_Surfactants.html?cm_mmc=wiki--social--surfactants--Surfactants
31. Silo-Suh L., Suh S., Sokol P. A., Ohman D. E., (2002) A simple alfalfa seedling infection model for *Pseudomonas aeruginosa* stains associated with cystic fibrosis shows AlfT (sigma-22) and RhlR contribute to pathogenesis. *PNAS* 99(24): 15699-15704
32. Stoodley P., Cargo R., Rupp C. J., Wilson S. and Klapper I., (2002) Biofilm material properties as related to shear-induced deformation and detachment phenomena. *Journal of Industrial Microbiology and Biotechnology* 29(6):361-367
33. Sundheim G., Langsrud S., Heir E., Holck A. L., (1998) Bacterial resistance to disinfectants containing quaternary ammonium compounds *International Biodeterioration & Biodegradation* 41(3-4): 235-239

34. Tortora G. J., Funke B. R., Case C. L. (2005) *Microbiology an Introduction*. Benjamin Cummings, San Francisco, CA.
35. Towler B. W., Rupp C. J, Cunningham A B, and Stoodley P (2003) Viscoelastic Properties of a Mixed Culture Biofilm from Rheometer Creep Analysis. *Biofouling* **19**: 279-285
36. Towler, B. (2004) Modeling the non-linear response of mixed culture biofilm structuresto turbulent flow. Doctoral Thesis, Montana State University, Bozeman, MT.
37. Van Benschoten J. E. and Edzwald J. K, (1990) Chemical aspects of coagulation using aluminum salts- I. Hydrolytic reactions of alum and polyaluminum chloride. *Wat. Res* 24(12): 1519-1526
38. Vance D., (1994) Iron: The environmental impact of a universal element. *NATL. ENVIRON. J.* 4(33): 24-25
39. Van der Wende E, Characklis WG, Smith DB (1989) Biofilms and bacterial drinking water quality. *Water Research* **23** 1313-1322
40. Vinogradov A. M., Winston M. Rupp C. J., Stoodley P., (2004) Rheology of biofilms formed from the dental plaque pathogen *Streptococcus mutans*. *Biofilms***1**: 49-56
41. Walters III M. C., Roe F., Bugnicourt A., Franklin M. J., Stewart P. S., (2003) Contributions of Antibiotic Penetration, Oxygen Limitations, and Low Metabolic Activity to Tolerance of *Pseudomonas aeruginosa* Biofilms to Ciprofloxacin and Tobramycin. *Antimicrobial Agents and Chemotherapy* 47(1): 317-323
42. Wloka M, Rehage H, Flemming H C, Wingender J (2005) Structure and rheological behavior of the extracellular polymeric substance network of mucoid *Pseudomonas aeruginosa* biofilms. *Biofilms* **2**: 275-283
43. Zheng Z. and Stewart P. S., (2002) Penetration of Rifampin through *Staphylococcus epidermidis* Biofilms. *Antimicrobial Agents and Chemotherapy* 46(3): 900-903

APPENDICES

APPENDIX A

DATA TABLE OF RESULTS FOR ALL TREATMENTS

FRD1 MgCl₂ 0.2 molar

Test #	G _K (Pa)	η _K (Pa.s)	η _M (Pa.s)	G _M (Pa)	Max γ	WGT ERR	Gap (μm)
1	599	19,442	117,804	1,443	0.0708	0.0181	100
2	1,066	12,522	67,899	3,340	0.0763	0.0174	85
3	1,011	63,428	175,212	4,361	0.0462	0.0119	80
4	282	7,056	43,876	1,576	0.1490	0.0234	115
5	707	18,115	99,414	3,271	0.0630	0.0251	95
6	991	26,645	241,051	5,348	0.0343	0.0250	90
7	493	14,276	82,476	2,295	0.0870	0.0216	90
8	411	8,518	63,690	1,460	0.1075	0.0248	90
9	900	36,211	132,794	3,976	0.0516	0.0146	85
10	1,532	40,463	134,493	2,455	0.0466	0.0181	95
11	2,750	51,445	362,125	7,018	0.0184	0.0249	75
12	1,907	67,171	321,764	6,251	0.0229	0.0197	70
13	306	9,598	34,696	759	0.1895	0.0162	80
14	241	9,442	25,230	559	0.2533	0.0128	70
15	1,121	39,917	214,019	5,611	0.0358	0.0167	80
16	2,715	29,981	211,771	7,363	0.0244	0.0343	90
17	374	10,213	63,928	1,480	0.1087	0.0219	95
18	1,211	18,201	204,618	5,074	0.0322	0.0407	75
Average	1,034	26,814	144,270	3,536	0.0787	0.0215	87
STDV	766	19,092	98,263	2,184	0.0634	0.0073	11
Control							
1	424	11,535	65,548	1,658	0.1016	0.0219	120
2	313	10,538	39,376	1,853	0.1581	0.0172	120
3	149	3,946	13,786	489	0.4299	0.0142	120
4	173	3,497	15,389	713	0.3739	0.0148	140
5	255	6,057	33,965	1,254	0.1897	0.0191	135
6	759	29,514	117,674	2,841	0.0609	0.0122	110
7	375	12,298	59,628	1,044	0.1224	0.0214	100
8	1,567	87,210	320,675	6,910	0.0255	0.0174	95
Average	502	20,574	83,255	2,095	0.1828	0.0173	118
STDV	471	28,158	101,567	2,080	0.1454	0.0035	16

FRD1 ALCL₃ 0.2 M

NAME	G _K (Pa)	η _K (Pa.s)	η _M (Pa.s)	G _M (Pa)	Max γ	WGT ERR	Gap (μm)
1	2,276	56,548	487,940	6,831	0.0167	0.0238	80
2	1,097	37,019	423,940	2,857	0.0287	0.0197	80
3	3,608	301,586	7,425,004	11,132	0.0063	0.0401	85
4	559	18,551	160,961	1,744	0.0604	0.0237	95
5	7,389	47,690	1,066,905	4,505	0.0089	0.0480	70
6	2,834	95,637	657,950	4,152	0.0158	0.0177	110
7	1,329	69,564	377,315	3,363	0.0287	0.0191	120
8	417	8,240	73,206	1,140	0.0999	0.0272	122
9	593	15,942	108,948	1,140	0.0730	0.0255	135
10	1,560	48,629	385,440	1,959	0.0271	0.0269	120
11	676	19,241	112,839	1,328	0.0676	0.0199	135
12	714	16,508	153,497	1,524	0.0548	0.0272	140
13	2,710	99,987	1,057,805	4,877	0.0127	0.0180	102
14	893	37,547	208,841	4,517	0.0395	0.0176	122
15	6,973	341,359	2,542,139	6,060	0.0065	0.0428	105
16	521	14,000	96,180	812	0.0857	0.0239	125
17	2,990	81,124	636,819	5,741	0.0142	0.0174	120
18	547	7,761	78,963	964	0.0894	0.0340	115
19	1,523	86,994	18,426,623	2,956	0.0152	0.0455	110
20	1,742	57,221	294,850	3,577	0.0267	0.0166	135
21	631	28,639	127,650	2,608	0.0633	0.0159	125
22	12,261	660,935	1,145,419	6,388	0.0079	0.0603	85
23	547	18,770	92,511	1,130	0.0833	0.0224	110
24	6,342	147,054	1,247,757	9,382	0.0073	0.0250	110
Average	2,531	96,523	1,557,896	3,779	0.0392	0.0274	111
STDV	2,928	147,014	3,899,879	2,738	0.0310	0.0117	20
Control							
1	654	6,359	64,237	987	0.0878	0.0434	90
2	328	5,677	50,583	783	0.1396	0.0267	95
3	302	4,861	31,174	541	0.1950	0.0237	120
4	331	8,050	56,843	617	0.1353	0.0267	110
5	491	14,910	96,874	1,546	0.0808	0.0242	100
6	479	10,268	64,765	956	0.1049	0.0269	120
7	136	3,245	12,004	267	0.5027	0.0158	110
8	1,209	20,315	77,201	3,229	0.0697	0.0147	150
9	312	7,005	35,983	671	0.1829	0.0198	140

10	120	2,284	10,310	377	0.5402	0.0215	150
11	159	4,943	13,517	354	0.4414	0.0145	130
12	2,433	60,097	234,747	6,613	0.0242	0.0308	135
13	159	6,730	10,918	229	0.5390	0.0110	150
14	251	7,395	25,247	529	0.2546	0.0146	140
15	334	7,111	28,105	1,048	0.1979	0.0208	132
16	253	6,691	27,468	565	0.2342	0.0174	140
Average	497	10,996	52,499	1,207	0.2331	0.0220	126
STDV	581	13,816	55,054	1,612	0.1749	0.0080	20

FRD1 CaCl₂ 0.2 M

Test #	G _K (Pa)	η _K (Pa.s)	η _M (Pa.s)	G _M (Pa)	Max γ	WGT ERR	Gap (μm)
1	1,668	96,899	1,136,639	1,802	0.0209	0.0303	90
2	764	20,015	132,596	1,232	0.0595	0.0255	120
3	1,615	50,092	330,995	5,826	0.0240	0.0183	110
4	2,071	47,741	507,416	2,582	0.0200	0.0289	100
5	2,263	65,186	735,269	8,836	0.0138	0.0243	90
6	1,939	63,372	365,212	1,332	0.0292	0.0220	97
7	988	22,426	121,188	585	0.0706	0.0225	110
8	1,701	82,331	292,698	605	0.0462	0.0154	125
9	305	3,776	30,213	318	0.1990	0.0398	125
10	893	4,670	73,760	1,338	0.0710	0.0468	112
11	3,014	157,945	966,707	10,735	0.0111	0.0207	125
12	839	23,970	183,466	470	0.0674	0.0270	115
13	1,893	33,065	285,088	2,974	0.0251	0.0286	100
14	1,562	25,447	216,023	905	0.0408	0.0316	110
15	1,130	29,486	164,748	592	0.0590	0.0263	115
16	1,343	40,229	186,438	673	0.0518	0.0232	105
17	880	19,777	83,707	342	0.1008	0.0280	120
18	6,369	77,168	234,591	4,559	0.0412	0.0132	120
Average	1,735	47,978	335,931	2,539	0.0528	0.0262	111
STDV	1,327	38,213	311,169	3,054	0.0437	0.0080	11
Control							
1	1,712	104,038	313,167	9,339	0.0258	0.0273	162
2	64	729	5,631	821	0.9115	0.0266	135
3	121	1,670	11,915	347	0.4576	0.0363	120
4	104	2,584	10,908	255	0.5649	0.0187	145
5	688	62,524	62,480	9,408	0.1073	0.0264	175

6	62	1,685	3,281	163	1.6456	0.0087	185
7	60	1,942	3,606	140	1.5562	0.0093	170
8	68	2,131	4,380	170	1.2895	0.0094	200
9	239	1,015	8,656	433	0.5563	0.0210	190
10	542	23,078	111,991	2,324	0.0716	0.0184	115
11	146	3,559	9,040	330	0.6213	0.0108	130
Average	346	18,632	49,551	2,157	0.7098	0.0194	157
STDV	500	33,885	93,810	3,622	0.5765	0.0092	30

FRD1 FeCl₂ 0.2 M

Test #	G _K (Pa)	η _K (Pa.s)	η _M (Pa.s)	G _M (Pa)	Max γ	WGT ERR	Gap (μm)
1	3,193	33,879	407,263	4,934	0.0157	0.0469	35
2	2,788	26,988	249,597	4,645	0.0223	0.0470	40
3	2,365	71,353	469,234	5,798	0.0170	0.0272	50
4	911	22,583	143,682	1,110	0.0562	0.0230	65
5	1,648	21,511	129,125	1,352	0.0467	0.0330	55
6	565	23,081	70,710	413	0.1160	0.0216	97
7	565	23,050	70,708	413	0.0414	0.0605	95
8	570	87,020	260,226	1,903	0.0486	0.0139	100
9	195	9,703	25,144	121	0.3636	0.0145	120
10	1,058	118,360	113,601	4,788	0.0723	0.0312	112
11	583	11,682	91,928	596	0.0878	0.0312	102
Average	1,203	37,434	169,268	2,173	0.0740	0.0292	73
STDV	1,030	35,315	145,013	2,192	0.0987	0.0145	31
Control							
1	5,642	42,397	415,096	2,424	0.0176	0.0357	45
2	281	6,576	29,408	500	0.2109	0.0241	50
3	546	8,385	88,952	1,267	0.0761	0.0364	45
4	302	7,568	38,238	855	0.1719	0.0197	105
5	161	4,155	13,030	377	0.4433	0.0163	102
6	219	4,583	20,035	509	0.2907	0.0215	105
Average	1,192	12,277	100,793	988	0.2017	0.0256	75
STDV	2,184	14,847	156,307	774	0.1529	0.0085	31

FRD1 EDTA 0.2 M

Test #	G_K (Pa)	η_K (Pa.s)	η_M (Pa.s)	G_M (Pa)	Max γ	WGT ERR	Gap (μm)
1	125	822	2306	928	1.9515	0.0119	132
2	not linear				30.7270	0.0759	147
3	3447	423912	322244	15500	0.0234	0.0223	165
5	not linear				0.0727	0.0124	150
6	2128	137035	426138	9819	0.0201	0.0213	95
7	not linear				9.8055	0.0521	160
8	369	4833	11	2	397.2100	0.0078	150
9	35	457	20	1	221.3400	0.0130	135
10	297	8272	25761	331	0.2305	0.0310	75
11	650	25347	70994	701	0.1015	0.0165	75
12	3640	98965	217823	3875	0.0231	0.0427	155
13	122	2923	1867	101	2.5234	0.0077	105
Average	1202	78063	118574	3473	55.3357	0.0262	129
STDV	1473	138823	162810	5529	124.7081	0.0209	33
Control							
1	2857	256079	361805	3785	0.0213	0.0083	125
2	171	6227	10295	224	0.5625	0.0112	145
3	180	8884	10100	235	0.5580	0.0117	125
4	142	7379	7215	147	0.7735	0.0141	165
5	166	12210	9463	218	0.6188	0.0063	185
6	205	8848	14029	230	0.4262	0.0150	170
7	183	6019	6746	148	0.7723	0.0152	195
8	693	50842	98874	804	0.0775	0.0196	95
9	369	18422	26824	482	0.2203	0.0139	100
10	264	9362	16375	280	0.3567	0.0149	140
11	3643	473648	136586	11412	0.0452	0.0273	122
12	6369	77168	234591	4559	0.0217	0.0251	162
Average	1270	77924	77742	1877	0.3712	0.0152	144
STDV	1989	143481	114185	3361	0.2890	0.0062	32

FRD1 NaCl 0.2 M

Test #	G_K (Pa)	η_K (Pa.s)	η_M (Pa.s)	G_M (Pa)	Max γ	WGT ERR	Gap (μm)
1	206	7,858	25,451	854	0.2651	0.0112	150
2	1,006	95,963	199,823	7,536	0.0466	0.0321	140
3	361	8,407	29,265	1,663	0.1869	0.0150	140
4	296	9,655	50,884	1,171	0.1460	0.0152	135
5	144	6,721	10,091	517	0.5593	0.0101	170
6	1,340	164,783	550,748	12,168	0.0266	0.0435	145
7	283	19,605	18,210	1,803	0.3267	0.0136	125
8	3,546	270,422	480,481	18,472	0.0154	0.0263	113
9	195	9,157	26,074	829	0.2636	0.0131	120
10	1,026	37,145	146,635	5,043	0.0463	0.0188	95
11	665	5,826	43,691	1,420	0.1170	0.0282	110
12	111	2,925	5,976	323	0.8945	0.0109	150
13	3,079	22,997	274,659	20,218	0.0183	0.0382	103
14	240	6,970	31,570	932	0.2033	0.0171	140
15	547	283,382	19,344	6,967	0.2775	0.0158	160
16	238	10,101	26,737	785	0.2445	0.0103	140
Average	830	60,120	121,228	5,044	0.2273	0.0200	134
STDV	1,038	94,800	172,270	6,503	0.2289	0.0105	21
Control							
1	180	4,981	11,949	385	0.4784	0.0102	120
2	171	5,290	18,765	704	0.3259	0.0159	160
3	297	10,738	40,893	1,375	0.1714	0.0128	160
4	946	85,949	284,257	8,362	0.0362	0.0315	145
5	577	30,195	100,895	5,625	0.0734	0.0163	135
6	163	5,218	15,436	496	0.3953	0.0127	130
7	844	13,250	91,287	2,787	0.0673	0.0216	125
8	298	9,570	38,730	1,033	0.1728	0.0172	110
9	266	7,239	34,647	963	0.1895	0.0170	145
10	677	37,741	215,803	5,802	0.0460	0.0201	145
11	279	8,209	33,122	692	0.1997	0.0167	145
12	1,905	168,863	401,959	19,886	0.0261	0.0498	150
Average	550	32,270	107,312	4,009	0.1818	0.0201	139
STDV	505	48,919	126,301	5,647	0.1488	0.0108	15

FRD1 AlCl₃ 0.02 M

Test #	G _K (Pa)	η _K (Pa.s)	η _M (Pa.s)	G _M (Pa)	Max γ	WGT ERR	Gap (μm)
1	330	7,752	40,887	599	0.1599	0.0249	115
2	860	44,021	363,595	6,035	0.0319	0.0173	120
3	512	13,549	120,780	932	0.0783	0.0201	125
4	9,041	169,898	272,107	5,327	0.0203	0.0125	95
5	190	6,258	46,641	159	0.2518	0.0222	85
6	5,060	140,790	1,037,848	6,434	0.0092	0.0258	95
7	2,220	29,880	346,823	2,597	0.0228	0.0304	70
8	1,334	3,850	23,247	1,184	0.2186	0.0142	80
9	1,895	40,107	186,993	2,753	0.0348	0.0153	70
10	150	1,117	14,008	101	0.4746	0.0376	100
11	728	10,024	119,159	1,179	0.0613	0.0353	95
12	1,212	42,354	146,126	1,725	0.0485	0.0152	65
13	371	28,845	75,755	137	0.1998	0.0153	100
14	6,282	116,708	920,704	5,090	0.0097	0.0383	70
Average	2,156	46,797	265,334	2,447	0.1158	0.0232	92
STDV	2,708	54,852	323,580	2,315	0.1329	0.0091	19
Control							
1	1,730	66,970	363,657	2,257	0.0238	0.0461	55
2	105	2,414	8,790	276	0.6454	0.0196	50
3	146	2,592	14,096	353	0.4148	0.0240	50
4	216	8,728	26,740	645	0.2508	0.0137	55
5	251	6,095	23,999	474	0.2639	0.0159	125
6	179	3,386	13,821	1,868	0.3647	0.0251	120
7	333	7,127	48,698	1,369	0.1312	0.0267	125
8	274	5,803	29,671	538	0.2115	0.0228	140
Average	404	12,889	66,184	973	0.2883	0.0242	90
STDV	540	21,966	120,838	758	0.1897	0.0099	41

FRD1 Barquat 50 mg/l

Test #	G_K (Pa)	η_K (Pa.s)	η_M (Pa.s)	G_M (Pa)	Max γ	WGT ERR	Gap (μm)
1	34	620	446	99	10.5690	0.0037	155
2	28	474	2,130	147	2.4173	0.0217	155
3	321	17,603	9,882	4,666	0.5166	0.0190	150
4	12	146	408	54	11.8380	0.0118	160
5	1	87,812	69	1,407	65.3220	0.0093	155
6	1	15,927	241	1,406	19.4940	0.0066	165
7	19	390	1,106	88	4.7211	0.0131	165
8	1	3,309,853	12,118	10,428	0.4383	0.0836	165
9	1	2,998,760	33,973	12,813	0.1428	0.0496	170
10	184	12,548	7,503	2,788	0.7100	0.0241	165
11	1	2,117,608	32,404	7,995	0.1629	0.0224	155
12	31	1,021	6,266	128	1.2335	0.0185	170
13	36	265	3,295	133	1.4555	0.0448	165
14	6,333	247,746	120,186	12,960	0.0394	0.0143	165
15	19	470	2,702	174	2.3442	0.0214	160
16	27	1,513	1,376	92	3.9838	0.0053	200
17	396	1,079	11,802	364	0.3900	0.0235	200
18	41	633	1,966	234	2.5819	0.0115	180
19	9,653	146,472	458,485	24,495	0.0105	0.0250	200
20	34	729	1,191	95	4.2713	0.0076	200
21	143	624	8,024	634	0.5604	0.0302	190
22	72	1,805	4,366	228	1.2199	0.0122	160
Average	790	2,661	3,454	1,152	6.1101	0.0218	170
STDV	2,389	996,917	98,535	6,316	14.0721	0.0181	17
Control							
1	446	3,405	31,556	1,535	0.1614	0.0243	130
2	256	8,037	19,897	1,214	0.2883	0.0092	132
3	1,002	13,925	88,850	2,980	0.0664	0.0134	120
4	846	94,441	74,744	3,305	0.0951	0.0238	140
5	886	65,596	292,046	4,057	0.0393	0.0239	132
6	135	4,307	9,601	378	0.5961	0.0094	132
7	495	30,951	57,150	7,528	0.1119	0.0153	140
8	278	4,626	16,740	541	0.3192	0.0167	145
9	84	3,049	6,150	187	0.9616	0.0104	170
10	7,752	80,098	531,012	22,221	0.0097	0.0214	160

11	5,734	257,944	345,264	25,316	0.0152	0.0135	155
Average	1,629	51,489	133,910	6,297	0.2422	0.0165	141
STDV	2,587	76,346	175,434	8,921	0.2956	0.0060	15

Staph. epi. CaCl₂ 0.2 M

Test #	G _K (Pa)	η _K (Pa.s)	η _M (Pa.s)	G _M (Pa)	Max γ	WGT ERR	Gap (μm)
1	2,826	49,045	405,038	1,064	0.0282	0.0193	72
2	224	3,519	19,078	349	0.3350	0.0099	80
3	511	6,718	66,381	534	0.1217	0.0103	75
4	2,059	37,888	456,993	1,990	0.0227	0.0192	75
5	1,512	21,002	292,209	812	0.0399	0.0302	62
6	521	3,489	76,359	609	0.0951	0.0395	75
7	1,379	16,839	283,807	1,275	0.0357	0.0259	72
8	381	6,660	34,260	473	0.1863	0.0168	80
9	4,902	133,531	448,863	1,306	0.0225	0.0216	75
Average	1,590	30,965	231,443	935	0.0986	0.0214	74
STDV	1,517	41,654	183,708	527	0.1049	0.0094	5
Control							
1	576	8,584	106,431	613	0.0914	0.0110	120
2	3,889	95,132	781,467	2,737	0.0146	0.0204	85
3	3,629	91,419	406,594	1,654	0.0215	0.0303	85
4	2,736	48,824	294,134	1,505	0.0281	0.0227	95
Average	2,707	60,990	397,157	1,627	0.0389	0.0211	96
STDV	1,504	40,767	284,557	871	0.0355	0.0079	17

Staph. epi EDTA 0.2 M

Test #	G _K (Pa)	η _K (Pa.s)	η _M (Pa.s)	G _M (Pa)	Max γ	WGT ERR	Gap (μm)
1	25497	1500975	5360259	8944	0.0195	0.0212	70
2	53998	1999206	8316803	29697	0.008549	0.0182	75
3	21953	741859	3155853	12455	0.0207	0.0141	70
4	11092	170750	1361351	5048	0.0454	0.0262	80
5	15126	1240448	2482982	4720	0.0371	0.0176	75
6	22935	1112249	4127570	9315	0.0221	0.0138	75
7	17168	1180961	2998491	15261	0.0213	0.0144	65
8	7197	154364	1057202	3830	0.0618	0.0243	75
Average	21871	1012602	3607564	11159	0.0296	0.0187	73

STDV	14370	634786	2357626	8477	0.0173	0.0048	5
Control							
1	20454	678167	6074163	10311	0.0196	0.0139	80
2	23039	831493	4834467	8785	0.0213	0.0125	80
3	17676	904065	3430031	6268	0.0286	0.0159	80
4	39010	526813	6736192	17257	0.0122	0.0226	75
Average	25044	735134	5268713	10655	0.0204	0.0162	79
STDV	9564	167795	1457345	4706	0.0067	0.0045	3

Staph. epi. FeCl₃ 0.2 M

Test #	G _K (Pa)	η _K (Pa.s)	η _M (Pa.s)	G _M (Pa)	Max γ	WGT ERR	Gap (μm)
1	42214	539764	3437139	25754	0.0134	0.0228	65
2	14196	685386	2304347	8973	0.0294	0.0123	75
3	8115	695903	914662	3389	0.0711	0.0126	60
4	12428	881776	3385065	11781	0.0252	0.0097	60
5	21368	1165788	3785278	14106	0.0183	0.0173	50
6	19824	3244587	7938740	9766	0.0174	0.0174	75
7	19563	3258762	2318985	5480	0.0343	0.0171	55
8	14060	348117	1745263	9016	0.0319	0.0212	55
9	10096	488048	1793205	7904	0.0383	0.0117	60
Average	17985	1256459	3069187	10686	0.031	0.016	62
STDV	10153	1155423	2050340	6467	0.017	0.004	9
Control							
1	65420	1330129	10631474	34944	0.0071	0.0323	55
2	44592	590170	7468990	21657	0.0099	0.0307	60
3	29921	315454	3587684	10666	0.0187	0.0274	65
4	16878	622295	3244862	8960	0.0261	0.0122	70
Average	39203	714512	6233253	19057	0.015	0.026	63
STDV	20824	432896	3502423	11993	0.009	0.009	6

Staph. epi. Glutaraldehyde 50 mg/l

Test #	G _K (Pa)	η _K (Pa.s)	η _M (Pa.s)	G _M (Pa)	Max γ	WGT ERR	Gap (μm)
1	336477	4129054	5328032	11165	0.0129	0.045975	80
2	53598	18269754	12572175	10831	0.0120	0.029894	85

3	23453	163743	7087902	6718	0.0276	0.014768	90
4	29203	742828	5515060	5206	0.0281	0.014635	100
5	28398	223689	5820380	7244	0.0224	0.019141	95
6	34380	1529016	8352850	5905	0.0287	0.015891	100
7	19956	100203	3927368	5650	0.0309	0.022565	102
8	40163	422942	6741646	10963	0.0148	0.023622	105
9	33487	393358	3993584	5593	0.0269	0.016636	115
Average	66568	2886065	6593222	7697	0.0227	0.0226	96.8889
STDV	101693	5907398	2653682	2542	0.0075	0.0101	10.7057
Control							
1	72465	456988	7009366	27301	0.0085	0.0217	60
2	19263	280887	2199018	11491	0.0243	0.0235	65
3	168747	1477728	2326022	9243	0.0193	0.0600	70
4	25654	1058972	5014383	6306	0.0250	0.0104	80
5	32698	1456787	13461218	8255	0.0170	0.0157	75
6	19878	248477	2756430	8181	0.0256	0.0196	90
7	36662	977684	3528616	8001	0.0228	0.0112	85
Average	53624	851075	5185008	11254	0.020	0.023	75
STDV	53907	526367	4032878	7247	0.006	0.017	11

Staph. epi. NaCl 0.2 M

Test #	G_K (Pa)	η_K (Pa.s)	η_M (Pa.s)	G_M (Pa)	Max γ	WGT ERR	Gap (μm)
1	1821	43845	92916	838	0.4507	0.0181	90
2	34113	542699	3996421	12747	0.0168	0.0202	85
3	8509	187307	1277033	4978	0.0486	0.0394	90
4	13032	294463	1501204	4383	0.0467	0.0200	75
5	11928	182326	1401607	4642	0.0449	0.0312	70
6	2141	27637	226369	1322	0.2136	0.0355	70
7	10240	216967	1175939	3680	0.0571	0.0194	77
Average	11684	213606	1381641	4656	0.125	0.026	80
STDV	10843	173169	1284555	3922	0.157	0.009	9
Control							
1	22590	1039370	7171031	14412	0.016	0.014	100
2	21797	781991	3200327	6858	0.027	0.014	100
3	14881	1136861	1255594	4332	0.050	0.016	95
4	31552	2062807	4307768	12112	0.016	0.049	90
Average	22705	1255257	3983680	9428	0.027	0.023	96

STDV	6839	558791	2471190	4641	0.016	0.017	5
------	------	--------	---------	------	-------	-------	---

Staph. epi.

Barquat 50 mg/l

Test #	G_K (Pa)	η_K (Pa.s)	η_M (Pa.s)	G_M (Pa)	Max γ	WGT ERR	Gap (μm)
1	1945	19920	78392	1078	0.4734	0.0229	75
2	1507	13257	71789	1240	0.5093	0.0188	70
3	2806	47314	165246	1596	0.2617	0.0112	70
4	NOT linear				70821.0000	0.0000	80
5	NOT linear				7104.1000	0.0000	75
6	5838	77107	412568	2380	0.1083	0.0434	70
7	Not linear				1194.0000	0.0000	70
Average	3024	39400	181999	1573	11302.9218	0.0138	73
STDV	1952	29140	159503	580	26373.0153	0.0161	4
Control							
1	31797	1233757	6003905	10095	0.0177	0.0104	70
2	19046	764435	2582485	4209	0.0384	0.0120	70
3	49289	1110503	6754380	15920	0.0118	0.0218	70
4	18828	466025	1909389	6158	0.0347	0.0166	70
Average	29740	893680	4312540	9096	0.0256	0.0152	70
STDV	14374	347495	2421537	5167	0.0129	0.0051	0

Staph. epi. rifampin 0.1 mg/l

Test #	G_K (Pa)	η_K (Pa.s)	η_M (Pa.s)	G_M (Pa)	Max γ	WGT ERR	Gap (μm)
1	2052	29150	168015	1289	0.2587	0.0363	60
2	7441	197517	907720	3520	0.0639	0.0393	65
3	809	10922	30887	505	1.058	0.0363	55
4	2584	25897	227364	2165	0.1769	0.0417	50
5	3165	19362	354766	2591	0.1195	0.0625	55
6	8062	172498	1257943	5373	0.0478	0.0371	50
7	8553	12792	829137	15862	0.0443	0.0403	55
8	3886	7736	515962	10878	0.0702	0.0637	50
9	13992	740989	1231717	4901	0.0460	0.0186	55
Average	5616	135207	613724	5231	0.2095	0.0418	55
STDV	4215	238627	460165	5028	0.3264	0.0139	5.00

Control							
1	15767	219153	1498499	6493	0.0358	0.0353	85
2	19481	1267613	3042431	10033	0.0228	0.0282	85
3	28139	1410475	3960645	10492	0.0181	0.0444	85
Average	21129	965747	2833859	9006	0.0256	0.0360	85
STDV	6348	650503	1244254	2189	0.0091	0.0081	0

Staph. epi. Urea 0.2 M

Test #	G_K (Pa)	η_K (Pa.s)	η_M (Pa.s)	G_M (Pa)	Max γ	WGT ERR	Gap (μm)
1	15657	413538	3351978	6270	0.0300	0.0140	65
2	7259	824529	2184110	5186	0.0388	0.0530	90
3	3927	22751	511413	3735	0.0949	0.0386	95
4	72	397	5165	149	5.8300	0.0649	85
5	4835	1302526	18051	123	1.7003	0.1057	65
6	553	9886	1696	17	17.6110	0.0625	95
Average	5384	428938	1012069	2580	4.218	0.056	83
STDV	5710	537425	1422835	2838	6.933	0.031	14
Control							
1	26092	1115937	3340144	9131	0.0215	0.0199	110
2	38923	519960	6327605	17741	0.0115	0.0324	105
3	39552	711171	7185410	18331	0.0111	0.0343	95
4	29648	3759721	5538370	7251	0.0205	0.0248	90
Average	33554	1526697	5597882	13114	0.0162	0.0279	100
STDV	6726	1509274	1648602	5741	0.0056	0.0067	9

FRD1 urea 0.2 M

Test #	G_K (Pa)	η_K (Pa.s)	η_M (Pa.s)	G_M (Pa)	Max γ	WGT ERR	Gap (μm)
1	215	23,975	18,846	394	0.3613	0.0095	160
2	13	133	785	100	5.8494	0.0312	175
3	112	1,649	12,065	519	0.4402	0.0371	150
4	161	18,952	460	141	10.0620	0.0028	160
5	67	857	2,383	1,026	2.0481	0.0074	150
6	362	22,886	29,960	2,313	0.2158	0.0187	150
7	1	69,094	314	1,534	14.8540	0.0096	195

8	546	17,454	59,383	5,475	0.0970	0.0214	190
9	365	3,796	43,627	762	0.1307	0.0460	185
10	179	5,051	16,719	914	0.3448	0.0148	180
11	242	8,298	9,719	461	0.5349	0.0076	190
12	2,166	238,156	32,009	16,797	0.1583	0.0173	180
13	196	1,829	3,446	1,579	1.4041	0.0029	195
14	2,747	122,058	226,445	5,310	0.0267	0.0172	140
15	18	281	197	55	23.2740	0.0045	145
16	411	15,743	46,133	373	0.1524	0.0249	145
17	2,104	200,760	63,066	4,304	0.0977	0.0256	147
18	916	32,801	19,036	168	0.2655	0.0453	125
19	77	1,933	4,348	222	1.2089	0.0121	140
Average	574	41,353	30,997	2,234	3.2382	0.0187	163
STDV	824	69,685	51,507	3,927	6.2677	0.0134	22
Control							
1	185	6,345	17,130	786	0.3590	0.0096	135
2	118	2,021	7,090	378	0.7458	0.0127	132
3	234	8,496	25,243	714	0.2579	0.0119	135
4	1,483	16,737	127,796	4,827	0.0452	0.0166	165
5	468	13,349	92,473	2,089	0.0845	0.0180	160
6	1,504	134,858	533,290	17,284	0.0217	0.0321	160
7	88	869	4,393	240	1.0923	0.0245	140
8	114	4,812	9,284	322	0.6539	0.0077	160
Average	524	23,436	102,088	3,330	0.4075	0.0166	148
STDV	610	45,342	180,077	5,845	0.3879	0.0082	14

FRD1 FeCl₂ 0.2 M

Test #	G _K (Pa)	η _K (Pa.s)	η _M (Pa.s)	G _M (Pa)	Max γ	WGT ERR	Gap (μm)
1	6,821	596,905	4,752,069	8,868	0.0053	0.0405	90
2	2,092	57,785	323,425	1,532	0.0284	0.0211	95
3	6,809	165,212	799,908	4,303	0.0102	0.0354	90
4	10,728	878,098	1,897,083	19,900	0.0044	0.0225	83
5	1,842	101,905	420,270	1,965	0.0257	0.0131	95
6	1,684	248,926	548,371	6,186	0.0226	0.0278	115
7	951	91,633	160,365	673	0.0619	0.0170	105
8	604	27,838	74,077	532	0.1050	0.0197	110

9	2,442	103,139	360,186	3,318	0.0213	0.0207	115
10	5,886	101,802	498,966	4,550	0.0130	0.0248	100
11	1,741	136,581	332,299	1,025	0.0343	0.0177	115
12	2,635	242,583	388,416	1,945	0.0250	0.0069	100
13	5,821	217,882	1,198,258	5,531	0.0088	0.0338	85
14	3,782	226,630	694,793	8,044	0.0124	0.0162	95
15	1,532	44,794	158,957	1,400	0.0443	0.0202	95
16	10,559	519,229	1,086,655	8,392	0.0062	0.0492	90
17	2,830	199,116	355,641	4,214	0.0237	0.0269	100
18	4,112	244,073	708,972	3,579	0.0136	0.0118	95
19	7,220	27,363	882,406	8,963	0.0080	0.0729	90
20	1,356	59,396	234,914	1,416	0.0381	0.0163	97
Average	4,072	214,545	793,802	4,817	0.0256	0.0257	98
STDV	3,075	216,595	1,027,497	4,539	0.0238	0.0151	10
Control							
1	939	88,927	156,387	870	0.0552	0.0244	105
2	1,180	18,265	151,216	1,272	0.0496	0.0258	110
3	263	10,401	18,527	273	0.3277	0.0169	115
4	163	5,805	11,159	189	0.5368	0.0139	145
5	195	8,357	10,948	205	0.5309	0.0121	145
6	704	14,528	38,648	432	0.1415	0.0338	105
7	633	44,586	59,332	446	0.1165	0.0251	100
8	629	17,887	39,869	429	0.1409	0.0333	135
9	515	30,131	43,915	410	0.1455	0.0237	105
Average	580	26,543	58,889	503	0.2272	0.0232	118
STDV	342	26,314	56,160	352	0.1914	0.0077	18

FRD1 FeCl₃ 0.02 M

Test #	G _K (Pa)	η _K (Pa.s)	η _M (Pa.s)	G _M (Pa)	Max γ	WGT ERR	Gap (μm)
1	1,108	14,211	87,054	2,029	0.0574	0.0449	100
2	3,445	35,226	390,120	4,069	0.0167	0.0323	85
3	292	6,430	40,420	556	0.1655	0.0266	100
4	5,216	149,230	584,398	11,096	0.0108	0.0369	95
5	728	18,329	132,698	1,451	0.0595	0.0214	82
6	4,022	24,108	359,629	5,970	0.0151	0.0402	135
7	3,294	8	142,173	5,245	0.0326	0.0406	150
8	174	2,892	21,205	449	0.2758	0.0385	122

9	531	18,657	129,599	256	0.1131	0.0208	160
10	743	15,387	170,852	685	0.0627	0.0252	130
11	349	9,559	62,201	1,755	0.1155	0.0231	120
12	1,607	52,850	381,075	1,719	0.0284	0.0188	55
13	1,444	24,176	158,235	922	0.0486	0.0298	70
14	3,783	53,705	312,070	4,923	0.0190	0.0278	50
15	2,807	37,052	447,562	6,398	0.0159	0.0250	75
16	1,158	25,677	218,674	920	0.0443	0.0361	80
17	1,078	22,618	159,813	862	0.0538	0.0251	90
18	10,897	210,844	1,127,147	9,064	0.0066	0.0406	70
19	2,068	20,590	188,891	1,526	0.0327	0.0514	80
20	3,722	495,665	1,561,655	2,144	0.0117	0.0684	90
21	895	12,565	134,867	998	0.0563	0.0358	92
22	5,225	132,529	1,141,651	5,556	0.0088	0.0265	65
Average	2,481	62,832	361,454	3,118	0.0569	0.0334	95
STDV	2,467	110,323	405,550	3,014	0.0633	0.0116	30
control							
1	251	6,095	24,002	474	0.2639	0.0159	125
2	179	3,397	13,823	1,868	0.3647	0.0251	120
3	333	7,137	48,698	1,369	0.1312	0.0267	125
4	274	5,803	29,671	538	0.2115	0.0228	140
5	620	9,026	84,428	712	0.0905	0.0214	62
6	877	34,852	93,960	2,409	0.0657	0.0223	50
7	707	14,326	96,773	1,638	0.0694	0.0206	80
8	462	14,694	61,805	1,080	0.1122	0.0182	110
9	245	3,063	18,736	1,312	0.2706	0.0247	95
10	218	3,978	10,111	533	0.5115	0.0090	85
11	150	2,267	10,683	330	0.5042	0.0214	105
12	157	3,803	16,274	339	0.3822	0.0181	95
Average	373	9,037	42,414	1,050	0.2481	0.0205	99
STDV	240	9,123	33,583	676	0.1626	0.0048	27

FRD1 FeCl₃ 0.2 M

Test #	G _K (Pa)	η _K (Pa.s)	η _M (Pa.s)	G _M (Pa)	Max γ	WGT ERR	Gap (μm)
1	14,506	301,386	1,377,098	24,524	0.0048	0.0459	100
2	17,994	233,934	2,290,391	12,288	0.0045	0.0917	95
3	7,031	294,951	1,341,849	3,380	0.0098	0.0217	130

4	8,737	378,629	2,236,117	6,634	0.0058	0.0216	120
5	14,349	332,158	2,064,251	9,409	0.0047	0.0399	100
6	16,325	395,332	1,896,395	10,291	0.0048	0.0494	105
7	15,817	339,559	1,896,714	9,136	0.0049	0.0297	95
8	11,523	331,342	3,515,350	7,085	0.0048	0.0391	120
9	4,260	150,417	1,535,431	5,466	0.0092	0.0219	120
10	14,953	689,066	2,568,043	8,400	0.0046	0.0335	155
11	6,416	846,315	6,563,445	5,786	0.0053	0.0329	115
12	8,155	298,323	3,359,970	8,488	0.0050	0.0369	130
13	11,067	475,504	2,461,336	8,991	0.0048	0.0224	110
14	6,464	15	362,221	90,063	0.0136	0.0524	97
15	12,969	216,198	1,377,507	11,660	0.0053	0.0252	95
Average	11,371	352,209	2,323,075	14,773	0.0061	0.0376	112
STDV	4,290	203,958	1,419,585	21,375	0.0026	0.0181	17
control							
1	1,682	122,528	327,770	3,997	0.0271	0.0225	115
2	475	14,176	66,414	2,488	0.0965	0.0191	95
3	171	2,107	10,723	556	0.4829	0.0215	135
4	4,498	86,327	310,102	7,984	0.0190	0.0191	90
5	128	2,481	10,356	337	0.5467	0.0192	150
6	178	3,862	13,608	538	0.4136	0.0143	130
7	3,153	7,230	174,122	6,950	0.0311	0.0230	135
8	1,209	20,315	77,201	3,229	0.0697	0.0147	150
9	312	7,005	35,983	671	0.1829	0.0198	140
10	120	2,284	10,310	377	0.5402	0.0215	150
11	14,104	44	474,565	21,662	0.0106	0.0388	105
12	1,778	68,369	442,566	4,536	0.0201	0.0348	60
Average	2,317	28,061	162,810	4,444	0.2034	0.0224	121
STDV	3,960	40,940	178,143	6,021	0.2234	0.0073	29

FRD1 ciprofloxacin 1 mg/l

Test #	G_K (Pa)	η_K (Pa.s)	η_M (Pa.s)	G_M (Pa)	Max γ	WGT ERR	Gap (μm)
1	185	2,963	16,067	893	0.3217	0.0262	80
2	6,260	486,558	665,738	7,962	0.0115	0.0389	105
3	1	31,437,549	139	778	32.0940	0.0281	90
4	10	111	316	78	14.4120	0.0151	140
5	895	46,629	34,284	2,358	0.1502	0.0145	90

6	7	93,407	49	980	90.2540	0.0075	110
7	10	5,368,709,220,000	79	940	56.3060	0.0071	90
8	15	32	64	56	69.7520	0.0051	85
9	123	6,276	49	160	91.3550	0.0030	90
10	1,558	80,740	458	225	9.8452	0.0030	130
Average	906	536,874,137,427	71,724	1,443	36.4502	0.0148	101
STDV	1,951	1,697,733,793,277	209,018	2,391	37.3807	0.0124	20
Control							
1	189	7,823	17,231	504	0.3653	0.0077	295
2	234	8,637	27,444	760	0.2407	0.0124	320
3	184	5,993	18,813	420	0.3464	0.0113	315
4	98	1,834	5,318	273	0.9724	0.0149	295
Average	176	6,072	17,202	489	0.4812	0.0116	306
STDV	57	3,034	9,105	204	0.3320	0.0030	13

FRD1 chlorine 50 mg/l

Test #	G_K (Pa)	η_K (Pa.s)	η_M (Pa.s)	G_M (Pa)	Max γ	WGT ERR	Gap (μ m)
1	2,161	66,845	195,318	4,553	0.0331	0.0088	200
2	95	618	8,224	733	0.5635	0.0425	135
3	75	1,623	11,198	581	0.5538	0.0266	185
4	1,366	44,002	215,873	3,365	0.0332	0.0202	165
5	24	317	3,232	104	1.7507	0.0421	175
6	67	5,480	7,345	904	0.9172	0.0270	180
7	925	28,924	60,346	3,211	0.0800	0.0611	200
8	628	11,314	44,823	2,820	0.1071	0.0397	190
9	361	18,598	20,095	8,475	0.2574	0.0476	130
10	655	1,443	10,664	3,655	0.4206	0.0126	215
11	107	3,940	12,495	352	0.5281	0.0110	130
12	34	308	867	463	5.4858	0.0058	240
13	490	36,269	37,842	2,666	0.1703	0.0155	215
14	1,595	123,245	75,135	13,061	0.0696	0.0293	220
Average	613	24,495	50,247	3,210	0.7836	0.0278	184
STDV	674	34,940	69,649	3,626	1.4305	0.0167	35
control							
1	3,543	239,544	106,501	4,168	0.0501	0.0067	200
2	56	205	3,646	1,555	1.2648	0.0308	175

3	67	1,836	3,957	218	1.3522	0.0118	155
4	1186	4100	15185	564	0.2981	0.0232	200
5	91	2,428	7,128	924	0.7958	0.0094	210
6	5,214	93,718	279,343	16,523	0.0173	0.0230	135
7	127	7,083	10,355	405	0.5893	0.0061	210
8	7,385	170,862	981,764	6,640	0.0089	0.0218	175
Average	2,813	85,606	233,379	5,018	0.2932	0.0150	188
STDV	3,069	101,434	381,269	6,107	0.3336	0.0084	29

FRD1 glutaraldehyde 50 mg/l

Test #	G_K (Pa)	η_K (Pa.s)	η_M (Pa.s)	G_M (Pa)	Max γ	WGT ERR	Gap (μ m)
1	28	725	2,623	120	2.1622	0.0192	170
2	10	69	499	715	8.8737	0.0308	165
3	43	395	3,386	283	1.4792	0.0275	180
4	1	223,555	153	1,533	29.8280	0.0064	165
5	29	333	845	92	5.6681	0.0098	155
6	76,811,525	10,124	22,479	8,818	0.2333	0.0465	180
7	58	985	5,806	194	0.9573	0.0268	160
8	98,637,359	10,712	664	5,342	7.0372	0.1060	150
9	84	722	10,624	190	0.5477	0.0530	125
10	1,965	56,553	182,200	19,908	0.0329	0.0285	120
Average	17,545,110	30,417	22,928	3,719	5.6819	0.0354	157
STDV	37,343,793	70,034	56,383	6,388	9.0394	0.0286	21
1	3,739	96,389	141,315	15,254	0.0327	0.0275	140
2	762	7,685	54,870	5,290	0.0852	0.0300	135
3	2,679	510,843	205,975	16,009	0.0298	0.0215	143
4	145	2,955	10,468	556	0.5117	0.0177	92
5	2,877	62,478	291,148	8,112	0.0202	0.0251	95
6	1,794	42,408	213,686	4,434	0.0302	0.0169	95
Average	1,999	120,460	152,910	8,276	0.1183	0.0231	117
STDV	1,362	194,401	105,504	6,194	0.1941	0.0053	25

APPENDIX B

MICROSOFT VISUAL BASIC CODE FOR CURVE FITTING BURGER
COEFFICIENTS

SolverOk SetCell:="\$M\$3", MaxMinVal:=2, ValueOf:="0", ByChange:="\$I\$3:\$L\$3"
SolverDelete CellRef:="\$L\$3", Relation:=1, FormulaText:="\$Q\$4"
SolverDelete CellRef:="\$L\$3", Relation:=3, FormulaText:="\$N\$4"
SolverAdd CellRef:="\$L\$3", Relation:=1, FormulaText:="\$Q\$4"
SolverAdd CellRef:="\$L\$3", Relation:=3, FormulaText:="\$N\$4"
SolverSolve UserFinish:=True
SolverOk SetCell:="\$M\$3", MaxMinVal:=2, ValueOf:="0", ByChange:="\$L\$3"
SolverSolve UserFinish:=True
SolverOk SetCell:="\$M\$3", MaxMinVal:=2, ValueOf:="0", ByChange:="\$I\$3"
SolverSolve UserFinish:=True
SolverOk SetCell:="\$M\$3", MaxMinVal:=2, ValueOf:="0", ByChange:="\$J\$3"
SolverSolve UserFinish:=True
SolverOk SetCell:="\$M\$3", MaxMinVal:=2, ValueOf:="0", ByChange:="\$K\$3"
SolverSolve UserFinish:=True
SolverOk SetCell:="\$M\$3", MaxMinVal:=2, ValueOf:="0", ByChange:="\$L\$3"
SolverSolve UserFinish:=True
SolverOk SetCell:="\$M\$3", MaxMinVal:=2, ValueOf:="0", ByChange:="\$I\$3"
SolverSolve UserFinish:=True
SolverOk SetCell:="\$M\$3", MaxMinVal:=2, ValueOf:="0", ByChange:="\$J\$3"
SolverSolve UserFinish:=True
SolverOk SetCell:="\$M\$3", MaxMinVal:=2, ValueOf:="0", ByChange:="\$K\$3"
SolverSolve UserFinish:=True
SolverOk SetCell:="\$M\$3", MaxMinVal:=2, ValueOf:="0", ByChange:="\$L\$3"
SolverSolve UserFinish:=True
SolverOk SetCell:="\$M\$3", MaxMinVal:=2, ValueOf:="0", ByChange:="\$I\$3"
SolverSolve UserFinish:=True
SolverOk SetCell:="\$M\$3", MaxMinVal:=2, ValueOf:="0", ByChange:="\$I\$3:\$L\$3"
SolverSolve UserFinish:=True
SolverOk SetCell:="\$M\$3", MaxMinVal:=2, ValueOf:="0", ByChange:="\$J\$3"
SolverSolve UserFinish:=True
SolverOk SetCell:="\$M\$3", MaxMinVal:=2, ValueOf:="0", ByChange:="\$K\$3"
SolverSolve UserFinish:=True
SolverOk SetCell:="\$M\$3", MaxMinVal:=2, ValueOf:="0", ByChange:="\$L\$3"
SolverSolve UserFinish:=True
SolverOk SetCell:="\$M\$3", MaxMinVal:=2, ValueOf:="0", ByChange:="\$I\$3"
SolverSolve UserFinish:=True
SolverOk SetCell:="\$M\$3", MaxMinVal:=2, ValueOf:="0", ByChange:="\$J\$3"
SolverSolve UserFinish:=True
SolverOk SetCell:="\$M\$3", MaxMinVal:=2, ValueOf:="0", ByChange:="\$K\$3"
SolverSolve UserFinish:=True
SolverOk SetCell:="\$M\$3", MaxMinVal:=2, ValueOf:="0", ByChange:="\$L\$3"
SolverSolve UserFinish:=True
SolverOk SetCell:="\$M\$3", MaxMinVal:=2, ValueOf:="0", ByChange:="\$I\$3"
SolverSolve UserFinish:=True

SolverOk SetCell:="\$M\$3", MaxMinVal:=2, ValueOf:="0", ByChange:="\$I\$3"
SolverSolve UserFinish:=True
SolverOk SetCell:="\$M\$3", MaxMinVal:=2, ValueOf:="0", ByChange:="\$K\$3"
SolverSolve UserFinish:=True
SolverOk SetCell:="\$M\$3", MaxMinVal:=2, ValueOf:="0", ByChange:="\$J\$3"
SolverSolve UserFinish:=True
SolverOk SetCell:="\$M\$3", MaxMinVal:=2, ValueOf:="0", ByChange:="\$I\$3"
SolverSolve UserFinish:=True
SolverOk SetCell:="\$M\$3", MaxMinVal:=2, ValueOf:="0", ByChange:="\$I\$3:\$L\$3"
SolverSolve UserFinish:=True
SolverOk SetCell:="\$M\$3", MaxMinVal:=2, ValueOf:="0", ByChange:="\$J\$3"
SolverSolve UserFinish:=True
SolverOk SetCell:="\$M\$3", MaxMinVal:=2, ValueOf:="0", ByChange:="\$K\$3"
SolverSolve UserFinish:=True
SolverOk SetCell:="\$M\$3", MaxMinVal:=2, ValueOf:="0", ByChange:="\$L\$3"
SolverSolve UserFinish:=True
SolverOk SetCell:="\$M\$3", MaxMinVal:=2, ValueOf:="0", ByChange:="\$I\$3"
SolverSolve UserFinish:=True
SolverOk SetCell:="\$M\$3", MaxMinVal:=2, ValueOf:="0", ByChange:="\$J\$3"
SolverSolve UserFinish:=True
SolverOk SetCell:="\$M\$3", MaxMinVal:=2, ValueOf:="0", ByChange:="\$K\$3"
SolverSolve UserFinish:=True
SolverOk SetCell:="\$M\$3", MaxMinVal:=2, ValueOf:="0", ByChange:="\$L\$3"
SolverSolve UserFinish:=True
SolverOk SetCell:="\$M\$3", MaxMinVal:=2, ValueOf:="0", ByChange:="\$I\$3"
SolverSolve UserFinish:=True
SolverOk SetCell:="\$M\$3", MaxMinVal:=2, ValueOf:="0", ByChange:="\$J\$3"
SolverSolve UserFinish:=True
SolverOk SetCell:="\$M\$3", MaxMinVal:=2, ValueOf:="0", ByChange:="\$K\$3"
SolverSolve UserFinish:=True
SolverOk SetCell:="\$M\$3", MaxMinVal:=2, ValueOf:="0", ByChange:="\$I\$3"
SolverSolve UserFinish:=True
SolverOk SetCell:="\$M\$3", MaxMinVal:=2, ValueOf:="0", ByChange:="\$K\$3"
SolverSolve UserFinish:=True
SolverOk SetCell:="\$M\$3", MaxMinVal:=2, ValueOf:="0", ByChange:="\$J\$3"
SolverSolve UserFinish:=True

```
SolverOk SetCell:="$M$3", MaxMinVal:=2, ValueOf:="0", ByChange:="$I$3"  
SolverSolve UserFinish:=True  
SolverOk SetCell:="$M$3", MaxMinVal:=2, ValueOf:="0", ByChange:="$L$3"  
SolverSolve UserFinish:=True  
SolverOk SetCell:="$M$3", MaxMinVal:=2, ValueOf:="0", ByChange:="$I$3"  
SolverSolve UserFinish:=True  
SolverOk SetCell:="$M$3", MaxMinVal:=2, ValueOf:="0", ByChange:="$J$3"  
SolverSolve UserFinish:=True  
SolverOk SetCell:="$M$3", MaxMinVal:=2, ValueOf:="0", ByChange:="$K$3"  
SolverSolve UserFinish:=True  
SolverOk SetCell:="$M$3", MaxMinVal:=2, ValueOf:="0", ByChange:="$I$3"  
SolverSolve UserFinish:=True  
SolverOk SetCell:="$M$3", MaxMinVal:=2, ValueOf:="0", ByChange:="$K$3"  
SolverSolve UserFinish:=True  
SolverOk SetCell:="$M$3", MaxMinVal:=2, ValueOf:="0", ByChange:="$J$3"  
SolverSolve UserFinish:=True  
SolverOk SetCell:="$M$3", MaxMinVal:=2, ValueOf:="0", ByChange:="$I$3"  
SolverSolve UserFinish:=True  
SolverOk SetCell:="$M$3", MaxMinVal:=2, ValueOf:="0", ByChange:="$L$3"  
SolverSolve UserFinish:=True  
SolverOk SetCell:="$M$3", MaxMinVal:=2, ValueOf:="0", ByChange:="$I$3"  
SolverSolve UserFinish:=True  
SolverOk SetCell:="$M$3", MaxMinVal:=2, ValueOf:="0", ByChange:="$J$3"  
SolverSolve UserFinish:=True  
SolverOk SetCell:="$M$3", MaxMinVal:=2, ValueOf:="0", ByChange:="$K$3"  
SolverSolve UserFinish:=True  
SolverOk SetCell:="$M$3", MaxMinVal:=2, ValueOf:="0", ByChange:="$I$3"  
SolverSolve UserFinish:=True  
SolverOk SetCell:="$M$3", MaxMinVal:=2, ValueOf:="0", ByChange:="$K$3"  
SolverSolve UserFinish:=True  
SolverOk SetCell:="$M$3", MaxMinVal:=2, ValueOf:="0", ByChange:="$J$3"  
SolverSolve UserFinish:=True  
SolverOk SetCell:="$M$3", MaxMinVal:=2, ValueOf:="0", ByChange:="$I$3"  
SolverSolve UserFinish:=True  
SolverOk SetCell:="$M$3", MaxMinVal:=2, ValueOf:="0", ByChange:="$I$3:$L$3"  
SolverSolve UserFinish:=True  
End Sub
```